AUS DEM LEHRSTUHL
FÜR INNERE MEDIZIN I
Prof. Dr. Martina Müller- Schilling

DER FAKULTÄT FÜR MEDIZIN
DER UNIVERSITÄT REGENSBURG

EXPRESSION, FUNCTION AND REGULATION OF METHYLTHIOADENOSINE PHOSPHORYLASE IN THE PATHOGENESIS OF CHRONIC LIVER DISEASE

Inaugural – Dissertation
zur Erlangung des Doktorgrades
der Biomedizinischen Wissenschaften

der
Fakultät für Medizin
der Universität Regensburg

vorgelegt von
Barbara Czech

2013

AUS DEM LEHRSTUHL
FÜR INNERE MEDIZIN I
Prof. Dr. Martina Müller- Schilling

DER FAKULTÄT FÜR MEDIZIN
DER UNIVERSITÄT REGENSBURG

EXPRESSION, FUNCTION AND REGULATION OF METHYLTHIOADENOSINE PHOSPHORYLASE IN THE PATHOGENESIS OF CHRONIC LIVER DISEASE

Inaugural – Dissertation
zur Erlangung des Doktorgrades
der Biomedizinischen Wissenschaften

der
Fakultät für Medizin
der Universität Regensburg

vorgelegt von
Barbara Czech

2013

Dekan: Prof. Dr. Dr. Torsten E. Reichert

Betreuer: Prof. Dr. Claus Hellerbrand

Tag der mündlichen Prüfung: 09.10.2013

Für meine Familie

NO PAIN- NO GAIN

Table of Contents

1 Zusammenfassung

Das Ziel dieser Arbeit war es, die Expression und Funktion der Methylthioadenosinphosphorylase (MTAP) in chronischen Lebererkrankungen zu analysieren.

Es zeigte sich, dass die MTAP mRNA und Proteinexpression in Hepatozyten im murinen Fibrosemodell sowie in Zirrhosepatienten vermindert vorliegt, während das Substrat 5'-Deoxy-5'-(Methylthio)adenosin (MTA) akkumuliert. Im Gegensatz dazu zeigen aktivierte hepatische Sternzellen (HSZ) starke MTAP Expression in zirrhotischen Lebern. Darüber hinaus konnte in den aktivierten HSZ im Vergleich zu Hepatozyten auch eine erhöhte Menge an intrazellulärem MTA nachgewiesen werden. Des weiteren ergab sich eine Korrelation der Collagen I Expression und der hepatischen MTA Spiegel in humanen Lebern von Patienten, die an einer nichtalkoholischen Steatohepatitis (NASH) litten, was darauf hinweist, dass die HSZ einen entscheidenden Beitrag zu den erhöhten MTA Spiegeln in den chronisch erkrankten Lebern leisten. Die Suppression von MTAP mittels siRNA in HSZ führte zu einer intrazellulären Akkumulation von MTA sowie einer Induktion von NFκB und erhöhter Apoptoseresistenz, während die Überexpression zu gegenteiligen Ergebnissen führte. Die anti-apoptotischen Effekte einer niedrigen MTAP Expression und demzufolge erhöhten MTA Spiegeln korrelierten mit der Expression von Survivin. Der anti-apoptotische Effekt wurde durch Inhibition von Survivin wieder aufgehoben. Behandlung mit einem demethylierenden Agens führte zu einer Induktion der MTAP und zu einer Reduktion der Survivin Expression, während, auf der anderen Seite die Stimulation mit reaktiven Sauerstoff Spezies (ROS) die Expression von MTAP verminderte und Survivin induzierte.

Zusammenfassend kann man sagen, dass die durch MTAP vermittelte Regulation von MTA den Polyaminstoffechsel mit der Apoptose von HSZ in Zusammenhang bringt. MTAP selbst sowie Mechanismen, die MTAP modulieren, erscheinen als vielversprechende prognostische Marker und therapeutische Angriffspunkte für die Behandlung von hepatischer Fibrose.

2 Summary

Objective: To study expression and function of methylthioadenosine phosphorylase (MTAP), the rate-limiting enzyme in the methionine and adenine salvage pathway, in chronic liver disease.

Design: MTAP expression was analyzed by qRT-PCR, Western blot and immunohistochemical analysis. Levels of MTA were determined by liquid chromatography-tandem mass spectrometry.

Results: MTAP was downregulated in hepatocytes in murine fibrosis models and in patients with chronic liver disease, leading to a concomitant increase in MTA levels. In contrast, activated hepatic stellate cells (HSCs) showed strong MTAP expression in cirrhotic livers. However, also MTA levels in activated HSCs were significantly higher than in hepatocytes, and there was a significant correlation between MTA levels and collagen expression in diseased human liver tissue indicating that activated HSCs significantly contribute to elevated MTA in diseased livers. MTAP suppression by siRNA resulted in increased MTA levels, NFκB activation and apoptosis resistance, while overexpression of MTAP caused the opposite effects in HSCs. The anti-apoptotic effect of low MTAP expression and high MTA levels, respectively, was mediated by induced expression of survivin, while inhibition of survivin abolished the anti-apoptotic effect of MTA on HSCs. Treatment with a DNA demethylating agent induced MTAP and reduced survivin expression, while oxidative stress reduced MTAP levels but enhanced survivin expression in HSCs.

Conclusion: MTAP mediated regulation of MTA links polyamine metabolism with NFκB activation and apoptosis in HSCs. MTAP and MTAP modulating mechanisms appear as promising prognostic markers and therapeutic targets for hepatic fibrosis.

3 Introduction

3.1 Liver function and physiology in health and disease

3.1.1 Liver Anatomy

Being the largest parenchymal organ and the largest gland in the body gives the liver special duties and responsibilities such as protein synthesis and detoxification. It is located in the right upper quadrant in the abdominal cavity and weighs about 1500 to 2000g. Macroscopically the liver can be divided into four lobes naming: *Lobus hepatis dexter, Lobus hepatis sinister, Lobus quadratus, and Lobus caudatus.* Connective tissue, namely Glisson's capsule surrounds the four lobes and is linked to intrahepatic tissue.

Arteria hepatica propria delivers arterial, oxygenated blood and the *vena portae hepatis* supplies venous, nutrient rich blood from the gastrointestinal tract. Liver sinusoids manage blood efflux by the *Vena hepatica* and the *Vena cava inferior*. The liver can be subdivided microscopically in eight segments which are consisting of *lobuli hepatis* which are 1-2mm of size and mainly containing hepatocytes with a vein in the center (*Vena centralis*).

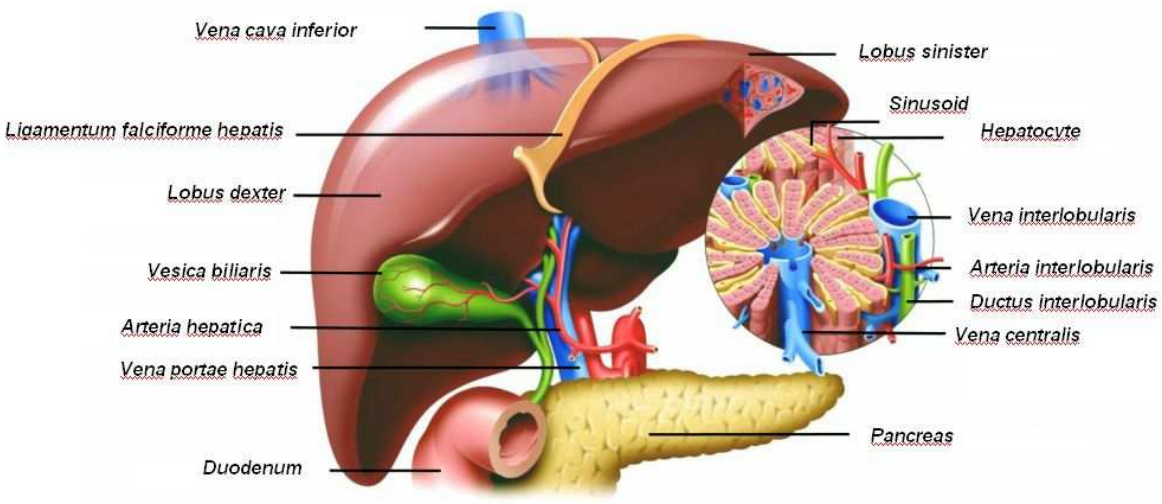

Figure 3.1 Schematical liver architecture (modified from Wissen Media Verlag GmbH, München).

In the contact area of several lobules the periportal field includes *Arteria* and *Vena interlobularis*, as well as bile ducts (*Ductuli interlobulares*) also known as Glisson's triangle. The bulk cellular mass in the liver is represented by hepatocytes which are divided by sinusoids, built by fenestrated, discontinuous endothelium without

basal membrane. Specialized macrophages called Kupffer cells are sitting in the sinusoids' walls. The space of Disse is called a 10 to 15µM wide perisinusoidal space which is located between hepatocytes and sinusoids containing blood plasma and hepatic stellate cells (HSCs, also called Ito cells). HSCs store lipids and vitamin A. Sinusoidal endothelial cells as well as Kupffer cells and HSCs are non parenchymatic cells and represent about 6% cellular volume while 94% of cellular mass constitute hepatocytes.

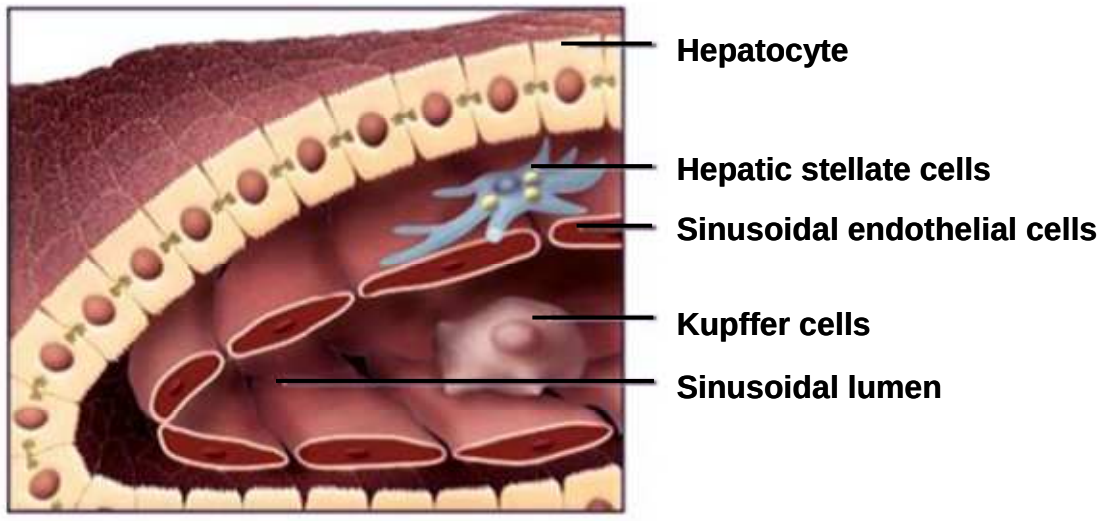

Figure 3.2 Schematical representation of hepatic cellular components (modified from Bataller and Brenner, 2005)

3.1.2 Liver Function

The liver represents the most important central organ concerning metabolism. Production of essential proteins salvaging carbohydrates and lipids, production of bile represent special tasks of the liver and herewith degradation and excretion of products of metabolism. Especially carbohydrate metabolism plays an important role so it regulates blood glucose concentration independent of food intake via gluconeogenesis and glucogenolysis. The liver is further responsible for the generation of albumin, globulin and coagulation factors (fibrinogen, prothrombin). Lipid metabolism is mediated via building up fatty acids and triglycerides (lipogenesis) and vice versa lipids are broken down to free fatty acids and glycerol (lipolysis). Synthesis of cholesterol and bile acid derivatives is further mediated by the liver. One of the most important tasks is detoxification of endo- and exogenic toxins which are metabolized to be discarded via bile or kidneys. During the degradation of amino acids ammonia is generated and will be used for the

synthesis of urea. Additional functions of the liver are biotransformation of xenobiotica and for example heme and storage of iron. By contrast to other organs the liver has the ability to regenerate but as a consequence of chronic liver disease this capability can be limited.

3.2 Chronic liver disease

Liver disease can be classified into acute and chronic liver disease. Acute infections or intoxications can be the cause of acute liver injury. This rarely results in complete liver failure thanks to the regenerative response of the liver. Development of chronic liver disease upon sustaining hepatic injury is characterized by chronic hepatic inflammation which can contribute to liver fibrosis and ultimately cirrhosis.

3.2.1 Fibrosis

Hepatic fibrosis describes an exuberant wound-healing response to chronic liver injury associated by hepatocellular damage, inflammation and continuous tissue remodeling (Bataller and Brenner, 2001; Bataller and Brenner, 2005; Friedman, 2003). Extracellular matrix (ECM), composed of collagen, elastin, structural glycoproteins, proteoglycans and some minor components, is either overproduced, degraded deficiently, or both. The trigger is chronic injury, especially, if there is an inflammatory component. Current evidence indicates that HSCs are central mediators of fibrogenesis (Friedman, 2004; Friedman, 2008). HSCs are the major cellular producer of ECM proteins (mainly collagen types I, III and IV). As already mentioned in 3.1.1 in healthy liver, HSCs are mainly in a quiescent state containing droplets of vitamin A in their cytoplasm. Quiescent HSCs are involved in ECM homeostasis as they express metalloproteinases (MMPs) for ECM degradation and inhibitors of metalloproteinases (TIMPs) for ECM maintenance, respectively (Atzori et al., 2009). As response to various stimuli during liver injury, quiescent HSCs undergo morphological changes associated with a loss of their vitamin A reservoir. This activation process is a hallmark of fibrogenesis (Friedman and Arthur, 1989). HSCs transform into highly proliferative myofibroblast like cells (activated HSCs) which express α smooth muscle actin (αsma), a histological marker of activated HSCs in injured liver (Mann and Mann, 2009). Activated HSCs migrate to and accumulate at the side of tissue repair. They overproduce ECM proteins (mainly collagen type I) and TIMPs (mainly TIMP-1) which in turn block

matrix degradation by MMPs. Further, activated HSCs up-regulate an array of cytokines (e.g. IL-6), chemokines (e.g. MCP-1), and mitogens (e.g. TGF-β and PDGF) which further activate HSCs in an autocrine manner. Moreover, activated HSCs are characterized by high resistance to apoptosis. They survive prolonged serum deprivation as well as established pro-apoptotic stimuli like e.g. Fas ligand (Novo et al., 2006). One key transcription factor in the activation of hepatic stellate cells is NFκB. This signaling pathway is mediating apoptosis resistance (Oakley et al., 2005; Watson et al., 2008). NFκB also induces proinflammatory gene expression such as MCP1 and RANTES (Elsharkawy et al., 2005; Hellerbrand et al., 1998; Schwabe et al., 2003).

3.2.2 Cirrhosis

Accumulation of ECM in advanced fibrosis deforms hepatic architecture by building up fibrous scar and subsequent development of nodules of regenerating hepatocytes ascertains cirrhosis. Patients suffering from cirrhosis exhibit disturbed hepatic blood flow and hepatocellular dysfunction. The outcome of this is hepatic insufficiency and portal hypertension (Gines et al., 2004; Iredale, 2003). Further pathological changes can occur such as liquid in the abdominal cavity (*ascites*) and formation and bleeding of esophagal varices, muscle wasting, bleeding from the intestines, enlarging of mens' breasts (*gynaecomastia*) and so on (Schuppan and Afdhal, 2008). Finally, cirrhosis results in loss of liver function (decompensated cirrhosis) a condition with high morbidity and mortality (Pinzani et al., 2011).

3.3 Trigger of chronic liver disease

Initiation of chronic hepatic inflammation, liver damage and ultimately liver failure caused by persisting fibrosis can result in complete cirrhosis and loss of liver function. Several mechanisms can be the cause for the progression of chronic liver disease. Namely chronic alcohol abuse (Gramenzi et al., 2006), 90% of heavy drinkers develop fatty liver and about 30% display more severe forms such as fibrosis and cirrhosis (Gao and Bataller, 2011). Further, drugs being metabolized by the liver can induce liver disease such as acute liver failure (ALF), acute hepatic necrosis, chronic hepatitis, triggered by various mechanisms of hepatotoxicity, such as cell death resulting from direct binding of the drug to cellular proteins, dysregulation of the cytoskeleton or inhibition of mitochondrial

function (Navarro and Senior, 2006). Autoimmune related disorders such as autoimmune hepatitis (Krawitt, 2006), and cholestatic autoimmune diseases like primary biliary cirrhosis and primary sclerosing cholangitis lead to the progression of chronic liver disease (Boonstra et al., 2012). Genetic disorders such as hereditary hemochromatosis which leads to liver iron overload (van Bokhoven et al., 2011), Wilson disease, an autosomal recessive disorder, that leads to an accumulation of copper in the liver (Rosencrantz and Schilsky, 2011) and Gilberts syndrome which affects billirubin levels (Strassburg, 2008) affect hepatic function and induce chronic liver disease. Beyond, viral hepatitis A-E influence liver function unequally, thus, leading from acute infection without chronic course (A) to fibrosis, cirrhosis and hepatocellular carcinoma (HCC) (C) (Qu and Lemon, 2010). Another common cause of chronic liver disease is the induction of non-alcoholic fatty liver disease (NAFLD) which will be illustrated in the subsequent chapter.

3.3.1 Non-alcoholic fatty liver disease (NAFLD)

Non-alcoholic fatty liver disease (NAFLD) is a clinico-pathological condition of rising importance. It is characterized by hepatic lipid accumulation which starts with simple hepatic steatosis and progresses towards hepatocellular injury and inflammation (non-alcoholic steatohepatitis [NASH]) in a significant number of patients NASH is the most common origin of abnormal liver tests in Western societies and its incidence is further increasing worldwide (Bosserhoff and Hellerbrand, 2011; Hellerbrand, 2010; Straub and Schirmacher, 2010). The pathology of NAFLD was first described in 1980 by Ludwig who obtained steatosis and inflammation in livers of patients without alcohol consumption (Ludwig et al., 1980). NAFLD ranges from simple hepatic steatosis with triglyceride accumulation in hepatocytes to Non-alcoholic steatohepatitis (NASH), which is histologically verifiable by ballooning hepatocytes and cell death. The prevalence of NAFLD correlates with obesity/BMI in adults and children (Bjornsson and Angulo, 2007) and advancing age (Frith et al., 2009). Obesity, type 2 diabetes, hypertension or dyslipidemia are frequently associated with NAFLD. Therefore, NAFLD is considered as the hepatic manifestation of the metabolic syndrome, and sedentary lifestyle combined with high caloric intake is the major cause of NAFLD (de Alwis and Day, 2008). A two hit model was raised to explain the progression (Day and James, 1998). The first hit resembles an imbalance between lipid intake and removal and the second hit induces inflammation. But it seems that a third hit

needs to be evaluated which explains ongoing fibrosis ultimately leading to cirrhosis in some patients. The outcome in patients suffering from simple hepatic steatosis is good involving change of lifestyle, food intake and weight loss. 20-30% of steatosis patients develop NASH and within 10 years in 10-30% of those patients evolve cirrhosis (Argo and Caldwell, 2009; Argo et al., 2009). The NASH induced cirrhosis can further be a trigger for the progression of HCC (Baffy et al., 2012).

3.3.2 Effects of reactive oxygen species (ROS) on fibrosis

Clinical and experimental data suggest that oxidative stress mediates the progression of fibrosis, and that oxidative stress related molecules may act as mediator of molecular and cellular events implicated in liver fibrosis. The generation of reactive oxygen species (ROS) plays an important role in producing liver damage and initiating hepatic fibrogenesis. Oxidative stress disrupts lipids, proteins and DNA, induces necrosis and apoptosis of hepatocytes and amplifies the inflammatory response. ROS also stimulate the production of profibrogenic mediators from Kupffer cells and circulating inflammatory cells and directly activate hepatic stellate cells, resulting in the initiation of fibrosis (Parola and Robino, 2001; Pinzani and Rombouts, 2004; Sanchez-Valle et al., 2012).

3.3.2.1 Effects of ROS formation on methylation

In addition to causing genetic changes, ROS may lead to epigenetic alterations that affect the genome and play a key role in the development of human malignant transformation (Campos et al., 2007; Ziech et al., 2011). More specifically, ROS production is associated with alterations in DNA methylation patterns (Campos et al., 2007; Donkena et al., 2010; Ziech et al., 2010). ROS-induced oxidative stress can contribute to gene silencing by mechanisms that involve aberrant hypermethylation of tumor suppressor gene promoter regions and thus lead towards progression to a malignant phenotype. Our group could show that in HCC the methylthioadenosine phosphorylase (MTAP) promoter is hypermethylated which results in decreased MTAP expression (Hellerbrand et al., 2006). Exposure of HCC cells to ROS induced hypermethylation of the E-cadherin (Lim et al., 2008) and catalase promoter (Min et al., 2010).

3.4 Characterisation of polyamine metabolism and methionine pathways

3.4.1 Methylthioadenosine phosphorylase (MTAP)

MTAP catalyzes the phosphorylation of 5'-deoxy-5'-(methylthio)adenosine (MTA) (**Figure 3.3**) which is formed as a by-product of polyamine synthesis to yield adenine and methylthioribose-1-phosphate (MTR-1P). MTR-1P is then converted in a series of enzymatic reactions to regain methionine (Backlund, Jr. and Smith, 1981). While adenine is subsequently recycled back into nucleotides through the action of phosphoribosyltransferases (Savarese et al., 1981). MTAP activity is responsible for essentially all of the free adenine generated in human cells (Kamatani and Carson, 1981), indicating that this enzyme performs an important function in the purine salvage pathway. Regaining methionine and adenine are essential responsibilities of MTAP. Beyond, MTAP is necessary to obtain polyamine metabolism to work properly.

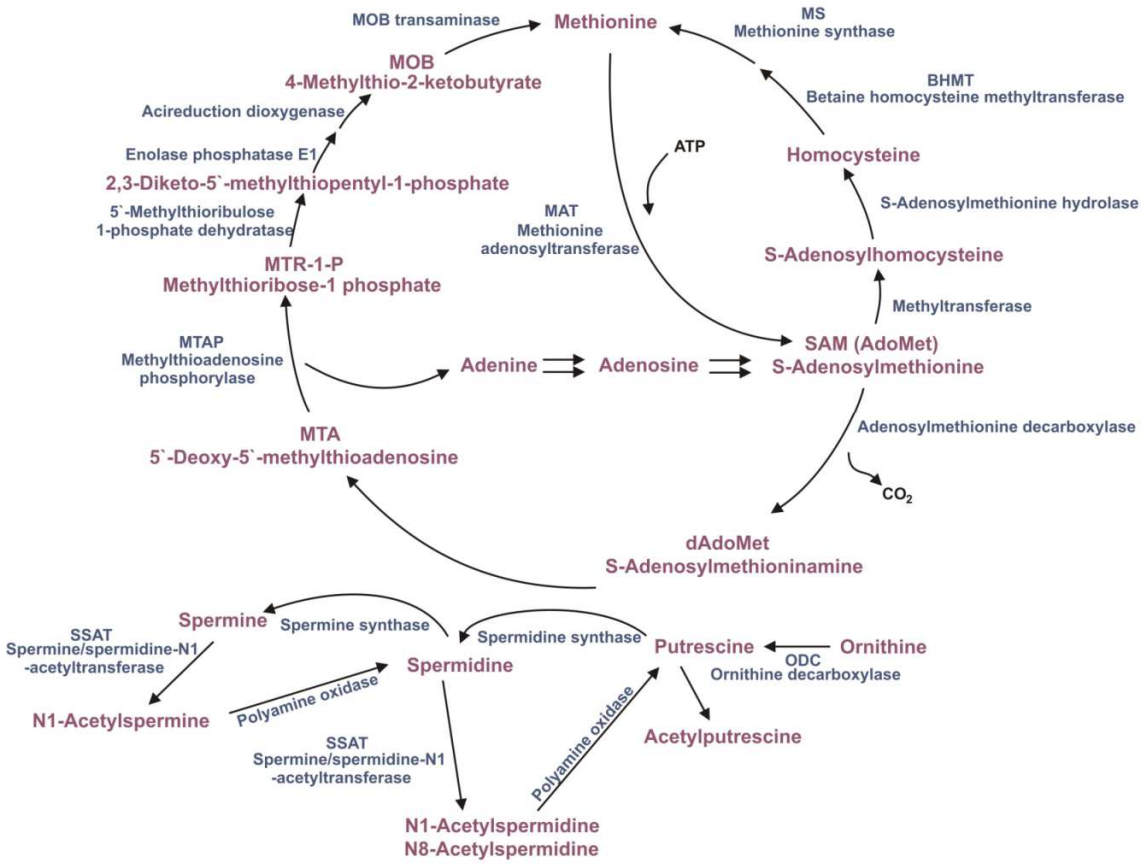

Figure 3.3 Metabolic pathways in which MTAP is involved. MTA resulting from polyamine pathway is metabolized by MTAP forming adenine necessary for DNA synthesis and MTR-1-P to regain methionine.

Loss of MTAP has been shown to cause a significant decrease in intracellular polyamine levels and alters the ratio of putrescine to total polyamines *in vitro* (Christopher et al., 2002; Subhi et al., 2003). The mechanism involves the accumulation of MTAP's substrate, MTA which in higher concentrations acts as a potent inhibitor of spermine and spermidine synthase, two key enzymes of the polyamine synthetic pathway (Subhi et al., 2003). MTAP activity was first characterized in rat ventral prostate in 1969 (Pegg and Williams-Ashman, 1969). Biochemical evidence suggests that mammalian MTAP is a trimer made up of three identical sub-units of 32 kDa (Della et al., 1990; Della et al., 1996). Each subunit in the human enzyme contains 283 amino acid residues. Consistent with its central metabolic role MTAP expression is high in normal liver tissue (Kamatani et al., 1981; Nobori et al., 1996). MTAP deficiency is common in human and murine malignant cell lines (Kamatani et al., 1981; Toohey, 1977). The abnormality is not confined to tissue culture cells, but is also present in primary leukemias, gliomas, and non-small cell lung cancers (Fitchen et al., 1986; Kamatani et al., 1981; Nobori et al., 1991; Nobori et al., 1993). In hepatocellular carcinoma (HCC) loss or downregulation of MTAP leads to an accumulation of MTA which promotes tumorigenicity (Berasain et al., 2004; Kirovski et al., 2011).

3.4.1.1 MTAP structure

The human MTAP gene (EC 2.4.2.28) resides on the short arm of chromosome 9, in the chromosomal region 9p21, from 21792543 to 22111094 (5'→ 3'). It consists of eight exons and seven introns. Exon 1 encodes 11 amino acids and the 5' noncoding region, the sizes of exons 2-7 range from 79 to 240 bp. The last (8th) exon encodes the C-terminal 12 amino acids and the 3' noncoding region (Nobori et al., 1996).

3.4.1.2 MTAP expression *in vivo*

Regarding the enzymatic responsibilities of MTAP it is obvious that MTAP is abundantly expressed in a wide range of healthy cells and tissues (Olopade et al., 1995). MTAP has been purified from rat liver (Ferro et al., 1978) and exhibits highest activity in liver and lung (Garbers, 1978). High hepatic MTAP expression can be explained by the key role of the liver in methionine metabolism (Avila et al., 2004). In various studies concerning malignancies it has been shown that MTAP expression is downregulated or even lost. Genomic or epigenetic alterations are

the cause of decreased MTAP expression. In leukemia (Hori et al., 1998), pancreatic adenocarcinoma (Hustinx et al., 2005; Subhi et al., 2004), osteosarcoma (Garcia-Castellano et al., 2002), endometrial cancer (Wong et al., 1998) and lung cancer (Watanabe et al., 2009) partial or complete deletions of MTAP account for lost expression. In contrast, MTAP is overexpressed in human colon carcinoma (Bataille et al., 2005). For hepatocellular carcinoma (HCC) (Hellerbrand et al., 2006), melanoma (Behrmann et al., 2003) as well as lymphoma (Ishii et al., 2005) hypermethylation has been shown to account for decreased MTAP expression. MTAP is located in the 9p21 chromosomal region (Carrera et al., 1984; Nobori et al., 1996), an area which has been described to play a role in various human malignancies such as type 2 diabetes (Cugino et al., 2012), coronary artery disease (Roberts and Stewart, 2012), melanoma (Cooper et al., 2012), leukemia (Ragione and Iolascon, 1997) and HCC (Liew et al., 1999). The 9p21 area contains p15-p16-MTAP-IFNa-IFNb (Olopade et al., 1995). P15 and p16 specifically inhibit cyclin D-associated kinases (Parry et al., 1995; Sandhu et al., 1997) and are both considered to be tumor suppressors (Tsihlias et al., 1999). Savarese and colleges could show co- deletions of MTAP and one or more genes in malignant cells (Chen et al., 1996; Zhang et al., 1996). MTAP deficiency *per se* was shown to induce accumulation of MTA in melanoma and HCC which promotes tumorigenicity (Kirovski et al., 2011; Stevens et al., 2009).

3.4.1.3 Effect of MTAP manipulation *in vivo* and *in vitro*

In vivo repression of MTAP enzyme activity with an inhibitor increased MTA levels in blood and urine and beyond tumor growth was inhibited in nude mouse models (Basu et al., 2011). *In vitro* contradictory results were obtained. In a MCF-7 breast cancer cells line it was shown that reexpression of the MTAP enzyme activity inhibits colony formation and suppressed tumor formation in implanted mice. The authors consider MTAP to have tumor suppressor activity and suggest that its effects may be mediated by altering intracellular polyamine pools (Christopher et al., 2002). A study by Subhi supports this idea so they showed that MTAP regulates ornithine decarboxylase (ODC) which is the rate limiting enzyme for polyamine production (**Figure 3.3**) (Subhi et al., 2003). For pancreatic carcinoma an inverse correlation of MTAP and ODC activity could be shown (Subhi et al., 2004). Inhibition of MTAP enzyme activity has been shown to induce apoptosis (Basu et al., 2011).

3.4.1.4 Regulation of MTAP

As already described in most malignancies loss of MTAP is due to homozygous deletions of the MTAP gene. Our group (Hellerbrand et al., 2006) and others (Berasain et al., 2004) have shown that in HCC MTAP is downregulated *via* promoter hypermethylation. This mechanism can also be observed for melanoma and lymphoma (Behrmann et al., 2003; Ishii et al., 2005). Transcriptional activation of the MTAP promoter by binding of CCAAT binding factor to a distal CCAAT motif in the MTAP promoter was also described (Kadariya et al., 2005).

MTAP activity was shown to be regulated by various mechanisms. In liver tissue of mice treated with LPS reduced MTAP activity, increased ODC activity and an accumulation of MTA was measured whereas no difference in MTAP protein could be obtained (Fernandez-Irigoyen et al., 2008). Further, treatment of HCC cells with reactive oxygen species (ROS) decreased MTAP activity (Fernandez-Irigoyen et al., 2008). Analogues of adenosine such as 5'- Deoxyadenosine can block MTAP activity (Fabianowska-Majewska et al., 1994).

3.4.2 5'-deoxy-5'-(methylthio)adenosine (MTA)- structure and abundance

The substrate of the enzyme MTAP is 5'-deoxy-5'-(methylthio)adenosine (MTA) whose occurrence was described about 100 years ago. The molecular structure was described in 1924 (Williams-Ashman et al., 1982). The biological importance of MTA became apparent in 1952, 1 year before the discovery of its metabolic precursor S-adenosylmethionine (AdoMet), in studies on the metabolic interrelationship of methionine and 5-thiomethylribose (Williams-Ashman et al., 1982). MTA is abundant in small amounts in all cell types, including prokaryotes, yeast, plants and higher eukaryotes. In mammalian tissues, MTA is mainly produced during the biosynthesis of polyamines (**Figure 3.4**) (Pegg, 1988; Williams-Ashman et al., 1982). For many years, this nucleoside has received by far much less attention than its precursor AdoMet. However, MTA exhibits a lot of different effects in various mammalian cells and tissue.

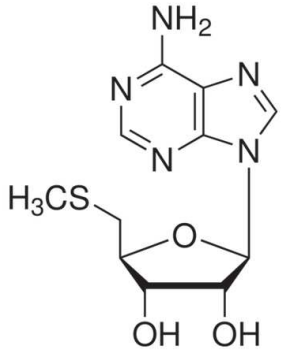

Figure 3.4 5'-deoxy-5'-(methylthio)adenosine (MTA) is a hydrophobic sulfur-containing adenine nucleoside in which the hydroxyl group in the 5 position of the ribose is substituted by a methylthio moiety. This methylthio moiety is derived from the amino acid methionine, while the rest of the molecule comes from ATP.

As already mentioned MTA is mainly produced in polyamine pathway and is synthesized in stochiometric amounts to spermidine and spermine. The biosynthesis of polyamines starts with the decarboxylation of AdoMet and decarboxylated AdoMet serves as substrate for aminopropyltransferases. These enzymes transfer the aminopropyl moiety from decarboxylated AdoMet to putrescine whereas spermidine is formed and to spermidine which forms spermine. MTA is metabolized by MTAP which results in the formation of adenine and MTR-1P. This metabolite is finally converted into methionine, and adenine is salvaged to ultimately replenish the AMP and ATP pools. Consequently, the two metabolites from which AdoMet and MTA are formed, namely methionine and ATP, are thus recovered (**Figure 3.3**) (Avila et al., 2004; Williams-Ashman et al., 1982). The conversion of MTR-1P into methionine involves a complex set of oxidations via the intermediate 4-methylthio-2-oxobutanoic acid (MTOB). This efficient cycle sustains the high rate of polyamine synthesis that occurs during cellular proliferation and provides methionine for AdoMet and protein synthesis. In addition, the removal of accumulating MTA by MTAP is necessary for the cell to carry out polyamine metabolism, since MTA is a strong inhibitor of spermine synthase, and to a lesser extent of spermidine synthase and of ODC (Pascale et al., 2002; Pegg and Williams-Ashman, 1969). The inhibition of ODC by MTA can be mediated in part by its metabolite MTOB, as has been recently demonstrated in yeast and human tumor cells (Subhi et al., 2003).

3.4.2.1 Effects of MTA *in vivo* and *in vitro*

Analyzing the literature there are contradictory results regarding the effects of MTA. But it is evident that MTA performs fundamental cellular functions and thus influences metabolism significantly. *In vivo* MTA was shown to rescue killing effect of LPS injection (Hevia et al., 2004), to inhibit tumor growth in a melanoma xenograft mouse model (Andreu-Perez et al., 2010) and to ameliorate malignant transformation of $Mdr2^{-/-}$ mice (Latasa et al., 2010). In an AOM/DSS experimental inflammation induced colon cancer model in mice MTA treatment reduced proinflammatory gene expression and proliferation and induced apoptosis (Li et al., 2012). For rats MTA donation slowered disease progression of experimental autoimmune encephalomyelitis (Moreno et al., 2010) and in a CCl_4 rat model MTA decreased proinflammatory and profibrogenic gene expression (Simile et al., 2001).

In vitro focussing on liver metabolism different results were obtained dependent on MTA concentrations used in the experiments. For hepatocellular carcinoma (HCC) MTA concentrations up to 5µM increased proliferative capacity, tumorigenicity as well as proinflammatory gene expression (Kirovski et al., 2011). MTA concentrations from 10 up to 500µM rescued rat hepatocytes from okadaic acid induced apoptosis while same doses of MTA promoted induction of apoptosis in hepatoma cell lines (Ansorena et al., 2002). The activation of hepatic stellate cells (HSCs) is considered to be the key event of hepatic fibrosis (Bataller and Brenner, 2005; Friedman, 2008) and MTA was shown to inhibit HSC activation at doses of 25-500µM (Simile et al., 2001). 200-500µM MTA blocked profibrogenic gene expression as well as proliferation of activating HSCs (Latasa et al., 2010). Further, decreased rather than increased invasiveness induced by MTA were suggested in a study examining two rat ascites hepatoma cell lines, possibly due to alterations in the phospholipid composition and fluidity of the tumor cell membranes (Kido et al., 1991). In cultured melanoma cell lines, exogenous addition of 50-100µM MTA caused up-regulation of tumor-promoting genes and enhanced invasiveness and vasculogenic mimicry while no similar gene up-regulation was observed in normal melanocytes (Stevens et al., 2009). Several pathways are affected by MTA. It is able to inhibit growth-factor induced protein tyrosine phosphorylation and to increase intracellular cAMP levels through the inhibition of cAMP phosphodiesterase (Maher, 1993; Riscoe et al., 1984). MTA

concentrations used in these experiments were much higher than physiologically occurring. NFκB was shown to be induced or inhibited depending on cells and concentrations (Hevia et al., 2004; Kirovski et al., 2011; Veal et al., 2004). One of the best-characterized actions of MTA is the inhibition of protein methylation (Williams-Ashman et al., 1982). This post-translational modification may occur at arginine residues or at the carboxyl terminus of proteins, and is thought to modulate cellular signaling and gene expression (Law et al., 1992; Lee and Cho, 1998; Mowen et al., 2001). To further complicate the understanding of the cellular responses to MTA, some of the effects of this molecule on the regulation of gene expression have been attributed to its ability to replenish the cellular AdoMet pool through the methionine salvage pathway (Martinez-Chantar et al., 2003).

3.4.3 AdoMet: MAT

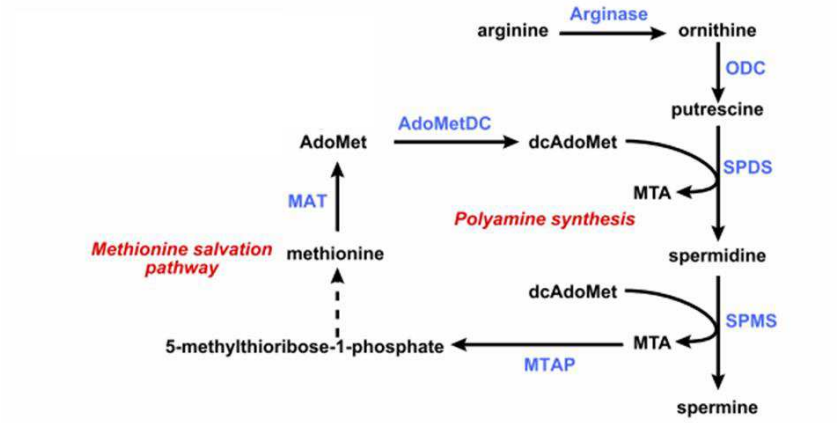

Figure 3.5 Methionine metabolism: Methionine adenosyltransferase (MAT) catalyzes the conversion of methionine and ATP into AdoMet (Lu and Mato, 2012).

S-Adenosyl-L-Methionine (AdoMet, SAM) was discovered 60 years ago and gained attention as major biological methyl donor but it has also principal roles in diverse cellular processes including growth and death (Lu and Mato, 2012). Methionine adenosyltransferase (MAT) is the enzyme that catalyzes the biosynthesis of AdoMet from ATP and methionine. MAT is one of the genes that is essential to sustain life (Glass et al., 2006). In mammals, all cells and tissues that have been studied express MAT, its activity being highest in the liver (Finkelstein, 1990). Consequently, individuals with hepatic MAT activity deficiency are characterized by isolated persistent hypermethioninemia (Ubagai et al., 1995). Mammals express two genes, MAT1A and MAT2A, which encode for two homologous MAT catalytic subunits, α1 and α2 (Kotb et al., 1997). MAT1A is

mostly expressed in normal liver, and the α1 subunit organizes into two MAT isoenzymes, MAT III (dimer) and MAT I (tetramer) (Kotb et al., 1997). MAT2A is widely distributed, and it encodes for a catalytic subunit (α2) found in the MAT isoenzyme MAT II that also exists in polymeric forms that vary from tissue to tissue (Horikawa et al., 1993; Kotb and Kredich, 1985). Fetal liver expresses MAT2A and MAT2B but not MAT1A (Gil et al., 1996; Yang et al., 2008). MAT1A expression increases a few days after birth and progressively takes over so that the adult liver (mostly hepatocytes) expresses mainly MAT1A, very little MAT2A, or MAT2B (Gil et al., 1996; Yang et al., 2008). Hepatic MAT1A gene expression is downregulated in HCC (Cai et al., 1996), during dedifferentiation (Lu and Mato, 2008; Vazquez-Chantada et al., 2010), in most cirrhotic patients (Avila et al., 2000), and in patients with alcoholic hepatitis (Lee et al., 2004). The mechanisms of MAT1A downregulation occur both at transcriptional and posttranscriptional levels. The Mat1a KO mouse model has provided much insight into the consequences of chronic hepatic AdoMet deficiency and altered signaling pathways that may lead to malignant degeneration. Mat1a KO mice appear normal at a young age but are more susceptible to steatosis induced by a choline-deficient diet and liver injury induced by CCl_4 , and they develop NASH and HCC spontaneously on a normal diet by 8 and 18 months, respectively (Lu et al., 2001; Martinez-Chantar et al., 2002). Mat1a KO mice have increased hepatic oxidative stress (Martinez-Chantar et al., 2002), show genomic instability (Tomasi et al., 2009), dysregulated signaling pathways (Chen et al., 2004; Tomasi et al., 2010; Varela-Rey et al., 2011; Vazquez-Chantada et al., 2009), have abnormal lipid homeostasis (Lu et al., 2001; Martinez-Chantar et al., 2002) and exhibit cancer cell expansion (Rountree et al., 2008).

Mouse models to study the effects of excess AdoMet resulted in spontaneous development of NASH and HCC (Liao et al., 2009; Martinez-Chantar et al., 2008). AdoMet treatment is well established to ameliorate liver injury in multiple animal models, including galactosamine, acetaminophen, alcohol, thioacetamide, endotoxemia, CCl_4 , bile duct ligation (BDL), NASH, and ischemia-reperfusion (Cave et al., 2007; Cederbaum, 2010; Ko et al., 2008; Lu and Mato, 2012; Mato et al., 1997; Yang et al., 2010; Yang et al., 2009). AdoMet not only protected against acute injury, it also reduced fibrosis in multiple experimental models (Cederbaum, 2010; Yang et al., 2010).

3.5 Aim of the study

Previous *in vitro* and *in vivo* studies in our group (Hellerbrand et al., 2006; Kirovski et al., 2011) suggested a functional role of MTAP in HCC progression. We wanted to expand our study on chronic liver disease which can be considered as a precancerous condition. Our goals were to investigate whether MTAP functionally affects hepatic stellate cells which can be called the cellular key players of hepatic fibrosis (Bataller and Brenner, 2005; Friedman, 2008). We further wanted to ascertain whether there is a correlation between MTAP expression an MTA levels in *vivo* as we have already shown in HCC (Kirovski et al., 2011). *In vitro* alteration of MTA levels was shown to have different effects depending on used MTA concentration (Kirovski et al., 2011; Latasa et al., 2010). We wanted to asses effects of physiologic relevant doses on hepatic stellate cells and the functional effects of those doses. There are not much regulatory mechanisms known affecting MTAP expression. It is known that MTAP activity is regulated by reactive oxygen species in HCC cells (Fernandez-Irigoyen et al., 2008) and the generation of ROS plays a pivotal role in the pathogenesis of chronic liver disease (Parola and Robino, 2001; Pinzani and Rombouts, 2004; Sanchez-Valle et al., 2012) so we wanted to know whether the generation of ROS has an impact on the regulation of MTAP expression. Induction of methylation is associated with cirrhosis (Ziech et al., 2011) and also it was described that ROS induce methylation reactions (Lim et al., 2008; Min et al., 2010). So, the aim was to assess whether methylation in combination with the induction of reactive oxygen species has an impact on MTAP expression.

4 Materials and Methods

4.1 Chemicals and Reagents

5- Azacytidine (Aza)	Sigma-Aldrich, Deisenhofen, Germany
Acrylamid	Carl Roth, Karlsruhe, Germany
Adenosine periodate oxidized (AdOx)	Sigma-Aldrich, Deisenhofen, Germany
Agar	Difco Laboratories, Augsburg
Agarose SeaKem® LE	Biozym, Hess/Oldendorf, Germany
Ampicillin	Sigma-Aldrich, Deisenhofen, Germany
APS	Sigma-Aldrich, Deisenhofen, Germany
Bovine serum albumine (BSA)	Biozym, Hess/Oldendorf, Germany
Ciprobay	Bayer, Leverkusen, Germany
Ciprofloxacin	Fresenius Kbi, Bad Homburg, Germany
Collagenase type IV	Sigma-Aldrich, Hamburg, Germany
DEPC	Carl Roth GmbH, Karlsruhe, Germany
Diflucan	Pfizer, Karlsruhe, Germany
DMEM medium	PAA Laboratories, Cölbe, Germany
DMSO	Sigma-Aldrich, Deisenhofen, Germany
Ethanol	J.T. Baker, Deventer, The Netherlands
Fatty Acid free BSA	Sigma-Aldrich, Deisenhofen, Germany
FCS (fetal calf serum)	PAN-Biotech, Aidenbach, Germany
FITC Annexin V	PromoKine, Heidelberg, Germany
Fluconazol	B. Braun, Melsungen, Germany
Geneticin	Gibco/Invitrogen
Methanol	Merck, Darmstadt, Germany
Milk powder	Carl Roth, Karlsruhe, Germany
5'-deoxy-5'-(methylthio)adenosine (MTA)	Sigma-Aldrich, Deisenhofen, Germany
Oleic acid	Sigma-Aldrich, Deisenhofen, Germany
PBS	PAA Laboratories, Cölbe, Germany
Penicillin	Invitrogen, Karlsruhe, Germany
Ponceau S	Sigma-Aldrich, Deisenhofen, Germany
Propidium iodie	Sigma-Aldrich, Deisenhofen, Germany

Roti Safe	Carl Roth, Karlsruhe, Germany
Staurosporine (STS)	Enzo Life Sciences, Lörrach, Germany
Streptomycin	Invitrogen, Karlsruhe, Germany
TEMED	Sigma-Aldrich, Deisenhofen, Germany
Trypan blue	Sigma-Aldrich, Deisenhofen, Germany
Trypsin/EDTA	PAA Laboratories, Cölbe, Germany
Tween 20®	Sigma-Aldrich, Deisenhofen, Germany
β-Mercaptoethanol	Sigma-Aldrich, Deisenhofen, Germany

4.2 Laboratory expendables

CryoTube vials	Nunc, Roskilde, Denmark
Pipet tips (10, 20, 100 und 1000µl)	Eppendorf, Hamburg, Germany
Falcon tubes (15 and 50ml)	Corning, New York, USA
Glassware (various)	Schott, Mainz, Germany
Multiwell plates (various sizes)	Corning, New York, USA
Pipettes (stripettes®) (5, 10, 25, 50ml)	Corning, New York, USA
Reaction vessels (1.5 and 2ml)	Eppendorf, Hamburg, Germany
Strip tubes (0.2ml)	Peqlab, Erlangen , Germany
Cell culture flasks T25, T75, T175	Corning, New York, USA
Neubauer hemocytometer	Marienfeld GmbH, Lauda- Königshofen, Germany
Scalpels (no.11)	Pfm, Cologne, Germany

4.3 Laboratory instruments

Heating block:	
Thermomixer comfort	Eppendorf, Hamburg, Germany
PCR-cycler:	
GeneAmp® PCR System 9700	Applied Biosystems, Foster City, USA
Q-PCR- cycler	Roche Applied Science, Mannheim,
LightCycler® 480 System	Germany

Pipettes:	
Eppendorf Research	
(1000, 200, 100, 20, 10, 2µl)	Eppendorf, Hamburg, Germany
Pipette controllers:	
Accu-jet®	Brand, Wertheim, Germany
Shaking devices:	
KS 260 Basic Orbital Shaker	IKA® Werke, Staufen, Germany
Power Supplies:	
Consort E145	Peqlab, Erlangen, Germany
Power Supply-EPS 301	Amersham Biosciences, Munich, Germany
Spectrophotometer:	
EMax® Microplate Reader	MWG Biotech, Ebersberg, Germany
SPECTRAFluor Plus	Tecan, Männedorf, Switzerland
Scale:	
MC1 Laboratory LC 620 D	Sartorius, Göttingen, Germany
Water bath:	
Haake W13/C10	Thermo Fisher Scientific, Karlsruhe, Germany
Centrifuges:	
Biofuge fresco	Heraeus, Hanau, Germany
Megafuge 1.0 R	Heraeus, Hanau, Germany
Microscope:	
Olympus CKX41 with	Olympus Hamburg, Germany
ALTRA20 soft imaging system	
Zeiss Axioskop2 mot plus microscope	Zeiss, Göttingen, Germany
Laminar flow:	Hera Safe, Heraeus, Osterode,
Biosafety Cabinet	Germany
Cell incubator:	Binder, Tuttlingen, Germany
Binder series CB	
UV/VIS spectrophotometer:	Peqlab, Erlangen, Germany
NanoDrop® ND-1000	
XCELLigence system:	Roche Applied Science, Mannheim,
Real- Time Cell Analyzer (RTCA)	Germany

Cell freezing machine:	Air Liquide, Düsseldorf, Germany
Nicool LM 10 freezing machine	

4.4 Buffers

PBS buffer	140mM	NaCl	
	10mM	KCl	
	6.4mM	Na_2HPO_4	
	2mM	KH_2PO_4	pH 7.4
TE buffer	10mM	Tris/HCl	
	1mM	EDTA	pH 8.0
TBS(T)	20mM	Tris	pH 7.4
	150mM	NaCl	
	(0.1% Tween 20®)		

4.5 Plasmids

MTAP	By courtesy of Prof. Bosserhoff (Institute of Pathology, University Hospital Regensburg)
pcDNA3.1	Invitrogen, Karlsruhe, Germany
pGL3	Promega, Mannheim, Germany
pRL-TK	Promega, Mannheim, Germany
NFκB luc	Promega, Mannheim, Germany

4.6 Working with bacteria

4.6.1 Bacterial strains

Top10	Invitrogen, Karlsruhe, Germany

4.6.2 Liquid media and agar plates

LB medium	10 g/L	peptone

	5 g/L	yeast extract
	10 g/L	NaCl
	Suspended in H_2O and autoclaved	
For plates	+ 15 g/L	Agar
For selection	+ 100 µg/ml	Ampicillin

4.6.3 Bacterial culture

E. coli strains were cultivated on solid LB-agar as well as in liquid medium. Ampicillin was added to LB medium for selection of insert-containing clones after transformation. Bacteria were spread out on agar plates using a Drigalski spatula and incubated overnight at 37°C. Liquid cultures were inoculated by a single bacterial colony with a sterile pipette tip and grown overnight at 37°C on a shaking device (250rpm).

4.6.4 Transformation

Top 10 cells were thawed on ice and 100ng plasmid DNA were added. After 30min incubation on ice cells were heat shocked at 42°C for 45s and immediately cooled on ice to enable plasmid DNA entering the cell. Thereafter, 500µl pre-warmed SOC medium was added and the cell suspension was incubated for 1h at 37°C with shaking. Then 50-150µl of the transformation mix were plated and incubated over night at 37°C on LB-agar containing the antibiotic necessary for selection of transformed cells.

4.6.5 Isolation of plasmid DNA (mini and midi preparation)

For mini preparation of plasmid DNA a single E.coli colony was picked and cultured with 3ml LB-selection medium at 37°C over night (250rpm).

To obtain greater amounts of plasmid DNA 50µl of this preculture was added to 50 ml LB-selection medium and incubated again at 37°C over night (250rpm). Then plasmids were isolated using HiSpeed^{TM} Plasmid Midi Kit (Qiagen, Hilden, Germany) following the supplier's instruction. Plasmid DNA was eluated with 500 µl sterile $H_2O_{dest.}$ and stored at -20°C.

4.7 Cell culture

4.7.1 Cell culture medium

DMEM(high glucose/10%FCS)	4.5 g/l	Glucose
	300 µg/ml	L-Glutamine
	supplemented with:	
	10% (v/v)	FCS
	400 U/ml	Penicillin
	50 µg/ml	Streptomycin
HSC medium	DMEM (high glucose/10% FCS)	
	supplemented with:	
	10 µg/ml	Fluconazol
	4 µg/ml	Ciprofloxacin
Freezing medium	5 Vol	DMEM (high glucose/10% FCS)
	3 Vol	FCS
	2 Vol	DMSO

4.7.2 Cultivation of cell lines

Cell culture work was always performed within a laminar flow biosafety cabinet (Hera Safe, Heraeus, Osterode, Germany). Cells were cultivated in a Binder series CB incubator (Binder, Tuttlingen, Germany) in 10% CO_2 atmosphere at 37°C. DMEM medium containing 4.5 g/l glucose and 300 µg/ml L-glutamine supplemented with 10% (v/v) FCS, 400 U/l penicillin and 50 µg/ml streptomycin was used as cell culture medium. For passaging adherent cells were washed with PBS and detached with trypsin (0.05%)/EDTA (0.02%) (PAA Laboratories, Cölbe, Germany) at 37°C. Trypsination was stopped adding DMEM containing 10% FCS. Subsequently, cells were centrifuged at 500g for 5min and the obtained cell pellet was resuspended in fresh culture medium and distributed to new cell culture flasks achieving a cell density thinning factor of 5 to 10. Medium was changed every second day. Cell growth and morphology were controlled and documented with a microscope (Olympus CKX41 with ALTRA20 Soft Imaging System, Olympus, Hamburg, Germany). Cell culture waste was autoclaved before disposal with a Sanoclav autoclave (Wolf, Geislingen, Germany).

4.7.3 Cell line of activated murine hepatic stellate cells

Activated murine hepatic stellate cells have immortalized spontaneously.

4.7.4 Isolation of primary human hepatocytes

Primary human hepatocytes (PHH) were isolated in cooperation with the Center of Liver Cell Research (Department of Paediatrics and Juvenile Medicine, University of Regensburg, Germany) from human liver resections using a modified two-step EGTA/collagenase perfusion procedure (Hellerbrand et. al., 2008; Hellerbrand et al., 2007; Pahernik et al., 1996; Ryan et al., 1993; Weiss et al., 2002). Experimental procedures were performed according to guidelines of the charitable state controlled foundation HTCR, with the informed patient's consent. For cell isolation only tissue which has been classified as not pathological after macroscopical and microscopical investigation was used. All used liver resections have been negatively tested for HBV, HCV and HIV infection. Viability of the isolated hepatocytes was determined by trypan blue exclusion, and cells with viability greater than 85% were used for further tests.

4.7.5 Isolation of hepatic stellate cells

Human hepatic stellate cells (HSCs) were isolated in cooperation with the Center of Liver Cell Research (Department of Paediatrics and Juvenile Medicine, University of Regensburg, Germany). After perfusion and separation of hepatocytes by an initial centrifugation step at 50g (5min, 4°C) the supernatant containing the non-parenchymal cells was centrifuged at 700g for 7min (4°C). The obtained cell pellet was resuspended in HSC medium and cells were seeded into T75 flasks. Within the first week, the medium was replaced daily, from the second week on medium change took place every 2-3 days. Under these conditions only HSCs proliferate. Liver sinusoidal endothelial cells (LSEC) die within the first 24h. By cultivation on uncoated plastic HSCs activate within the first 2 weeks and transdifferentiate to myofibroblast-like cells. Liver disease mediated HSC activation can be simulated *in vitro* that way. After 2 weeks the cell culture was split 1:3 by incubating the cells with Trypsin (0.05%)/EDTA (0.02%) solution. Thereby, only HSCs detach whereas Kupffer cells remain adherent to the plastic surface. Therefore, after the first passage only activated HSCs remain in the cell culture which was confirmed by previously done analysis (Mühlbauer et al. 2006).

Further, isolation of primary murine HSCs was performed on a regular basis within our group from 8-12 weeks old female BALB/c mice (Charles River Labortatories, Sulzfled, Germany) according to procedures described previously (Hellerbrand et al., 1996).

4.7.6 Determination of cell number and viability

Cell number and viability was determined by trypan blue exclusion test. The cell suspension was diluted 1:2 with trypan blue solution (Sigma, Deisenhofen, Germany) and applied on a Neubauer hemocytometer (Marienfeld GmbH, Lauda-Königshofen, Germany). Cell with impaired cell membrane integrity are stained blue, and therefore, can be clearly distinguished from intact cells which appear white under microscopic inspection. The cell number could be calculated after counting cells in all four quadrants of the hemocytometer, each containing sixteen smaller squares, with the following equation:

Cell number/ml = Z x DF x 10^4 ÷ 4

Z: counted cell number

DF: dilution factor (in the described procedure the factor is 2)

The ratio of viable cells could be determined by setting the number of unstained cells in relation to the total cell number (blue and unstained cells).

4.7.7 Freezing cells for storage

To freeze cells for storage, cells were trypsinized, centrifuged and resuspended in 5ml DMEM. Cells were counted, and 1 x 10^6 cells were pipetted in cryotube vials (Nunc, Roskilde, Denmark) and centrifuged again. The supernatant was discarded and the obtained cell pellet was resuspended in 1ml of freezing medium. To gently freeze the cell suspension the temperature was lowered stepwise using a Nicool LM freezing machine (Air Liquide, Düsseldorf, Germany) following the listed program:

Level 4: 30min

Level 8: 30min

Level 10: 30min

Thereafter, the cryotube vials containing the frozen cell suspension were transferred to a liquid nitrogen storage tank.

Thawing of the frozen cell stocks was done quickly with a water bath adjusted to 37°C. The defrosted cell suspension was transferred into 8ml of warm DMEM and centrifuged at 300g for 5minutes. The obtained cell pellet was resuspended in 10ml of warm DMEM and pipetted into a T25 cell culture flask.

4.7.8 Transient siRNA transfection

siRNA and HiPerFect Transfection Reagent® were purchased from Qiagen (Hilden, Germany).

name	target sequence
MTAP siRNA1	CCCGGCGATATTGTCATTATT
MTAP siRNA2	AGGCTGGAATTTGTTACGCAA
All stars negative control siRNA	not disclosed

Transfection of cells was performed according to the manufacturer's fast-forward siRNA transfection protocol.

Shortly before transfection, 2 x 10^5 cells per well were seeded on a 6 well plate in 2,300µl DMEM culture medium containing 10% FCS. 150ng siRNA per well was diluted in 100µl DMEM without FCS and 12µl of HiPerFect Transfection Reagent was added to the diluted siRNA and mixed. The samples were incubated for 10min at room temperature to allow the formation of transfection complexes which were then added drop-wise onto the cells. After 24h cell medium was changed and the cells were grown for another 24- 72h (according to individual experiment set-up). Successful gene silencing was documented on the mRNA and protein levels by quantitative RT-PCR and Western blotting.

4.7.9 Transient plasmid transfection

Lipofectamine method with Lipofectamine™ and PLUS™ reagent (Invitrogen, Karlsruhe, Germany) was used to transfect cells with plasmid DNA.

For transfection 2x10^5 cells per well were seeded on a 6-well plate. After 3h medium was changed and cells are cultivated in DMEM without FCS over night. On the next day medium was again changed to DMEM containing 10% FCS (1ml per well) and after 3h cells transfection mix was added to the cells. Transfection mix was prepared according the manufacturer's instructions containing 0.5µg plasmid DNA per well. Cell medium was changed after incubation over night.

4.7.10 Luciferase reporter gene assay

Regulatory DNA sequences can be examined by using reporter gene analysis. To determine the activity of a promoter, the corresponding DNA fragment containing the promoter region, is cloned into the reporter plasmid pGL3 basic prior to the firefly luciferase gene. Expression of the reporter gene is then proportional to the activation potential of the cloned DNA fragment. By addition of a substrate (luciferin) for the luciferase enzyme chemiluminescence is achieved which can be measured in a luminometer.

Considering different transfection efficiencies in individual experimental assays, cells were cotransfected with an additional vector containing the luciferase gene from Renilla reniformis (pRL-TK). Chemiluminescence of Renilla luciferase was also measured in the luminometer and used for the normalization of the values depending on the transfection efficiency. Dual-Luciferase® Reporter Assay System (Promega, Mannheim, Germany) was used to perform luciferase assays.

2×10^5 cells per well were seeded on a 6-well plate and transfected with 0.5µg NFκB or AP-1 reporter construct or empty control plasmid and pRL-TK using lipofectamine (see 3.7.11). After 24h medium is removed and cells are rinsed twice with water. Subsequently, 300µl lysis buffer are added per well and cells were gently shaked for 20min at room temperature. Then, 50µl of each approach were measured in the luminometer using the provided chemicals in the kit.

4.8 Isolation and analysis of RNA

4.8.1 RNA isolation and determination of RNA concentration

RNA isolation was performed with the RNeasy® mini kit (Qiagen, Hilden, Germany) according to the manufacturer's instructions. The principle of RNA isolation is based on the absorption of RNA to hydrophilic silicon-gel membranes in presence of suitable buffer systems. Biological samples were first lysed and homogenized in the presence of a highly denaturing guanidine isothiocyanate containing buffer, which immediately inactivates RNases to ensure isolation of intact RNA. To homogenize tissue samples a MICCRA D1 homogenizer (ART Prozess- & Labortechnik, Müllheim, Germany) was used.

After lysis, ethanol has been added to provide ideal conditions for the binding of RNA to the silica-gel membranes. Contaminants have been washed away with suitable buffers before RNA was eluted in water and stored at -80°C. The

concentration of RNA was measured with the NanoDrop® ND-1000 UV/VIS spectrophotometer (Peqlab, Erlangen, Germany).

4.8.2 Reverse transcription of RNA to cDNA

Transcription of RNA to complementary DNA (cDNA) was conducted with the Reverse Transcription System Kit (Promega, Mannheim, Germany) which uses avian myeloblastosis virus reverse transcriptase (AMV-RT). The working solution was pipetted with contamination-free aerosol filter pipet tips after the following pipetting scheme:

0.5µg	RNA
4µl	$MgCl_2$ (25mM)
2µl	10x reverse transcription buffer
2µl	dNTP mix (10mM)
1µl	random primer
0.5µl	RNasin ribonuclease inhibitor
0.6µl	AMV RT
ad 25µl	$H_2O_{dest.}$

For reverse transcription samples were incubated in a GeneAmp® PCR cycler (Applied Biosystems, Foster City, USA) for 30min at 42°C. For denaturation of the AMV RT the temperature was raised to 99°C for 5min. After cooling down to 4°C the obtained cDNA was diluted with 75µl $H_2O_{dest.}$ and used immediately or stored at -20°C.

4.8.3 Quantitative real time polymerase chain reaction

To quantify the expression of specific mRNA, quantitative real time polymerase chain reaction (qRT-PCR) was performed with the LightCycler® 480 System (Roche Diagnosics, Mannheim, Germany). The qRT-PCR is principally based on a conventional polymerase chain reaction (PCR), but offers the additional possibility of quantification, which is accomplished by fluorescence measurements at the end and/or during a PCR cycle. As fluorescent reagent SYBR® Green (SensiFAST™ SYBR No-ROX Kit, Bioline, Luckenwalde, Germany) was used. SYBR® Green intercalates with double-stranded DNA whereby the fluorescence emission rises significantly. Therefore, the fluorescence signal increases proportionally with the amount of PCR products. To quantify the expression of a specific gene of interest, the results were normalized to housekeeper 18S mRNA. The results were

evaluated with the LightCycler® 480 software release 1.5.0 SP4 following the manufacturer's instructions. qRT-PCR was performed according following protocol:

2.5µl	$H_2O_{dest.}$
0.25µl	forward primer (20µM)
0.25µl	reverse primer (20µM)
5µl	SYBR® Green

Following standard scheme was used and adapted to particular primer melting point temperature:

Initial denaturation:	95°C	2min
Two step PCR (45 cycles):	95°C	5s
	60°C	18s
Analysis of melting curve:	95°C	5s
	65°C	1min
	97°C	0sec

For validation, after qRT-PCR, PCR product was mixed with loading buffer (Peqlab, Erlangen, Germany) and loaded on a agarose gel with ROTI safe (50 µg/100ml gel) to determine the PCR product length. Each experimental condition was performed in triplicates and experiments were repeated at least three times.

Table 1 Sets of used forward and reverse primers for qRT-PCR, species: mouse or human

name	forward primer	reverse primer
18s	5' AAACGGCTACCACATCCAAG	5' CCTCCAATGGATCCTCGTTA
human α-sma	5' CGTGGCTATTCCTTCGTTAC	5' TGCCAGCAGACTCCATCC
human BAX	5' GGCCCACCAGCTCTGAGCAGA	5' GCCACGTGGGCGTCCCAAAGT
human BclXl	5' GCGGATTTGAATCTCTTTCTC	5' CACTAAACTGACTCCAGCTG
human Coll I	5' CGGCTCCTGCTCCTCTT	5' GGGGCAGTTCTTGGTCTC
human MTAP	5' GCGAACATCTGGGCTTTG	5' GCACCGGAGTCCTAGCTTC
human survivin	5' AGTGAGGGAGGAAGAAGGCA	5' ATTCACTGTGGAAGGCTCTGC
human XIAP	QIAGEN QuantiTect Primer Assay	
murine α-sma	QIAGEN QuantiTect Primer Assay	
murine BAX	5' TGCAGAGGATGATTGCTGAC	5' GATCAGCTCGGGCACTTTAG
murine BclXl	QIAGEN QuantiTect Primer Assay	
murine CCl2	5' TGGGCCTGCTGTTCACA	5' TCCGATCCAGGTTTTTAATGTA
murine CCl5	QIAGEN QuantiTect Primer Assay	
murine Coll I	5' CGG GCA GGA CTT GGG TA	5' CGG AAT CTG AAT GGT CTG ACT

murine HMOX	5’ CACGCATATACCCGCTACCT	5’ CCAGAGTGTTCATTCGAGCA
murine MTAP	5’ CGGTGAAGATTGGAATAATTGG	5’ ATGTTTGCCTGGTAGTTGAC
murine p47phox	QIAGEN QuantiTect Primer Assay	
murine survivin	5’ GTACCTCAAGAACTACCGCA	5’ TCTATGCTCCTCTATCGGGT
murine XIAP	QIAGEN QuantiTect Primer Assay	

Primers were synthesized by SIGMA Genosys (Hamburg, Germany) or purchased as QuantiTect Primer Assays from Qiagen (Hilden, Germany). The lyophilized primers were solved in $H_2O_{dest.}$ or TE buffer (QuantiTect Primer Assays), respectively, and stored at -20°C.

4.9 Protein analysis

4.9.1 Preparation of protein extracts

To extract whole cell protein from cell lines, cultivated in 6-well plates the cell culture medium was discarded and cells were washed once with PBS, then scraped off with a cell scraper (Corning, New York, USA) and taken up into 350µl cell lysis buffer (Cell Signaling Technology, Boston, USA) supplemented with 1mM PMSF and a protease inhibitor cocktail (cOmplete Mini Protease Inhibitor Cocktail Tablets from Roche Diagnostics, Mannheim, Germany). Liver tissue extracts were obtained by homogenization of snap-frozen liver tissue in cell lysis buffer containing 1mM PMSF and protease inhibitors using a MICCRA D1 homogenizer (ART Prozess- & Labortechnik, Müllheim, Germany). Subsequently, probes were treated with an ultrasonoscope (Sonoplus hp 70, Bandelin electronics, Berlin, Germany) 5 x 3s at an intensity of 70% for cell lysis. Subsequently, the solved proteins were separated from the non-soluble cell components by centrifugation at 20.000g (15min, 4°C). The protein solution was transferred into new reaction tubes and stored at -20°C.

4.9.2 Determination of protein concentration

To determine the protein concentrations of protein solutions the BCA^{TM} Protein Assay Kit (Pierce, Rockford, USA) was used. The assay combines the reduction of Cu^{2+} to Cu^{1+} by protein in an alkaline medium with the highly sensitive and selective colorimetric detection of the cuprous cation Cu^{1+} by bicinchoninic acid (BCA). The first step is the chelation of copper with protein in an alkaline

environment to form a blue-colored complex. In this reaction, known as biuret reaction, peptides containing three or more amino acid residues form a colored chelate complex with cupric ions in an alkaline environment. One cupric ion forms a colored coordination complex with four to six nearby peptides bound. In the second step of the color development reaction, BCA, a highly sensitive and selective colorimetric detection reagent reacts with the cuprous cation Cu^{1+} that was formed in step 1. The purple-colored reaction product is formed by the chelation of two molecules of BCA with one cuprous ion. The BCA/copper complex is water-soluble and exhibits a strong linear absorbance at 562 nm with increasing protein concentrations. 200µl of alkaline BCA/copper(II) solution (50 parts of solution A mixed with 1 part of solution B) was added to 2µl of protein solution using a 96-well plate and were incubated for 15min at 37°C. Thereafter the purple color was measured at 562 nm with a spectrophotometer (EMax® Microplate Reader, MWG Biotech, Ebersberg, Germany). The optical absorbance values could be translated into specific protein concentrations by parallel quantification of a BSA standard.

4.9.3 SDS polyacrylamid gel electrophoresis (SDS-PAGE)

Used buffers:

Laemmli buffer	62.5mM	Tris/HCl; pH6.8
	2% (w/v)	SDS
	10% (v/v)	Glycerine
	5% (v/v)	β-Mercaptoethanol
Running buffer	25mM	Tris/HCl; pH8.5
	200mM	Glycine
	0.1% (w/v)	SDS
10% Resolving gel	7.9ml	$H_2O_{dest.}$
	5.0ml	1.5 M Tris/HCl; pH8.8
	0.2ml	10% (w/v) SDS
	6.7ml	Acrylamide/Bisacrylamid 30%/0.8% (w/v)
	0.2ml	Ammonium persulfate 10% (w/v)
	0.008ml	TEMED

5% Stacking gel	2.7ml	$H_2O_{dest.}$
	0.5ml	1.0 M Tris/HCl; pH6.8
	0.04ml	10% (w/v) SDS
	0.67ml	Acrylamide/Bisacrylamid 30%/0.8% (w/v)
	0.04ml	Ammonium persulfate 10% (w/v)
	0.004ml	TEMED

The protein solutions were heated at 95°C for 5min in Laemmli buffer and applied on a SDS polyacrylamid gel for protein fractionation by size at 35mA/150V (XCell SureLock™ Mini-Cell, Invitrogen, Karlsruhe, Germany). As size marker HiMark™ Pre-Stained High Molecular Weight Protein Standard (Invitrogen, Karlsruhe Germany) and peqGOLD Protein-Marker V (Peqlab, Erlangen, Germany) were used.

4.9.4 Western Blotting

Used buffers:

Standard transfer buffer	10% (v/v)	Methanol
	25mM	Tris
	190mM	Glycine

To detect the proteins after SDS-PAGE by use of specific antibodies proteins were transferred electrophoretically to a nitrocellulose membrane (Invitrogen, Karlsruhe, Germany) at 220mA/300 V for 1.5h (XCell II Blot Module, Invitrogen, Karlsruhe, Germany). To block unspecific binding sites, the membrane was bathed in TBST containing 5% BSA or 5% milk powder for 1h at RT. Then, the membrane was incubated with a specific primary antibody (Table 2) over night at 4°C. After washing with TBST, the membrane was incubated with a secondary horseradish peroxidase (HRP) conjugated antibody for 1h at RT. Thereafter, the membrane was washed and incubated with ImmunStar™ WesternC™ Kit (BioRad, München, Germany) for 3min. This system utilizes chemiluminescence, which was detected by the ChemiDoc XRS (BioRad, München, Germany) imaging system.

Table 2 Antibodies used for Western Blot, immunohistochemistry and Western Blot

Primary antibodies		
Antibody	Dilution	Company
Actin	1:20000	Biomol, Hamburg, Germany

αsma	1:200	Abcam, Cambridge, UK
MTAP	1:500	Abcam, Cambridge, UK
survivin	1:1000	Abcam, Cambridge, UK
phospho IκBα	1:1000	Cell signaling, Danvers, USA
phospho p65	1:1000	Cell signaling, Danvers, USA
Secondary antibodies		
anti rabbit Cy2	1:400	Dianova, Hamburg, Germany
anti mouse TRITC	1:400	Dianova, Hamburg, Germany
anti mouse HRP	1:3000	Santa Cruz, Heidelberg, Germany
anti rabbit HRP	1:3000	Santa Cruz, Heidelberg, Germany

4.9.5 Quantification of caspase-3/7 activity

Caspases, or cysteine-aspartic acid proteases, are a family of cysteine proteases, which play essential roles in apoptosis. There are two types of apoptotic caspases: initiator (apical) caspases and effector (executioner) caspases. Initiator caspases (*e.g.* caspase-2, -8, -9, -10) cleave inactive pro-forms of effector caspases, thereby activating them. Effector caspases (*e.g.* caspase-3, -6, -7) in turn cleave other protein substrates within the cell, to trigger the apoptotic process. To analyze caspase-3/7 activity we used the Apo-One Homogeneous Caspase-3/7 Assay Kit (Promega, Mannheim, Germany) according to the manufacturer's instructions. We used 6000 cells/well (96-well plate) and incubated cells with the provided caspase substrate Z-DEVD-R110 for 1h. Cleavage of the non-fluorescent caspase substrate Z-DEVD-R110 by caspase-3/7 liberates the fluorescent rhodamine 110, which was detected fluoro-spectrometrically with a SPECTRAFluor Plus microplate reader (Tecan, Männedorf, Switzerland) at wavelengths of 485nm (excitation) and 520nm (emission). Each experimental condition was performed in triplicates and experiments were repeated at least twice.

4.9.6 5'-deoxy-5'-(methylthio)adenosine (MTA) extraction and analysis

Medium was collected, centrifuged, and the supernatant was snap-frozen and stored at -80°C. Further, cell number in corresponding cell culture plates was determined by counting trypsinised cells. For intracellular MTA measurements, cells were harvested by incubation in a solution containing 0.05% (w/v) trypsin and

0.02% (w/v) EDTA. Trypsination was stopped after 5min with cell culture medium. Following centrifugation, the supernatant was removed, the cell pellet was washed with PBS, centrifuged again, snap-frozen and stored at -80°C. Samples were further processed by the Institute of Functional Genomics, University of Regensburg, as described in greater detail in (Stevens et al., 2010; Stevens et al., 2008). Briefly, cell culture medium was spiked with stable isotope labeled MTA, dried by means of an infrared evaporator, and the residues reconstituted in 0.1mol/l acetic acid. Frozen cell pellets were extracted by three repeated freeze/thaw cycles in 600µl of MeOH / 0.1mol/l acetic acid (80:20, v/v) after the addition of stable isotope labeled MTA. After centrifugation the supernatant was transferred in a glass vial and the protein pellet was washed twice with MeOH/acetic acid. The combined extracts were dried and reconstituted in 0.1mol/l acetic acid. Tissue samples were weighed and then homogenized in 600µl of MeOH/ 0.1mol/l aqueous acetic acid (80:20, v/v) using “Precelly-Keramik-Kit 1.4mm” vials (Peqlab Biotechnologie GmbH, Erlangen, Germany). The samples were centrifuged at 9.000g for 5min at 4°C. Subsequently, the supernatant was transferred to a 1.5ml glass vial and the pellet was washed twice. After solvent evaporation, the residues were reconstituted in 0.1mol/l acetic acid. Liquid chromatography-electrospray ionization-tandem mass spectrometry (LC-ESI-MS/MS) was carried out as described (Stevens et al., 2010). The analysis was performed using an Agilent 1200 SL HPLC system (Böblingen, Germany) and a PE Sciex API 4000 QTrap mass spectrometer (Applied Biosystems, Darmstadt, Germany). An Atlantis T3 3µm (2.1mm i.d.×150mm) reversed-phase column (Waters, Eschborn, Germany) was used. LC separation was carried out using a water-acetonitrile gradient consisting of 0.1% acetic acid and 0.025% HFBA in both solvents at a flow-rate of 400µl/min with an injection volume of 10µl. The API 4000 QTrap mass spectrometer was operated in positive mode and quantitative determination was performed with multiple reaction monitoring (MRM).

4.10 Flow cytometry

4.10.1 Annexin V / Propidium iodide double staining

At early stages of apoptosis cells change the structure of their membrane, which leads to the exposure of phosphatidylserine on the membrane surface. In living cells, phosphatidylserine is transported to the inside of the lipid bilayer by the

aminophospholipid translocase, a Mg^{2+} ATP dependent enzyme. At the onset of apoptosis, phosphatidylserine is translocated to the external membrane and serves as a recognition signal for phagocytes.

Annexins are ubiquitous homologous proteins that bind phospholipids in the presence of calcium. Since the redistribution of phosphatidylserine from the internal to the external membrane surface represents an early indicator of apoptosis, Annexin V and its conjugates can be used for the detection of apoptosis because they interact strongly and specifically with exposed phosphatidylserine.

The differentiation between apoptotic and necrotic cells can be performed by simultaneous staining with propidium iodide (PI), a dye that stains by intercalating into nucleic acid molecules. The cell membrane integrity excludes PI in viable cells, whereas necrotic cells are permeable to PI. Thus, dual parameter flow cytometric analysis allows for the discrimination between viable, early apoptotic and late apoptotic/necrotic cells.

To quantify apoptotic cells we used the Annexin V-FITC Detection Kit (PromoKine, Heidelberg, Germany). Therefore, we resuspended 2 x 10^5 cells in 500µl of the provided binding buffer and added 5µl of the FITC-labeled Annexin V reagent and 5µl of PI solution. After incubation for 5min at room temperature in the dark flow cytometric analysis was performed. The FITC-Annexin V signal was detected at a wavelength of 525 ± 12.5nm, the PI signal at a wavelength of 620 ± 12.5nm. The result of the dual parameter flow cytometric analysis were depicted as dotplot and evaluated by quadrant analysis. The y-axis of the dotplot shows PI fluorescent signal intensity, the x-axis FITC-Annexin V fluorescent signal intensity. Discrimination of viable, early apoptotic and late apoptotic/necrotic cells were done by means of different intensities of FITC-Annexin V of PI fluorescent signals. Viable cells show low FITC-Annexin V and PI fluorescence (lower left quadrant), early apoptotic cells show high FITC-Annexin V but low PI fluorescence (lower right quadrant) and late apoptotic/necrotic cells show both high FITC-Annexin V and PI fluorescence (upper right quadrant).

To asses the effects of a specific apoptosis or necrosis inducing reagent the percental distribution of viable, early apoptotic and late apoptotic/necrotic cells related to the total of counted cell (10^4 cells) were calculated.

4.11 Measurement of reactive oxygen formation (ROS)

Reactive oxygen species (ROS) formation was analyzed with an assays applying cell-permeant 2',7'-dichlorodihydrofluorescein diacetate (H2DCFDA) according to the manufacturer's instructions (Invitrogen). Briefly, cells were incubated with H2DCFDA at a concentration of 100µM for 30min at 37°C, and after washing with PBS, ROS formation was detected using a multi-well fluorescence plate reader (Spectra Fuor Plus, Tecan, Männedorf, Switzerland) with excitation and emission filters of 485 and 535nm, respectively.

4.12 Animal experiments

4.12.1 BDL

Experimental cholestasis induced by bile duct ligation (BDL) is a commonly used model of liver injury. BDL or sham surgeries were performed in 5 female C57Bl/6 mice each as described (Gabele et al., 2009). After midline laparotomy the common bile duct was exposed and ligated. Then, the abdomen was closed again in layers. After 3 weeks, blood and livers were collected for further analysis.

4.12.2 NASH

Male BALB/c mice were purchased at 6 weeks of age, divided into two groups (n=5 each) and fed either with control diet or a non-alcoholic steatohepatitis (NASH) inducing high fat diet containing 30% lard, 1.25% cholesterol and 0.5% sodium cholate (Matsuzawa et al., 2007). After 30 weeks feeding animals were sacrificed and liver tissue was immediately frozen.

4.13 Histology and Immunohistochemistry

For histological and immunohistochemical analysis tissue was fixed for 24h in buffered formaldehyde solution (3.7% in PBS) at room temperature, dehydrated by graded ethanol and embedded in paraffin. Sections were cut at 5µm and stuck on glass slides.

4.13.1 Histology and Immunohistochemistry

Human liver biopsies were collected in the Molecular Pathology of the University Hospital Regensburg. The formalin-fixed and paraffin-embedded biopsies were dewaxed and rehydrated. The biopsies were then boiled for 30min in citrate buffer

(pH 6.0). Endogenous peroxidase activity was blocked in 3% v/v H_2O_2 in PBS for 10min. The sections were placed in a humidified chamber and covered with blocking solution (Zytomed, Berlin, Germany) for 5min. Sections were incubated with primary anti-MTAP antibody in a 1:200 dilution in TBS–Tween (0.1% v/v) overnight at 4°C. After washing with TBS–Tween, sections were incubated with biotinylated secondary antibody for 20min (Zytomed), before incubation with Streptavidine-HRP conjugate for 20min and AEC (3-amino-9-ethylcarbazole) for 30min (Zytomed) according to the manufacturers' instructions.

Deparaffinized sections were blocked with 1%BSA/PBS and incubated with anti MTAP and anti αsma antibody in 10% FCS and 1%BSA/PBS. After washing sections were incubated with Cy2- and TRITC conjugated secondary antibodies and a DAPI staining was performed to identify cellular nuclei. Images were collected by fluorescence microscopy using a Zeiss Axioskop2 mot plus microscope (Zeiss, Göttingen, Germany).

4.13.2 Immunofluorescent cell staining

For immunofluorescence analysis, 2 x 10^4 cells were seeded in permanox coated 4-well chamber slides (Thermo Fisher Scientific, Karlsruhe, Germany) and cultured overnight. The following day, cells were fixed. Subsequently, cells were washed with PBS and fixed using 4% paraformaldehyd for 5 minutes. For permeabilization of cell membranes, 0.1% Triton X-100 (Sigma-Aldrich, Munich, Germany) was added for 15minutes. After two washing steps with PBS, a blocking solution (PBS and 5% BSA, w/v) was added for 30 ,minutes. Thereafter, cells were incubated with a MTAP antibody overnight at 4°C. Next day, cells were washed three times with PBS, followed by incubation with the secondary antibody (Invitrogen, Carlsbad, USA) for 1h. After extensively washing, hard set mounting medium including DAPI (Vector Laboratories, Burlingame, USA) was added and images were collected by fluorescence microscopy using a Zeiss Axioskop2 mot plus microscope (Zeiss, Göttingen, Germany).

4.14 Statistical analysis

Values are presented as mean ± SEM or mean ± SD as indicated. All experiments were repeated at least three times. Comparison between groups was made using the Student's unpaired t-test. A p-value < 0.05 was considered statistically significant. Correlations were performed applying Pearson test. All calculations

were performed using the statistical computer package GraphPad Prism version 4.00 for Windows (GraphPad Software, San Diego, CA, USA).

5 Results

Our group could show that MTAP is downregulated in HCC and this downregulation results in an accumulation of the substrate MTA (Kirovski et al., 2011). Further, in earlier studies we investigated the regulation of decreased MTAP expression in HCC which was mediated via hypermethylation of the MTAP promoter (Hellerbrand et al., 2006). Establishment of chronic liver disease can be seen as a deciding risk factor for developing HCC (Hernandez-Gea et al., 2013; White et al., 2012; Zhang and Friedman, 2012) so we wanted to unravel the role of MTAP in the progression of chronic liver disease.

5.1 Expression and function of MTAP in chronic liver disease

5.1.1 MTAP expression in chronic liver disease

First, we analyzed hepatic tissue from patients with alcoholic liver disease and chronic viral infection and found significant lower MTAP mRNA and protein expression in liver cirrhosis compared to normal liver tissue (**Figure 5.1**).

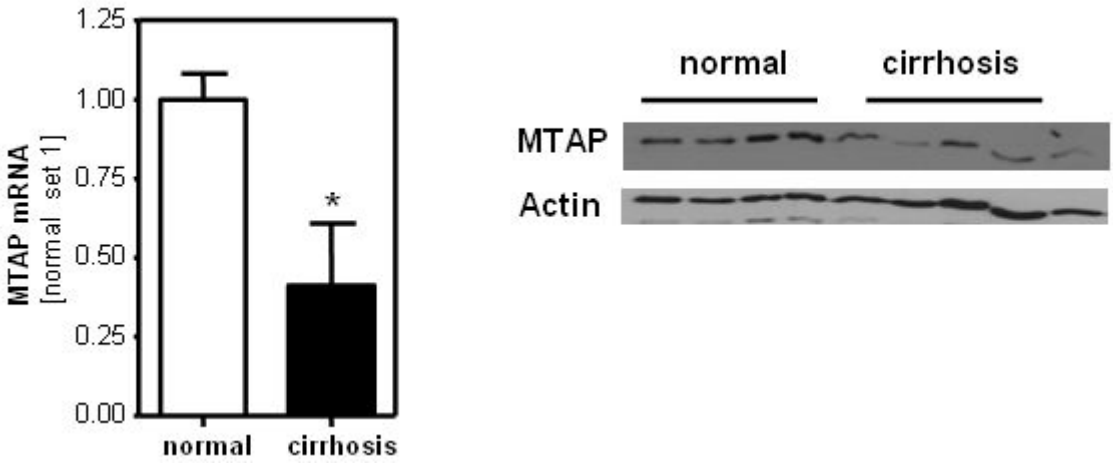

Figure 5.1 Analysis of MTAP mRNA and protein expression in normal (n=5) and cirrhotic (n=5) liver tissue by means of pRT-PCR and Western Blot. Actin served as loading control. (*p<0.05)

In line with the downregulation of MTAP, which catalyzes the phosphorylation of MTA, hepatic levels of this metabolite were significantly higher in cirrhotic compared to normal human liver tissue (**Figure 5.2**).

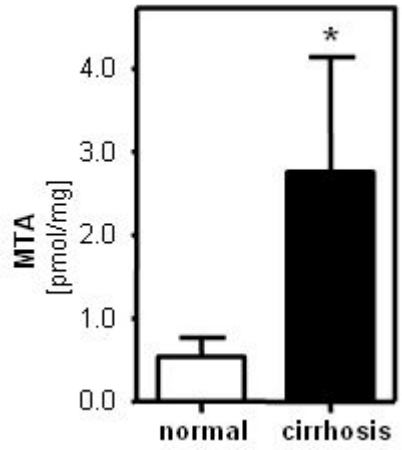

Figure 5.2 Hepatic MTA levels of tissue of normal versus cirrhotic origin were determined by LC-ESI-MS/MS. (*p<0.05)

5.1.2 MTAP expression in non-alcoholic steatohepatitis (NASH)

Next, we assessed patients with non-alcoholic steatohepatitis (NASH), in which fibrosis was less advanced. Although MTAP mRNA and protein expression were similar as in normal hepatic tissue (**Figure 5.3**), MTA levels were significantly higher (**Figure 5.4**).

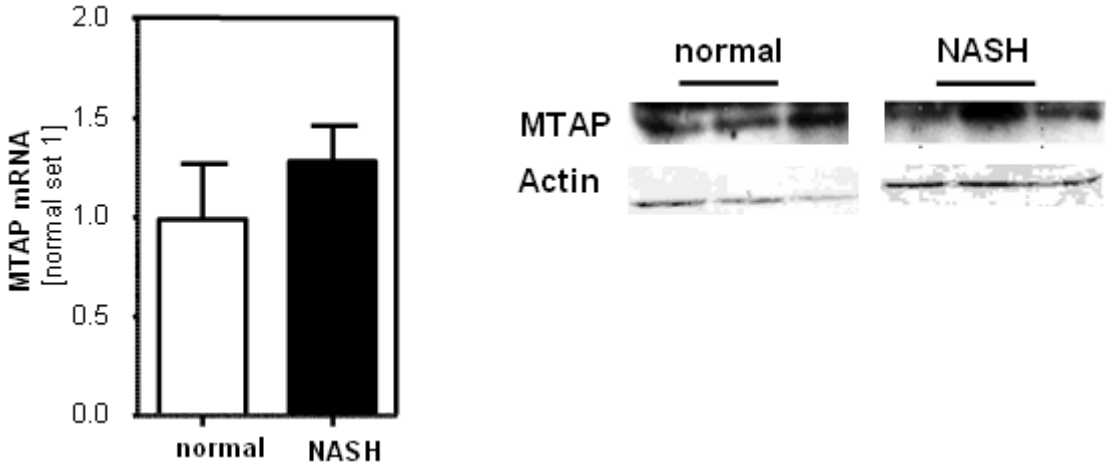

Figure 5.3 Hepatic MTAP mRNA and protein levels of tissue of normal and NASH origin measured by pRT-PCR and Western Blot. Actin served as control for equal protein loading.

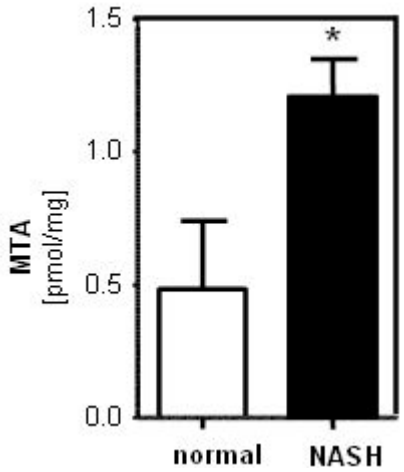

Figure 5.4 Hepatic MTA levels of hepatic tissue of normal and NASH origin by LC-ESI-MS/MS. (*p<0.05)

To verify these findings in experimental models of chronic hepatic injury, we analyzed MTAP expression in mice subjected to three weeks bile duct ligation (BDL) or fed with a NASH-inducing diet for 30 weeks. Similar as in human cirrhosis, MTAP mRNA and protein expression were significantly reduced in the BDL model (**Figure 5.5**).

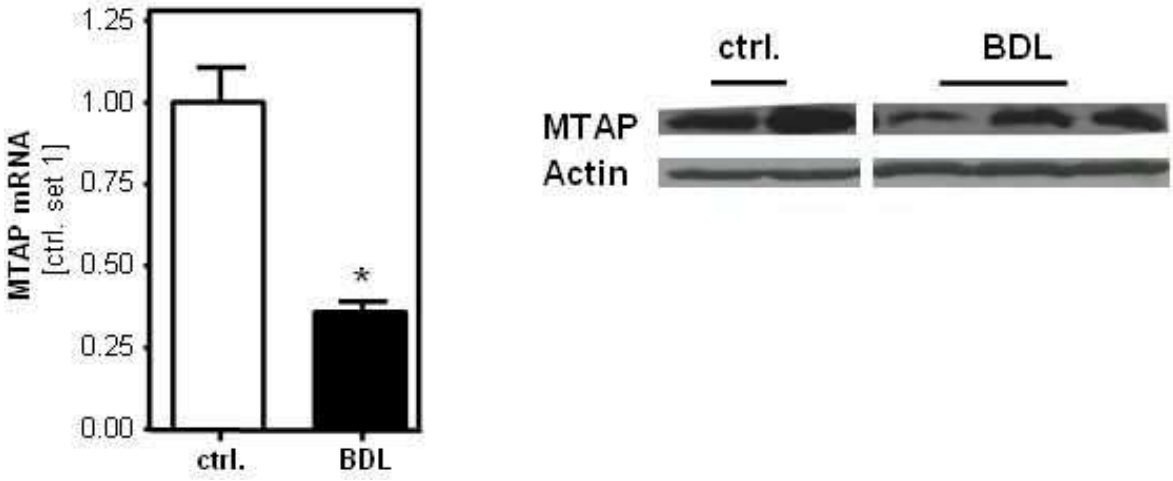

Figure 5.5 MTAP mRNA and protein expression in mice subjected to BDL (n=5) and control mice (n=5). (*p<0.05)

In murine NASH-livers MTAP expression was neither affected on mRNA nor on protein level (**Figure 5.6**). However, hepatic MTA levels were significantly higher in murine NASH livers (**Figure 5.7**) paralleling the findings in human NASH.

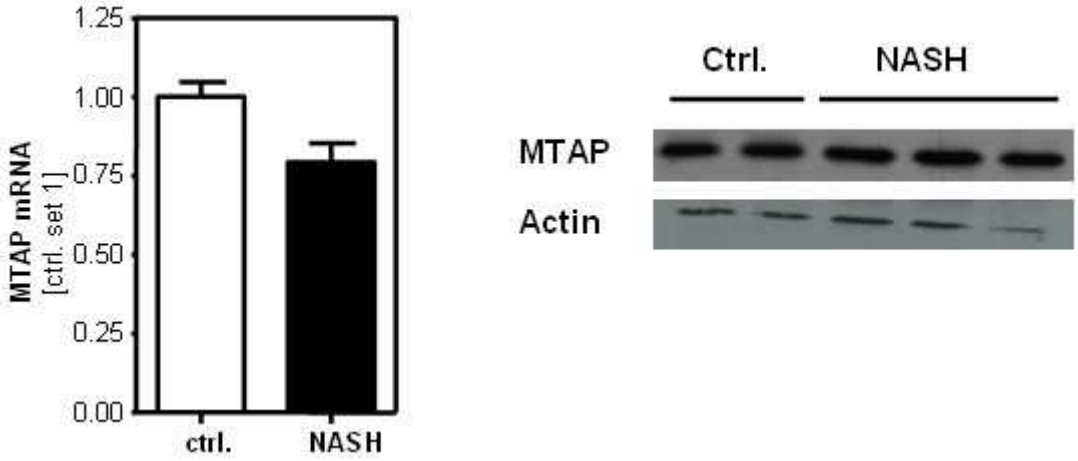

Figure 5.6 MTAP mRNA and protein expression in mice which were fed a NASH inducing diet (n=5) versus control mice (n=5).

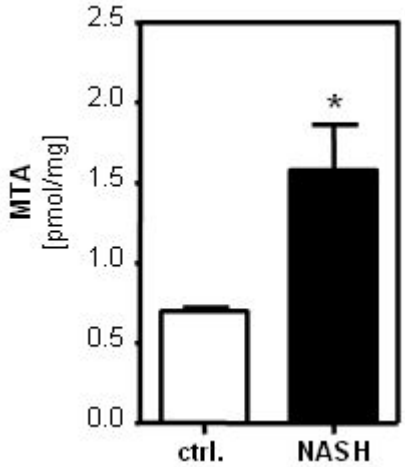

Figure 5.7 Hepatic MTA levels in mice which were fed a NASH inducing diet versus control mice. (*p<0.05)

5.2 MTAP expression in hepatic stellate cells

Immunohistochemical analysis revealed reduced MTAP expression in hepatocytes in both human cirrhotic liver tissue (**Figure 5.8 II**) and murine BDL-livers (**Figure 5.9**). In contrast, myofibroblast-like cells in fibrotic septa showed a strong MTAP immunosignal (**Figure 5.8 panel III**).

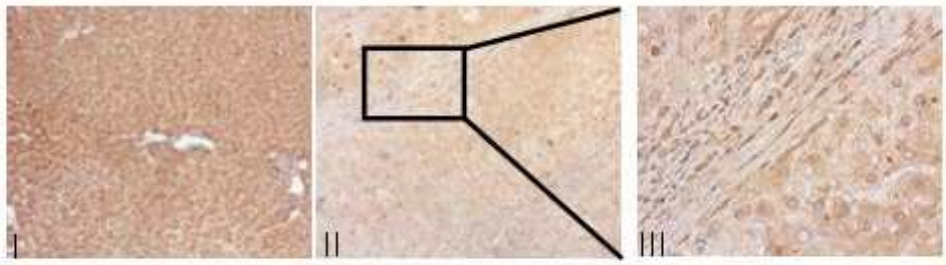

Figure 5.8 Immunohistochemical analysis of MTAP in ctrl. (panel I) and cirrhotic (II, III) human liver tissue (Magnifications I (200x) and II (400x)). Myofibroblast like cells in fibrotic septa revealed a strong MTAP immunosignal (III).

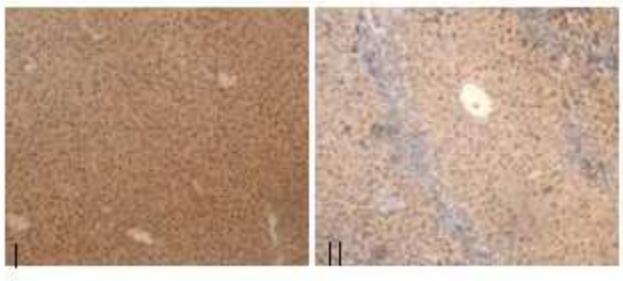

Figure 5.9 Immunohistochemical analysis of MTAP in ctrl. (panel I) and fibrotic (II) murine liver tissue (Magnification 200x).

Also *in vitro* activated hepatic stellate cells (HSCs) revealed higher MTAP expression than primary human hepatocytes (PHHs) (**Figure 5.10**). Still, hepatocytes constitute the bulk mass of hepatic cells in healthy as well as in diseased livers, and thus, reduced MTAP expression in these cells likely accounts for reduced MTAP levels observed in fibrotic liver tissues. Furthermore, lowered MTAP in hepatocytes appeared as one probable reason for increased MTA levels in diseased livers.

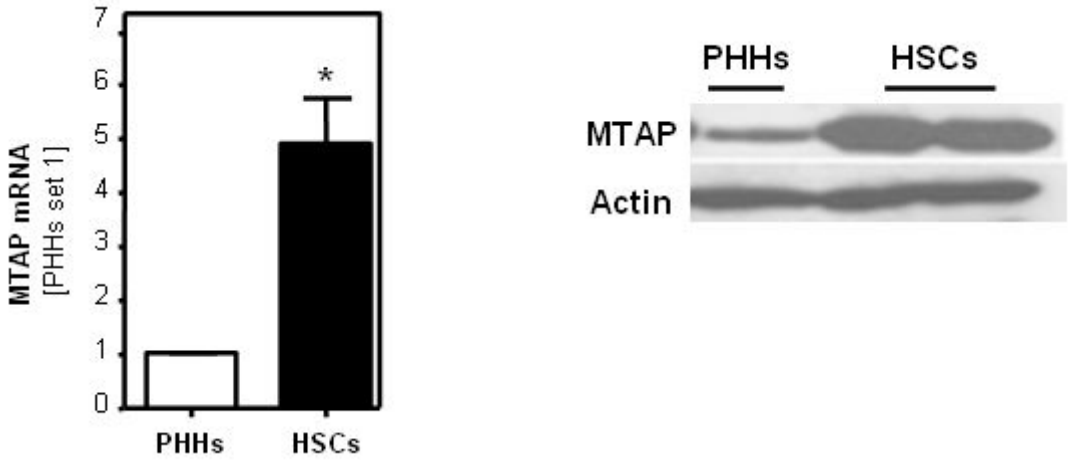

Figure 5.10: Measurement of MTAP mRNA and protein levels in primary human hepatocytes (PHHs) and activated HSCs. In Western Blot analysis actin was used to demonstrate equal protein loading. (*p<0.05)

However, MTA levels were strikingly higher in activated HSCs compared to PHHs *in vitro* (**Figure 5.11**), and MTA levels correlated significantly with collagen I mRNA expression in diseased human liver tissue (**Figure 5.12**).

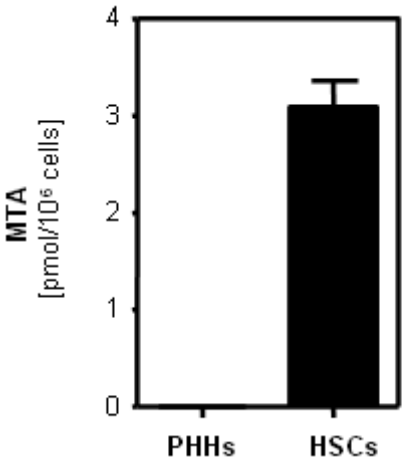

Figure 5.11: Measurement of intracellular MTA with LC-ESI-MS/MS in primary human hepatocytes (PHHs) and activated HSCs.

Further, we could show a colocalization of MTAP and αsma in hepatic sections of fibrotic liver tissue (**Figure 5.13**). As described in chapter 3.2, hepatic stellate cells express collagen I and αsma which can be considered markers of fibrosis.

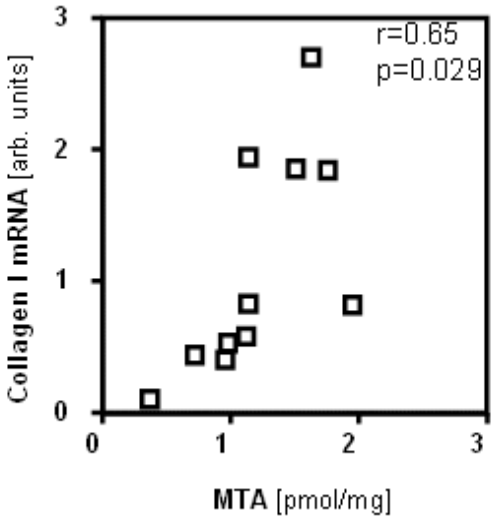

Figure 5.12 Correlation of hepatic MTA content, measured with LC-ESI-MS/MS and hepatic Collagen I expression measured with pRT-PCR.

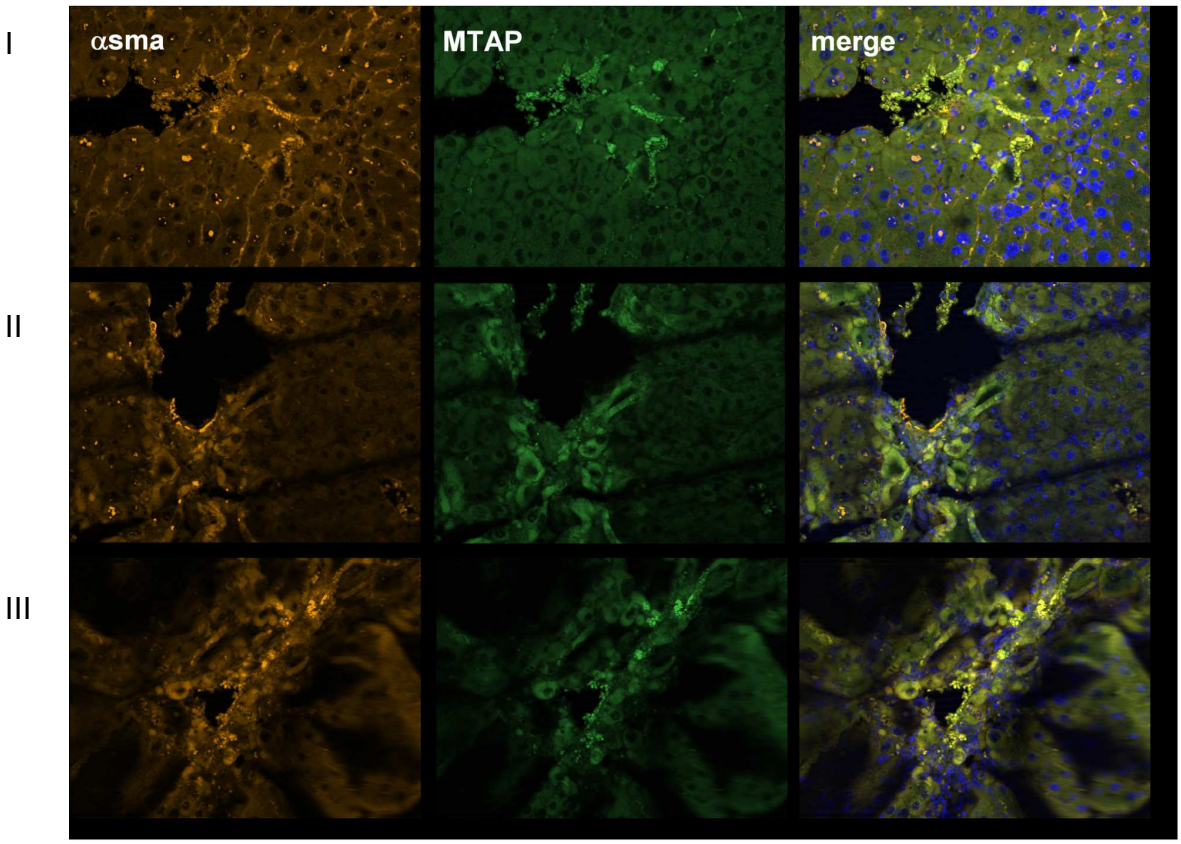

Figure 5.13 Immunofluorescent staining of αsma (red) and MTAP (green) and αsma and MTAP (merge) in fibrotic murine livers. Dapi staining (blue) identifies cellular nuclei. (Magnifications: I (x200), II (x400), III (x800))

Together these findings indicated that activated HSCs significantly contribute to elevated MTA levels and MTAP expression in diseased livers. Higher expression of both MTAP expression and MTA levels in activated HSCs compared to hepatocytes might be explained by a generally more active methionine and adenine salvage pathway in response to high proliferation and cellular transdifferentiation in activated HSCs. Furthermore, these findings may explain the observed increase in MTA levels in murine and human NASH tissues despite unaltered MTAP expression (**Figure 5.3, Figure 5.4, Figure 5.6, Figure 5.7**).

5.3 Functional role of MTAP in activated hepatic stellate cells

5.3.1 Functional role of MTAP suppression

To get an insight into the functional role of MTAP in HSCs, we transiently transfected activated HSCs with siRNA directed against MTAP, which led to significantly reduced MTAP mRNA and protein expression compared to HSCs transfected with control siRNA (**Figure 5.14**).

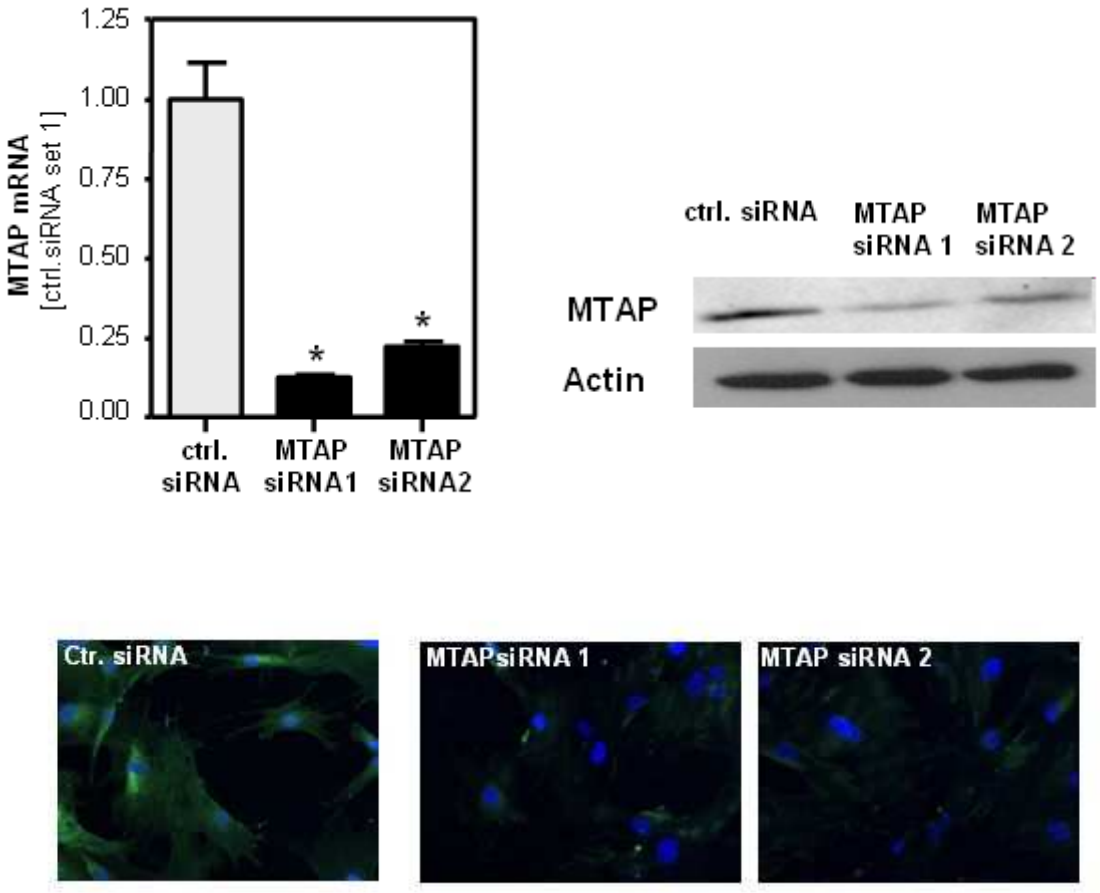

Figure 5.14 Activated HSCs were transfected with siRNA against MTAP (siRNA1 and siRNA2) or control siRNA. Analysis of MTAP downregulation on mRNA by pRT-PCR and protein level in MTAP siRNA treated activated HSCs via Western Blot and immunofluorescence. Actin staining confirms equal loading in Western Blot. Immunofluorescent staining of MTAP protein (green) in MTAP siRNA transfected HSCs, DAPI identified cellular nuclei (blue). (*p<0.05)

Furthermore, MTAP suppression led to increased MTA levels in activated HSCs (**Figure 5.15**).

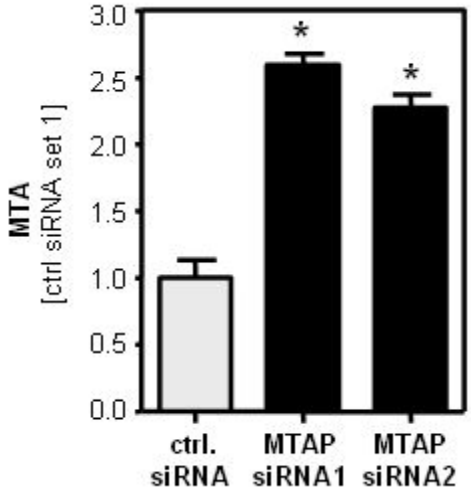

Figure 5.15 Analysis of intracellular MTA in activated HSCs treated with MTAP siRNA by means of LC-ESI-MS/MS. (*p<0.05)

We have previously shown that MTA affects NFκB activity in hepatocellular carcinoma (Kirovski et al., 2011), and thus, we assessed whether this signaling pathway is also affected by MTA in activated HSCs. MTAP suppressed HSCs revealed higher levels of phosphorylated p65 (**Figure 5.16 A**) indicative of increased NFκB activation. Further, a NFκB reporter gene assay (**Figure 5.16 B**) revealed increased NFκB activity in MTAP suppressed cells.

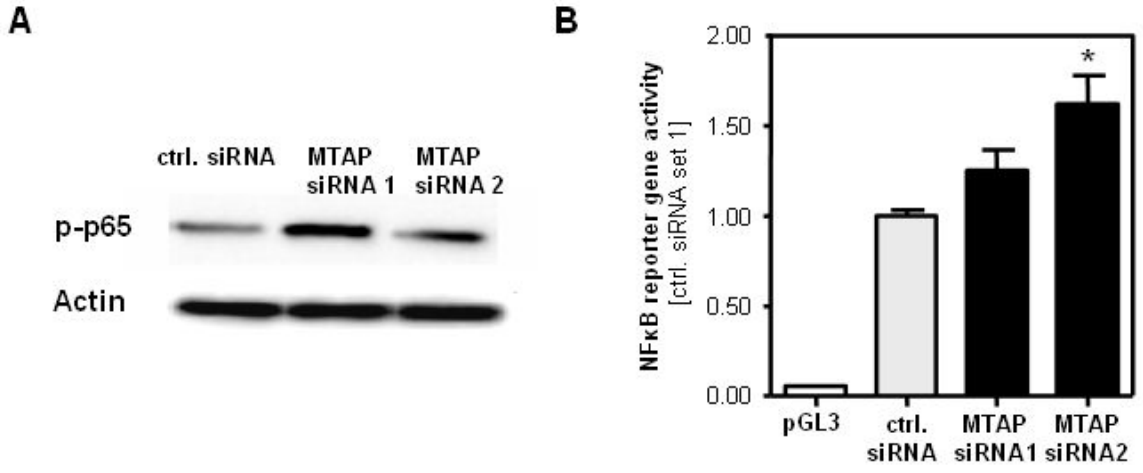

Figure 5.16 Effect of MTAP suppression on NFκB signaling: phospho p65 (A). Actin demonstrated equal protein loading. NFκB reporter gene assay (pGL3: empty vector) (B). (*p<0.05)

The NFκB signaling pathway is increased during the activation of HSCs and protects these cells from apoptosis (Elsharkawy et al., 2005; Hellerbrand et al., 1998). Consequently, analysis of caspase3/7 activity (**Figure 5.17 A**) and FACS analysis (**Figure 5.17 B**) revealed that HSCs with suppressed MTAP expression were less susceptible for staurosporine (STS) induced apoptosis compared to control siRNA transfected cells.

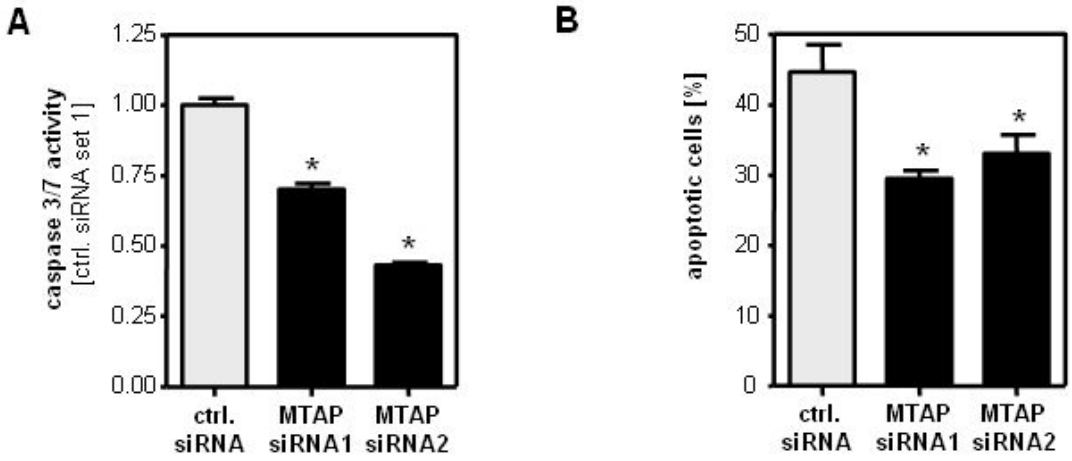

Figure 5.17 Analysis of caspase 3/7 activity after induced apoptosis (Staurosporine (STS) 500nM; 4h) (A). Assessment of STS-induced apoptosis by flow cytometric analysis of annexin V-FITC / propidium iodide stained cells. Depicted are the mean percentages of total apoptotic cells from 3 independent experiments. (*p<0.05 compared to ctrl. siRNA)

In a second approach we enhanced MTAP expression in activated HSCs by transient transfection with a MTAP-expression plasmid (**Figure 5.18**).

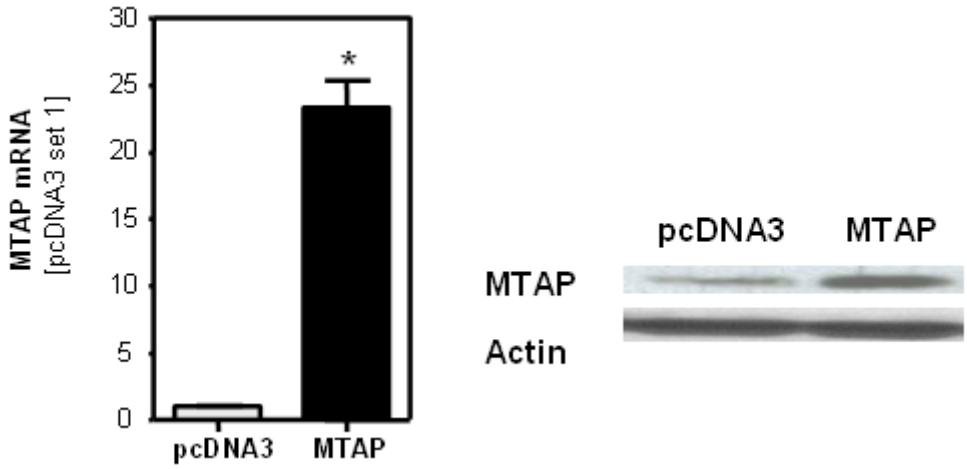

Figure 5.18 Activated HSCs were transiently transfected with control vector (pcDNA3) and an MTAP expression vector (MTAP). Analysis of MTAP expression by pRT-PCR and Western Blot. (*p<0.05)

Consequently, MTAP overexpressing HSCs revealed reduced MTA levels (**Figure 5.19**), reduced p65-phosphorylation (**Figure 5.20 A**) and NFκB reporter gene activity (**Figure 5.20 B**).

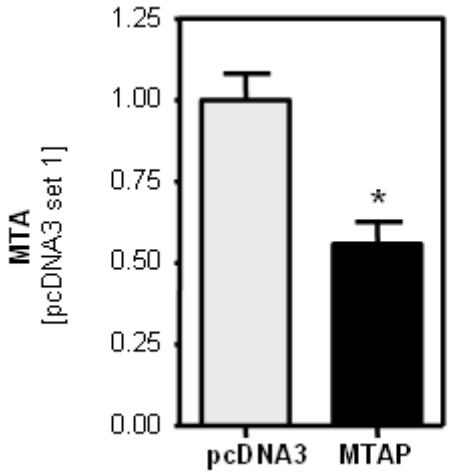

Figure 5.19 Quantification of cellular MTA levels by LC-ESI-MS/MS in activated HSCs transiently transfected with control vector (pcDNA3) and MTAP expression vector (MTAP). (*p<0.05)

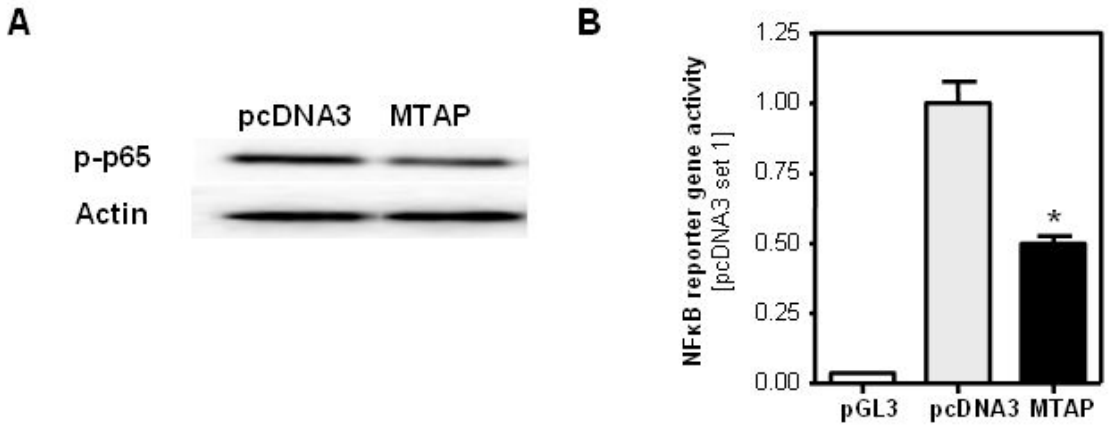

Figure 5.20 Effect of MTAP overexpression on NFκB signaling: phospho p65 Western Blot (A) as well as NFκB reporter gene assay (pGL3: empty vector) (B). (*p<0.05)

Furthermore, elevated MTAP expression made HSCs more susceptible for STS induced apoptosis (**Figure 5.21**) than control vector (pcDNA3) transfected cells. Together, these data indicate that MTAP expression is a critical regulator of MTA levels in activated HSCs, and herewith significantly affects NFκB activity and apoptosis in HSCs.

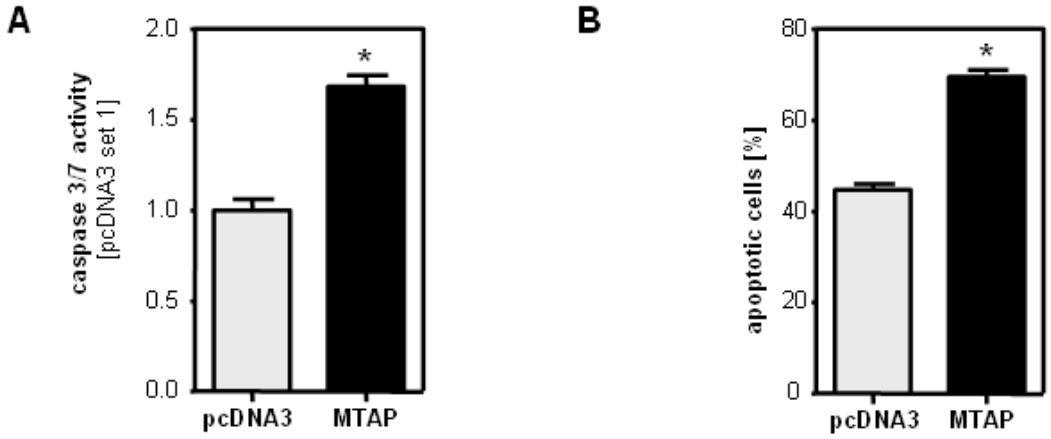

Figure 5.21 Functional effect of MTAP overexpression on resistance towards apoptosis in MTAP overexpressing activated HSCs: Analysis of caspase3/7 activity (A) after induced apoptosis (Staurosporine (STS) 500nM; 4h) and (B) assessment of STS induced apoptosis by cytometry applying annexin V and propidium iodide staining. Depicted is mean-percentage of total apoptotic cells from 3 independent experiments. (*p<0.05 compared to pcDNA3)

5.4 Effect of MTA on hepatic stellate cells

5.4.1 During activation

The activation of hepatic stellate cells is the key event in the progression of chronic liver disease. We wanted to know whether stimulation of HSCs during the course of activation influences profibrogenic gene expression. Markers of HSC activation αsma and Collagen I were further increased with MTA stimulation (**Figure 5.22**).

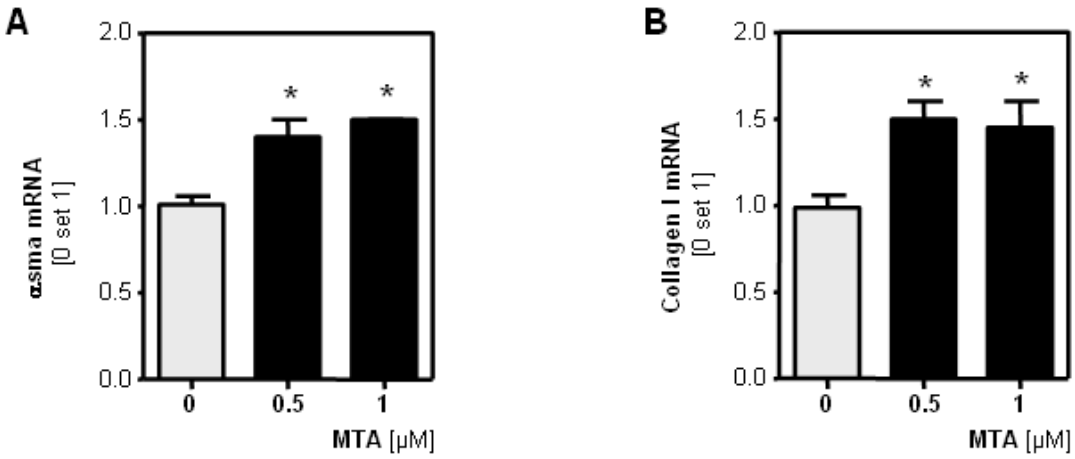

Figure 5.22: Profibrogenic gene expression of αsma (A) and Collagen I (B) in HSCs stimulated with MTA during activation. (*p<0.05)

5.4.2 In activated HSCs

Loss and gain of function studies indicated that MTAP regulated MTA levels exhibit profibrogenic effects on HSCs. In contrast, previous studies by Simile *et al.* and Latasa *et al.* showed that MTA stimulation in a dose range between 25µM and 500µM or 200µM and 500µM, respectively, caused impaired fibrogenic characteristics of activated HSCs (Latasa et al., 2010; Simile et al., 2001). To unravel these putative discrepancies we stimulated activated HSCs with MTA in a wide dose range comprising MTA levels found in diseased murine and human liver tissues (up to 5µM) and MTA doses as high as 1mM. In concentrations up to 5µM MTA stimulation led to dose-dependent induction of CCL5 (also called RANTES (Regulated on Activation, Normal T cell Expressed and Secreted)) and CCL2 (also referred to as monocyte chemotactic protein-1 (MCP-1)) expression, while higher MTA doses reduced the expression of both chemokines in activated HSCs (**Figure 5.23, Figure 5.24**). These findings indicated a nonmonotonic dose-response

relationship between MTA levels and profibrogenic gene expression in activated HSCs. While the studies of Simile *et al.* and Latasa *et al.* (Latasa et al., 2010; Simile et al., 2001) comprehensively assessed the effects of exogenously applied MTA doses, we subsequently focused on the assessment of the effects of (endogenous) MTA levels found in diseased livers. In this dose range, MTA caused a time-dependent induction of CCL5 (**Figure 5.23**) expression in activated HSCs *in vitro*.

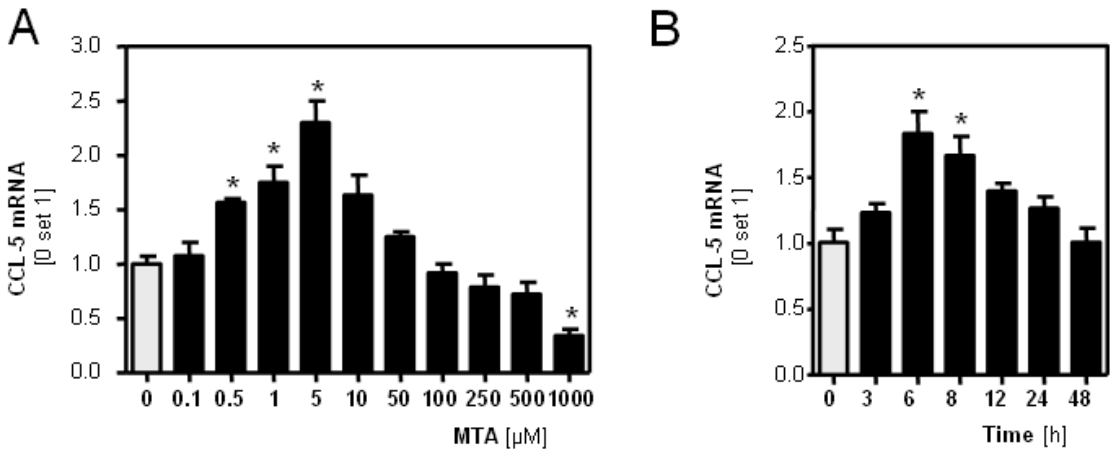

Figure 5.23: Dose (A) and time (MTA 1µM) (B) dependent proinflammatory gene expression of CCL5 in activated HSCs treated with MTA. (*p<0.05)

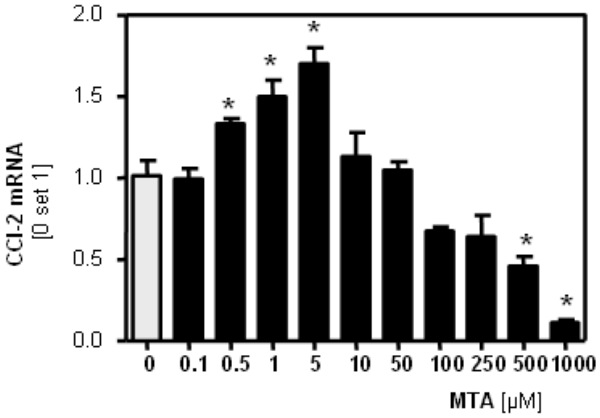

Figure 5.24: Dose dependent induction of CCL2 mRNA in activated HSCs treated with MTA. (*p<0.05)

Rapid induction of chemokine expression pointed to an effect on transcriptional regulation, and NFκB is a known critical regulator of these chemokines (Mezzano et al., 2004). MTA stimulation of HSCs induced a dose-dependent phosphorylation of IκBα (**Figure 5.25**) and activation of NFκB-reporter gene activity (**Figure 5.25**). Moreover, analysis of caspase3/7 activity and FACS analysis revealed, that MTA stimulation increased the resistance of activated HSCs towards apoptosis (**Figure 5.26**).

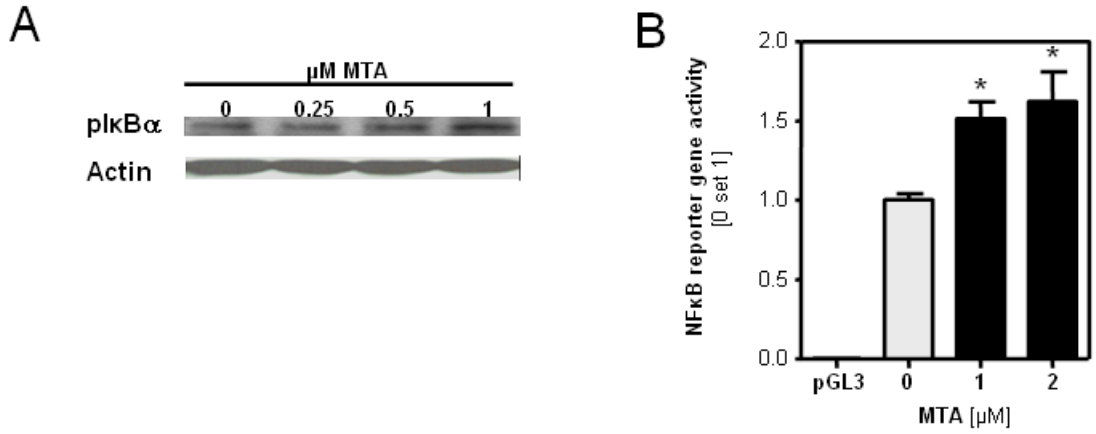

Figure 5.25: Induction of NFκB in activated HSCs treated with MTA (1µM) measured with phospho IκBα Western Blot (A) and a NFκB reporter gene assay (pGL3= empty vector) (B). (*p<0.05)

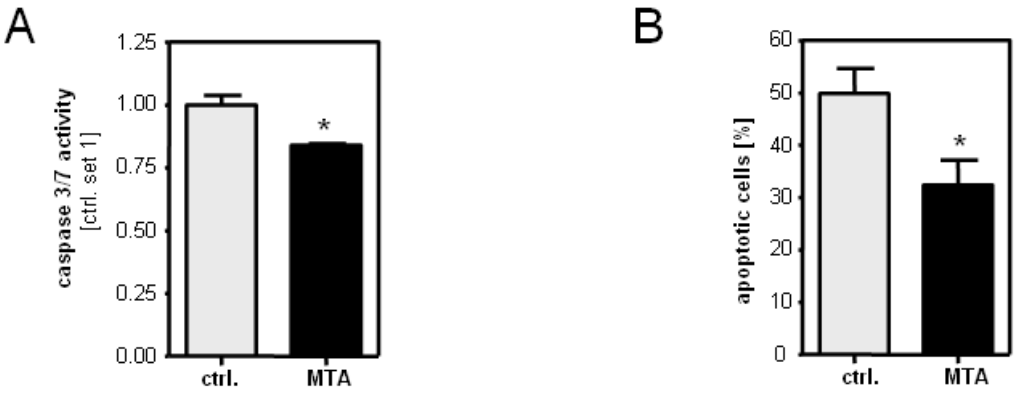

Figure 5.26 Reduced resistance towards STS induced apoposis in MTA (1µM) treated activated HSCs. (*p<0.05)

5.4.3 Functional effect of MTAP/MTA on survivin expression in activated hepatic stellate cells

Manipulation of MTAP expression or MTA stimulation did not significantly affect BAX, BCLXL and XIAP expression in activated HSCs (**Figure 5.27**).

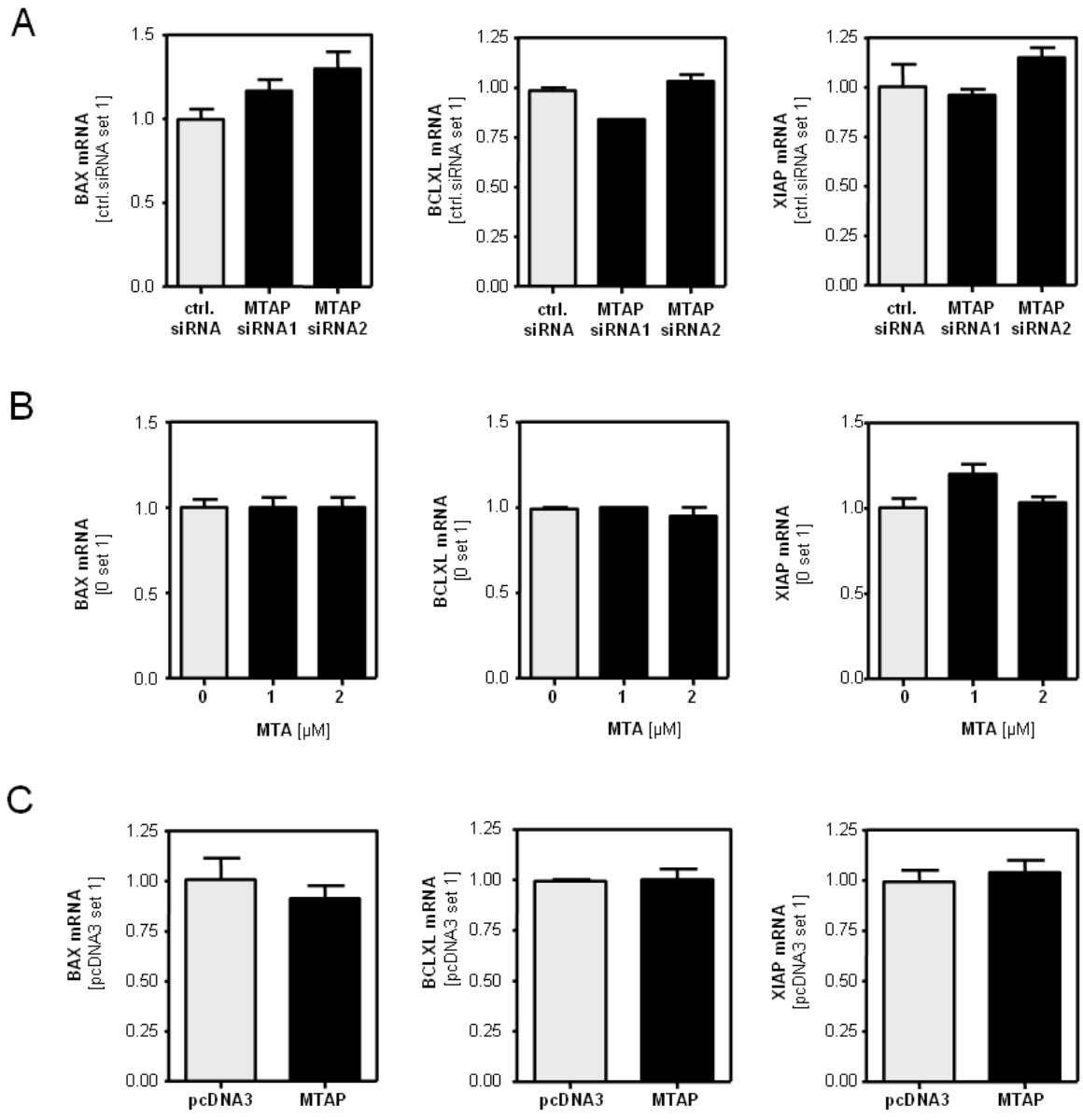

Figure 5.27 Expression of apoptosis related genes in MTAP manipulated and MTA treated activated HSCs. Quantitative RT-PCR analysis of BAX, BCLXL, and XIAP mRNA expression in activated HSCs (A) transfected with MTAP siRNA or control siRNA, (B) stimulated with MTA, and (C) transfected with MTAP expression plasmid or control vector (pcDNA3) .

However, MTAP suppressed cells (**Figure 5.28 A**) and wildtype HSCs stimulated with MTA (**Figure 5.28 B**) revealed an increased expression of survivin. In contrast, survivin expression was downregulated in MTAP overexpressing HSCs compared to pcDNA3 transfected control cells (**Figure 5.28 C**).

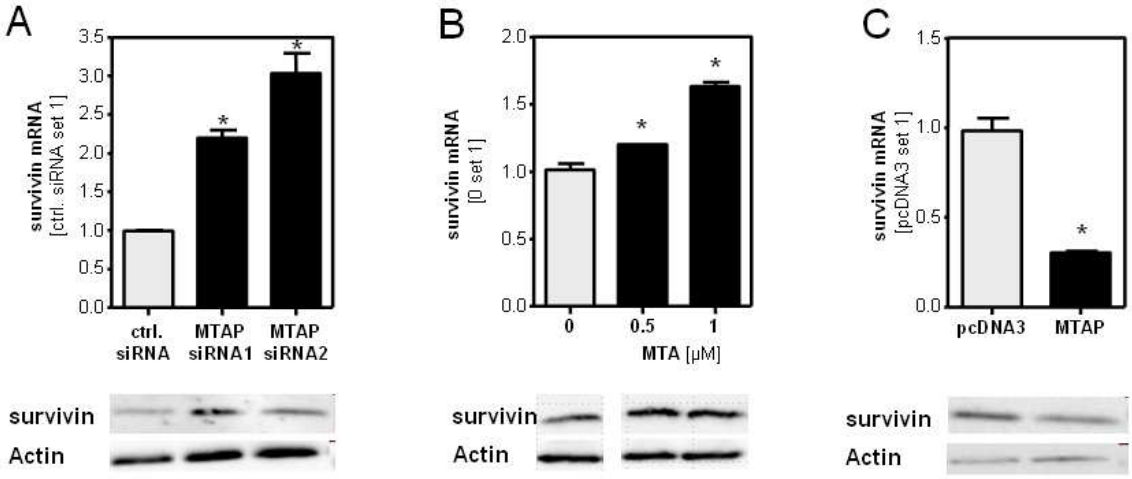

Figure 5.28 Survivin mRNA and protein expression in activated HSCs (A) transfected with MTAP siRNA or control siRNA, (B) stimulated with MTA, and (C) transfected with an MTAP expression plasmid or empty vector (pcDNA3). (*p<0.05)

Survivin is a target of NFκB (Basseres and Baldwin, 2006) and can prevent caspase-induced apoptosis (Tamm et al., 1998). This suggested that the regulation of this anti-apoptotic factor accounts at least in part for the effects of the manipulation of MTAP levels and MTA stimulation, respectively, on apoptosis resistance of HSCs. Accordingly, pretreatment with the survivin inhibitor YM-155 abolished the apoptosis protecting effect of MTA stimulation in HSCs (**Figure 5.29**). In summary, these findings indicated, that NFκB-mediated regulation of survivin expression was responsible for the effects of MTAP and MTA on apoptosis resistance of activated HSCs.

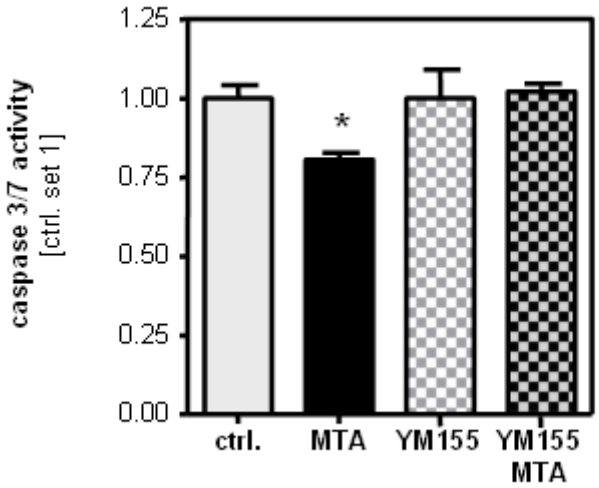

Figure 5.29 Assessment of caspase3/7 activity in MTA-treated HSCs with and without preincubation with the survivin inhibitor YM155 (5µM) following staurosporine (500nM; 4h) induced apoptosis.

5.4.4 Role of methylation and the generation of reactive oxygen species (ROS) on MTAP regulation in activated HSCs

Next, we analyzed the mechanisms regulating MTAP expression in activated HSCs. Previously, we have shown that promotor methylation causes downregulation of MTAP expression in HCC (Hellerbrand et al., 2006), and Ramani et al. described decreased global DNA methylation during HSC activation (Ramani et al., 2010). To assess whether this mechanism also affects MTAP expression in HSCs, we incubated activated HSCs with the demethylating agent 5-azacytidine (5-Aza) and found that this treatment further enhanced MTAP expression in a dose dependent manner (**Figure 5.30**).

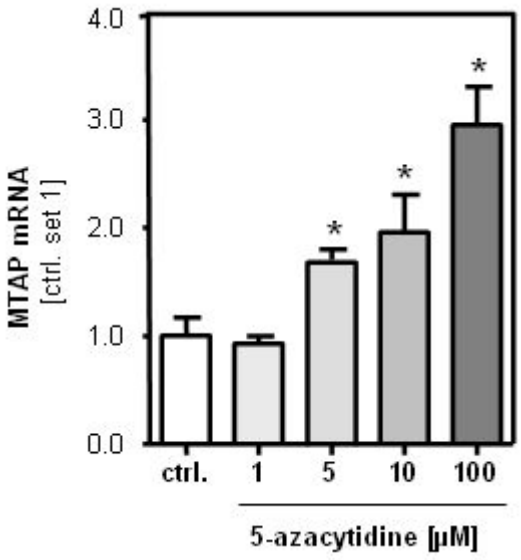

Figure 5.30 Analysis of MTAP mRNA in activated murine HSCs stimulated with 5-azacytidine (1-100µM). (*p<0.05)

Liver damage, which leads to HSC activation, is characterized by increased reactive oxygen species (ROS) formation, and oxidative stress has been shown to induce promoter methylation (Min et al., 2010; Ziech et al., 2011). Arsenic trioxide (AT) induces ROS production *via* up-regulation of NADPH oxidase (Chou et al., 2004) (**Figure 5.31 A, B**). Furthermore, we analyzed expression of heme oxygenase (decycling) 1 (HMOX). HMOX is an essential enzyme in heme catabolism, it cleaves heme to form biliverdin and is increased *via* induction of ROS (**Figure 5.31 C**) (Jaeschke, 2011; Tanaka et al., 2007).

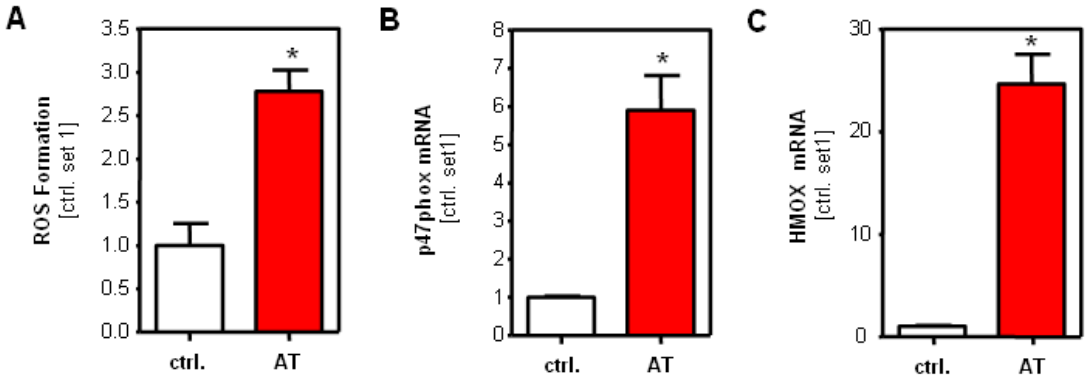

Figure 5.31. A dichlorodihydrofluorescein diacetate (H2DCFDA) assay confirmed induced ROS formation in AT (10µM) treated HSCs (A). Analysis of p47phox mRNA (B) and HMOX (heme oxygenase (decycling) 1) (C) expression in AT (10µM) treated HSCs. (*p<0.05)

Treatment of activated HSCs with AT downregulated MTAP expression (**Figure 5.32**).

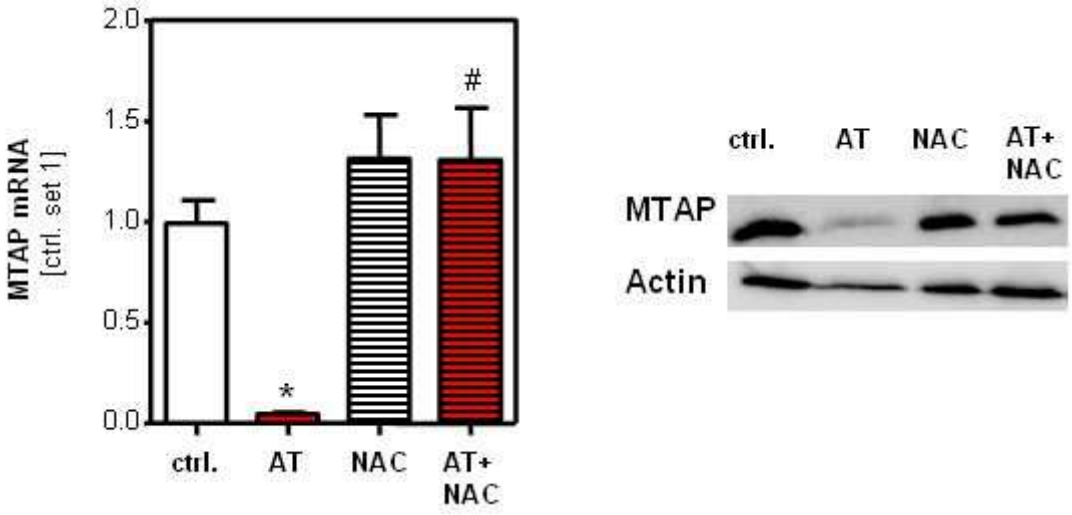

Figure 5.32 MTAP mRNA and protein expression in activated HSCs treated with As_2O_3 (AT) and NAC (10mM). (*p<0.05)

Preincubation with the ROS-scavenger N-Acetyl- L-Cysteine (NAC) abrogated AT induced downregulation of MTAP mRNA and protein (**Figure 5.32**). Also stimulation with hydrogen peroxide (H_2O_2) dose dependently downregulated MTAP in HSCs while HMOX and p47phox are induced (**Figure 5.33**) confirming that oxidative stress caused a downregulation of MTAP in HSCs.

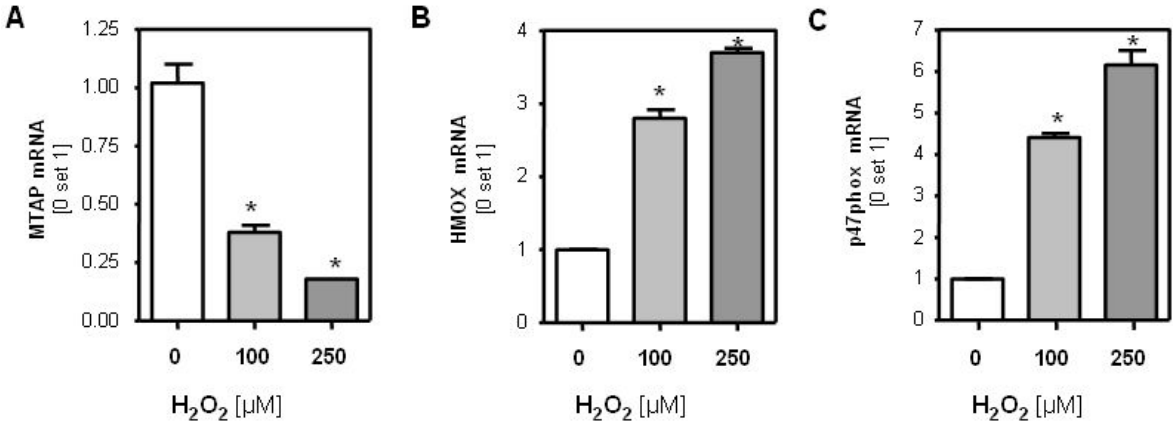

Figure 5.33 Activated HSCs were treated with different doses of hydrogen peroxide (H_2O_2) and quantification of (A) MTAP (B) HMOX1 (heme oxygenase (decycling) 1 and (C) p47phox mRNA expression was performed with quantitative RT-PCR. (*p<0.05)

In contrast, pretreatment with methyltransferase inhibitor adenosine periodate oxidized (AdOx) abolished ROS induced MTAP downregulation (**Figure 5.34**).

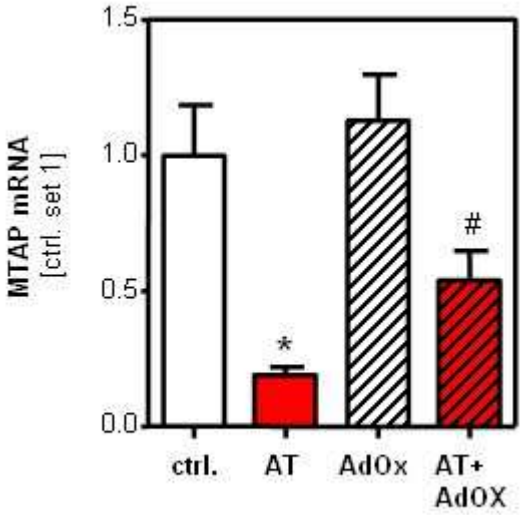

Figure 5.34 Analysis of MTAP mRNA in activated murine HSCs stimulated with 10µM As_2O_3 (AT), AdOx (50µM) alone and in combination with AT. (*p<0.05 compared to ctrl.; #p<0.05 compared to AT)

On the contrary, AT stimulation increased survivin expression in activated HSCs, and this induction was blunted by AdOx treatment (**Figure 5.35**). Together, these data indicate that epigenetic mechanisms account at least in part for the increased MTAP expression during HSC activation, while oxidative stress causes a downregulation of MTAP expression in activated HSCs, and herewith functionally affects the profibrogenic phenotype of these cells.

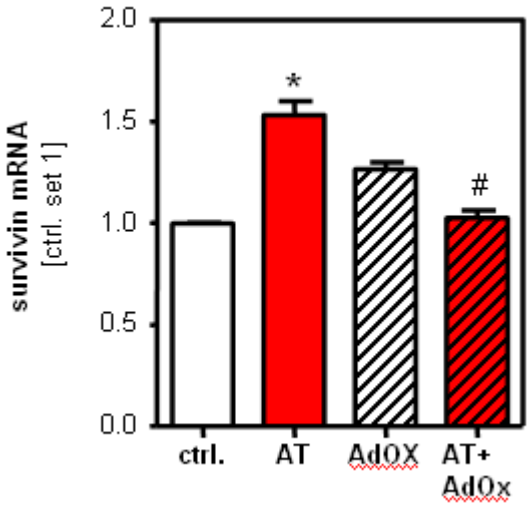

Figure 5.35 Survivin mRNA expression in activated HSCs treated with As_2O_3 (AT) (10µM) and methylation inhibitor AdOx (50µM) alone and in combination with AT. (*p<0.05 compared to ctrl.; #p<0.05 compared to AT)

6 Discussion

Recently, we have shown downregulation and tumor suppressor activity of MTAP in hepatocellular carcinoma (HCC) (Kirovski et al., 2011). Here, we expanded our investigation on chronic liver disease, which is the major HCC precondition (Hernandez-Gea et al., 2013; White et al., 2012; Zhang and Friedman, 2012). The observed downregulation of MTAP mRNA expression in cirrhotic human livers and experimental models of liver cirrhosis was in line with a previous study by Berasain *et al.* (Berasain et al., 2004). Here, we confirmed this finding at the protein level, and applying immunohistochemistry we revealed that hepatocytes of cirrhotic livers have lower MTAP expression than hepatocytes in normal liver tissue. In contrast, we found strong MTAP expression in activated HSCs in cirrhotic livers. Moreover, we demonstrated that not only MTAP but also its metabolite MTA are abundant in activated HSCs. This may be caused by an upregulation of polyamine biosynthesis in response to enhanced proliferation and cellular transdifferentiation during the course of HSC activation. In line with this, activated HSCs showed markedly higher MTA levels than hepatocytes *in vitro*. Moreover, hepatic MTA levels strongly correlated with collagen I expression in diseased hepatic tissue. And further, MTAP expression is colocalized with αsma. Together these findings indicated that also *in vivo* activated HSCs significantly contribute to MTA abundance in fibrotic livers despite their relatively lower quantity compared to hepatocytes, which are the main cellular source of total MTA in normal liver tissue. Differences in the cellular sources of MTAP and MTA could also account for enhanced MTA levels in NASH, although MTAP levels in total liver tissue were similar as in normal liver tissue. Furthermore, this may be an explanation why Berasain *et al.* did not find MTA accumulation in the model of carbon tetrachloride (CCl_4)-induced liver injury in spite of a compromised expression of MTAP (Berasain et al., 2004). In addition, it has to be considered that MTA is produced during polyamine biosynthesis from S-adenosylmethionine (AdoMet, SAM), its metabolic precursor. Interestingly, Berasain *et al.* found that AdoMet was strongly reduced in CCl_4-treated rats, and herewith, identified one further potential mechanism why reduced MTAP levels in diseased livers may not always coincide with lowered MTA levels in particular experimental models.

In the present study, we observed increased MTA levels in two experimental models of hepatic injury as well as in patients with NASH and cirrhosis of different origin. We could show that treatment of HSCs during *in vitro* activation with physiologic relevant doses of MTA enhanced profibrogenic gene expression. Beyond, stimulation of activated HSCs with MTA at concentrations similar to those found in diseased liver tissues caused increased proinflammatory gene expression and NFκB activation, as well as enhanced apoptosis resistance. In contrast to our findings, some groups have reported proapoptotic effects of MTA on hepatoma cells (Ansorena et al., 2002), and found antifibrotic effects of MTA on HSCs *in vitro* and in experimental models of hepatic fibrosis (Latasa et al., 2010; Simile et al., 2001). However, in those studies significantly higher, pharmacological doses had been administered, whereas the MTA levels achieved here mirrored endogenous hepatic levels. Moreover, pharmacological doses of MTA have been shown to exhibit protective effects on hepatocytes *in vitro* (Ansorena et al., 2006; Ansorena et al., 2002; Hevia et al., 2004), while MTA accumulation in HCC promotes tumorigenicity (Kirovski et al., 2011). Our *in vitro* findings clearly showed a biphasic effect of MTA stimulation levels on profibrogenic response in activated HSCs, and it is reasonable that also in other cells such a nonmonotonic dose-response relationship exists. Together, these findings indicate that hepatic effects of MTA are a double-edged sword and warrant the exercise of caution in the pharmacological use of MTA in treating liver disease, as pharmacological levels may drop to levels at which pro-fibrogenic and pro-tumorigenic effects predominate.

In addition to exogenous MTA stimulation also manipulation of MTAP expression and subsequent alterations of intracellular MTA levels functionally affected activated HSCs. Survivin has been described as a NFκB target gene in tumor cells (Basseres and Baldwin, 2006), and De Minicis *et al.* described increased survivin expression in HSCs isolated from murine fibrosis models (De et al., 2007). Here, we showed that survivin functionally affected apoptosis resistance of activated HSCs and identified this member of the Inhibitor of Apoptosis (IAP) family as a transcriptional target of exogenous MTA mediated NFκB activation in activated HSCs. Moreover, loss and gain of function studies revealed that MTAP-regulated levels of intracellular MTA affect NFκB activity and survivin expression in activated HSCs. NFκB activity in HSCs is critical for their resistance against apoptosis, and

herewith, the extent of fibrosis in chronic liver injury (Wright et al., 2001). Hepatic fibrosis and cirrhosis are HCC preconditions, and we have shown downregulation and tumor suppressor activity of MTAP in HCC (Kirovski et al., 2011). Together, these findings suggest (induction of) MTAP as therapeutic strategy against both fibrosis and cancerogenesis in chronic liver disease. Noteworthy, we found that promoter methylation is a critical regulator of MTAP expression in HSCs similar as we and others have shown before in HCC cells (Berasain et al., 2004; Hellerbrand et al., 2006). DNA methylation inhibitors have been suggested for treatment of HCC (Sceusi et al., 2011) and have been shown to inhibit HSC activation and fibrogenesis (Mann et al., 2007). Our study unraveled a novel mechanism by which epigenetic mechanisms critically affect the fibrogenic potential of HSCs. Furthermore, we identified oxidative stress to impair MTAP expression in HSCs. This finding is complementary to a previous study by Fernandez-Irigoyen *et al.*, who demonstrated redox regulation of MTAP activity in hepatocytes (Fernandez-Irigoyen et al., 2008).

In conclusion, we identified regulation of MTAP expression and corresponding MTA levels as a novel mechanism affecting profibrogenic gene expression, NFκB activity and apoptosis resistance in HSCs. This may be exploited for the prognosis or treatment of fibrosis progression in chronic liver disease.

7 References

Andreu-Perez, P., J. Hernandez-Losa, T. Moline, R. Gil, J. Grueso, A. Pujol, J. Cortes, M. A. Avila, and J. A. Recio, 2010, Methylthioadenosine (MTA) inhibits melanoma cell proliferation and in vivo tumor growth: BMC.Cancer, v. 10, p. 265.

Ansorena, E., C. Berasain, M. J. Lopez Zabalza, M. A. Avila, E. R. Garcia-Trevijano, and M. J. Iraburu, 2006, Differential regulation of the JNK/AP-1 pathway by S-adenosylmethionine and methylthioadenosine in primary rat hepatocytes versus HuH7 hepatoma cells: Am.J.Physiol Gastrointest.Liver Physiol, v. 290, no. 6, p. G1186-G1193.

Ansorena, E., E. R. Garcia-Trevijano, M. L. Martinez-Chantar, Z. Z. Huang, L. Chen, J. M. Mato, M. Iraburu, S. C. Lu, and M. A. Avila, 2002, S-adenosylmethionine and methylthioadenosine are antiapoptotic in cultured rat hepatocytes but proapoptotic in human hepatoma cells: Hepatology, v. 35, no. 2, p. 274-280.

Argo, C. K., and S. H. Caldwell, 2009, Epidemiology and natural history of non-alcoholic steatohepatitis: Clin.Liver Dis., v. 13, no. 4, p. 511-531.

Argo, C. K., P. G. Northup, A. M. Al-Osaimi, and S. H. Caldwell, 2009, Systematic review of risk factors for fibrosis progression in non-alcoholic steatohepatitis: J.Hepatol., v. 51, no. 2, p. 371-379.

Atzori, L., G. Poli, and A. Perra, 2009, Hepatic stellate cell: a star cell in the liver: Int.J.Biochem.Cell Biol., v. 41, no. 8-9, p. 1639-1642.

Avila, M. A. et al., 2000, Reduced mRNA abundance of the main enzymes involved in methionine metabolism in human liver cirrhosis and hepatocellular carcinoma: J.Hepatol., v. 33, no. 6, p. 907-914.

Avila, M. A., E. R. Garcia-Trevijano, S. C. Lu, F. J. Corrales, and J. M. Mato, 2004, Methylthioadenosine: Int.J.Biochem.Cell Biol., v. 36, no. 11, p. 2125-2130.

Backlund, P. S., Jr., and R. A. Smith, 1981, Methionine synthesis from 5'-methylthioadenosine in rat liver: J.Biol.Chem., v. 256, no. 4, p. 1533-1535.

Baffy, G., E. M. Brunt, and S. H. Caldwell, 2012, Hepatocellular carcinoma in non-alcoholic fatty liver disease: an emerging menace: J.Hepatol., v. 56, no. 6, p. 1384-1391.

Basseres, D. S., and A. S. Baldwin, 2006, Nuclear factor-kappaB and inhibitor of kappaB kinase pathways in oncogenic initiation and progression: Oncogene, v. 25, no. 51, p. 6817-6830.

Basu, I. et al., 2011, Growth and metastases of human lung cancer are inhibited in mouse xenografts by a transition state analogue of 5'-methylthioadenosine phosphorylase: J.Biol.Chem., v. 286, no. 6, p. 4902-4911.

Bataille, F. et al., 2005, Strong expression of methylthioadenosine phosphorylase (MTAP) in human colon carcinoma cells is regulated by TCF1/[beta]-catenin: Lab Invest, v. 85, no. 1, p. 124-136.

Bataller, R., and D. A. Brenner, 2001, Hepatic stellate cells as a target for the treatment of liver fibrosis: Semin.Liver Dis., v. 21, no. 3, p. 437-451.

Bataller, R., and D. A. Brenner, 2005, Liver fibrosis: J.Clin.Invest, v. 115, no. 2, p. 209-218.

Behrmann, I., S. Wallner, W. Komyod, P. C. Heinrich, M. Schuierer, R. Buettner, and A. K. Bosserhoff, 2003, Characterization of methylthioadenosin phosphorylase (MTAP) expression in malignant melanoma: Am.J.Pathol., v. 163, no. 2, p. 683-690.

Berasain, C. et al., 2004, Methylthioadenosine phosphorylase gene expression is impaired in human liver cirrhosis and hepatocarcinoma: Biochim.Biophys.Acta, v. 1690, no. 3, p. 276-284.

Bjornsson, E., and P. Angulo, 2007, Non-alcoholic fatty liver disease: Scand.J.Gastroenterol., v. 42, no. 9, p. 1023-1030.

Boonstra, K., U. Beuers, and C. Y. Ponsioen, 2012, Epidemiology of primary sclerosing cholangitis and primary biliary cirrhosis: a systematic review: J.Hepatol., v. 56, no. 5, p. 1181-1188.

Bosserhoff, A., and C. Hellerbrand, 2011, Obesity and fatty liver are 'grease' for the machinery of hepatic fibrosis: Dig.Dis., v. 29, no. 4, p. 377-383.

Cai, J., W. M. Sun, J. J. Hwang, S. C. Stain, and S. C. Lu, 1996, Changes in S-adenosylmethionine synthetase in human liver cancer: molecular characterization and significance: Hepatology, v. 24, no. 5, p. 1090-1097.

Campos, A. C., F. Molognoni, F. H. Melo, L. C. Galdieri, C. R. Carneiro, V. D'Almeida, M. Correa, and M. G. Jasiulionis, 2007, Oxidative stress modulates DNA methylation during melanocyte anchorage blockade associated with malignant transformation: Neoplasia., v. 9, no. 12, p. 1111-1121.

Carrera, C. J., R. L. Eddy, T. B. Shows, and D. A. Carson, 1984, Assignment of the gene for methylthioadenosine phosphorylase to human chromosome 9 by mouse-human somatic cell hybridization: Proc.Natl.Acad.Sci.U.S.A, v. 81, no. 9, p. 2665-2668.

Cave, M., I. Deaciuc, C. Mendez, Z. Song, S. Joshi-Barve, S. Barve, and C. McClain, 2007, Nonalcoholic fatty liver disease: predisposing factors and the role of nutrition: J.Nutr.Biochem., v. 18, no. 3, p. 184-195.

Cederbaum, A. I., 2010, Hepatoprotective effects of S-adenosyl-L-methionine against alcohol- and cytochrome P450 2E1-induced liver injury: World J.Gastroenterol., v. 16, no. 11, p. 1366-1376.

Chen, L. et al., 2004, Impaired liver regeneration in mice lacking methionine adenosyltransferase 1A: FASEB J., v. 18, no. 7, p. 914-916.

Chen, Z. H., H. Zhang, and T. M. Savarese, 1996, Gene deletion chemoselectivity: codeletion of the genes for p16(INK4), methylthioadenosine phosphorylase, and the alpha- and beta-interferons in human pancreatic cell carcinoma lines and its implications for chemotherapy: Cancer Res., v. 56, no. 5, p. 1083-1090.

Chou, W. C., C. Jie, A. A. Kenedy, R. J. Jones, M. A. Trush, and C. V. Dang, 2004, Role of NADPH oxidase in arsenic-induced reactive oxygen species formation and cytotoxicity in myeloid leukemia cells: Proc.Natl.Acad.Sci.U.S.A, v. 101, no. 13, p. 4578-4583.

Christopher, S. A., P. Diegelman, C. W. Porter, and W. D. Kruger, 2002, Methylthioadenosine phosphorylase, a gene frequently codeleted with p16(cdkN2a/ARF), acts as a tumor suppressor in a breast cancer cell line: Cancer Res., v. 62, no. 22, p. 6639-6644.

Cooper, C., J. Sorrell, and P. Gerami, 2012, Update in molecular diagnostics in melanocytic neoplasms: Adv.Anat.Pathol., v. 19, no. 6, p. 410-416.

Cugino, D., F. Gianfagna, I. Santimone, G. G. de, M. B. Donati, L. Iacoviello, and C. A. Di, 2012, Type 2 diabetes and polymorphisms on chromosome 9p21: a meta-analysis: Nutr.Metab Cardiovasc.Dis., v. 22, no. 8, p. 619-625.

Day, C. P., and O. F. James, 1998, Steatohepatitis: a tale of two "hits"?: Gastroenterology, v. 114, no. 4, p. 842-845.

de Alwis, N. M., and C. P. Day, 2008, Non-alcoholic fatty liver disease: the mist gradually clears: J.Hepatol., v. 48 Suppl 1, p. S104-S112.

De, M. S., E. Seki, H. Uchinami, J. Kluwe, Y. Zhang, D. A. Brenner, and R. F. Schwabe, 2007, Gene expression profiles during hepatic stellate cell activation in culture and in vivo: Gastroenterology, v. 132, no. 5, p. 1937-1946.

Della, R. F., A. Oliva, V. Gragnaniello, G. L. Russo, R. Palumbo, and V. Zappia, 1990, Physicochemical and immunological studies on mammalian 5'-deoxy-5'-methylthioadenosine phosphorylase: J.Biol.Chem., v. 265, no. 11, p. 6241-6246.

Della, R. F. et al., 1996, Purification and characterization of recombinant human 5'-methylthioadenosine phosphorylase: definite identification of coding cDNA: Biochem.Biophys.Res.Commun., v. 223, no. 3, p. 514-519.

Donkena, K. V., C. Y. Young, and D. J. Tindall, 2010, Oxidative stress and DNA methylation in prostate cancer: Obstet.Gynecol.Int., v. 2010, p. 302051.

Elsharkawy, A. M., F. Oakley, and D. A. Mann, 2005, The role and regulation of hepatic stellate cell apoptosis in reversal of liver fibrosis: Apoptosis., v. 10, no. 5, p. 927-939.

Fabianowska-Majewska, K., J. Duley, L. Fairbanks, A. Simmonds, and T. Wasiak, 1994, Substrate specificity of methylthioadenosine phosphorylase from human liver: Acta Biochim.Pol., v. 41, no. 4, p. 391-395.

Fernandez-Irigoyen, J. et al., 2008, Redox regulation of methylthioadenosine phosphorylase in liver cells: molecular mechanism and functional implications: Biochem.J., v. 411, no. 2, p. 457-465.

Ferro, A. J., A. Barrett, and S. K. Shapiro, 1978, 5-Methylthioribose kinase. A new enzyme involved in the formation of methionine from 5-methylthioribose: J.Biol.Chem., v. 253, no. 17, p. 6021-6025.

Finkelstein, J. D., 1990, Methionine metabolism in mammals: J.Nutr.Biochem., v. 1, no. 5, p. 228-237.

Fitchen, J. H., M. K. Riscoe, B. W. Dana, H. J. Lawrence, and A. J. Ferro, 1986, Methylthioadenosine phosphorylase deficiency in human leukemias and solid tumors: Cancer Res., v. 46, no. 10, p. 5409-5412.

Friedman, S. L., 2003, Liver fibrosis -- from bench to bedside: J.Hepatol., v. 38 Suppl 1, p. S38-S53.

Friedman, S. L., 2004, Mechanisms of disease: Mechanisms of hepatic fibrosis and therapeutic implications: Nat.Clin.Pract.Gastroenterol.Hepatol., v. 1, no. 2, p. 98-105.

Friedman, S. L., 2008, Mechanisms of hepatic fibrogenesis: Gastroenterology, v. 134, no. 6, p. 1655-1669.

Friedman, S. L., and M. J. Arthur, 1989, Activation of cultured rat hepatic lipocytes by Kupffer cell conditioned medium. Direct enhancement of matrix synthesis and stimulation of cell proliferation via induction of platelet-derived growth factor receptors: J.Clin.Invest, v. 84, no. 6, p. 1780-1785.

Frith, J., C. P. Day, E. Henderson, A. D. Burt, and J. L. Newton, 2009, Non-alcoholic fatty liver disease in older people: Gerontology, v. 55, no. 6, p. 607-613.

Gabele, E., M. Froh, G. E. Arteel, T. Uesugi, C. Hellerbrand, J. Scholmerich, D. A. Brenner, R. G. Thurman, and R. A. Rippe, 2009, TNFalpha is required for cholestasis-induced liver fibrosis in the mouse: Biochem.Biophys.Res.Commun., v. 378, no. 3, p. 348-353.

Gao, B., and R. Bataller, 2011, Alcoholic liver disease: pathogenesis and new therapeutic targets: Gastroenterology, v. 141, no. 5, p. 1572-1585.

Garbers, D. L., 1978, Demonstration of 5'-methylthioadenosine phosphorylase activity in various rat tissues. Some properties of the enzyme from rat lung: Biochim.Biophys.Acta, v. 523, no. 1, p. 82-93.

Garcia-Castellano, J. M., A. Villanueva, J. H. Healey, R. Sowers, C. Cordon-Cardo, A. Huvos, J. R. Bertino, P. Meyers, and R. Gorlick, 2002, Methylthioadenosine phosphorylase gene deletions are common in osteosarcoma: Clin.Cancer Res., v. 8, no. 3, p. 782-787.

Gil, B., M. Casado, M. A. Pajares, L. Bosca, J. M. Mato, P. Martin-Sanz, and L. Alvarez, 1996, Differential expression pattern of S-adenosylmethionine synthetase isoenzymes during rat liver development: Hepatology, v. 24, no. 4, p. 876-881.

Gines, P., A. Cardenas, V. Arroyo, and J. Rodes, 2004, Management of cirrhosis and ascites: N.Engl.J.Med., v. 350, no. 16, p. 1646-1654.

Glass, J. I., N. Assad-Garcia, N. Alperovich, S. Yooseph, M. R. Lewis, M. Maruf, C. A. Hutchison, III, H. O. Smith, and J. C. Venter, 2006, Essential genes of a minimal bacterium: Proc.Natl.Acad.Sci.U.S.A, v. 103, no. 2, p. 425-430.

Gramenzi, A., F. Caputo, M. Biselli, F. Kuria, E. Loggi, P. Andreone, and M. Bernardi, 2006, Review article: alcoholic liver disease--pathophysiological aspects and risk factors: Aliment.Pharmacol.Ther., v. 24, no. 8, p. 1151-1161.

Hellerbrand, S. C. Wang, H. Tsukamoto, D. A. Brenner, and R. A. Rippe, 1996, Expression of intracellular adhesion molecule 1 by activated hepatic stellate cells: Hepatology, v. 24, no. 3, p. 670-676.

Hellerbrand, C., 2010, Pathophysiological similarities and synergisms in alcoholic and non-alcoholic steatohepatitis: Dig.Dis., v. 28, no. 6, p. 783-791.

Hellerbrand, C., C. Jobin, L. L. Licato, R. B. Sartor, and D. A. Brenner, 1998, Cytokines induce NF-kappaB in activated but not in quiescent rat hepatic stellate cells: Am.J.Physiol, v. 275, no. 2 Pt 1, p. G269-G278.

Hellerbrand, C., M. Muhlbauer, S. Wallner, M. Schuierer, I. Behrmann, F. Bataille, T. Weiss, J. Scholmerich, and A. K. Bosserhoff, 2006, Promoter-hypermethylation is causing functional relevant downregulation of methylthioadenosine phosphorylase (MTAP) expression in hepatocellular carcinoma: Carcinogenesis, v. 27, no. 1, p. 64-72.

Hernandez-Gea, V., S. Toffanin, S. L. Friedman, and J. M. Llovet, 2013, Role of the microenvironment in the pathogenesis and treatment of hepatocellular carcinoma: Gastroenterology, v. 144, no. 3, p. 512-527.

Hevia, H. et al., 2004, 5'-methylthioadenosine modulates the inflammatory response to endotoxin in mice and in rat hepatocytes: Hepatology, v. 39, no. 4, p. 1088-1098.

Hori, Y., H. Hori, Y. Yamada, C. J. Carrera, M. Tomonaga, S. Kamihira, D. A. Carson, and T. Nobori, 1998, The methylthioadenosine phosphorylase gene is frequently co-deleted with the p16INK4a gene in acute type adult T-cell leukemia: Int.J.Cancer, v. 75, no. 1, p. 51-56.

Horikawa, S., H. Ozasa, K. Ota, and K. Tsukada, 1993, Immunohistochemical analysis of rat S-adenosylmethionine synthetase isozymes in developmental liver: FEBS Lett., v. 330, no. 3, p. 307-311.

Hustinx, S. R., L. M. Leoni, C. J. Yeo, P. N. Brown, M. Goggins, S. E. Kern, R. H. Hruban, and A. Maitra, 2005, Concordant loss of MTAP and p16/CDKN2A expression in pancreatic intraepithelial neoplasia: evidence of homozygous deletion in a noninvasive precursor lesion: Mod.Pathol., v. 18, no. 7, p. 959-963.

Iredale, J. P., 2003, Cirrhosis: new research provides a basis for rational and targeted treatments: BMJ, v. 327, no. 7407, p. 143-147.

Ishii, M., K. Nakazawa, H. Wada, J. Nishioka, K. Nakatani, Y. Yamada, S. Kamihira, M. Kusunoki, and T. Nobori, 2005, Methylthioadenosine phosphorylase gene is silenced by promoter hypermethylation in human lymphoma cell line DHL-9: another mechanism of enzyme deficiency: Int.J.Oncol., v. 26, no. 4, p. 985-991.

Jaeschke, H., 2011, Reactive oxygen and mechanisms of inflammatory liver injury: Present concepts: J.Gastroenterol.Hepatol., v. 26 Suppl 1, p. 173-179.

Kadariya, Y., K. Nakatani, J. Nishioka, T. Fujikawa, W. D. Kruger, and T. Nobori, 2005, Regulation of human methylthioadenosine phosphorylase gene by the CBF (CCAAT binding factor)/NF-Y (nuclear factor-Y): Biochem.J., v. 387, no. Pt 1, p. 175-183.

Kamatani, N., and D. A. Carson, 1981, Dependence of adenine production upon polyamine synthesis in cultured human lymphoblasts: Biochim.Biophys.Acta, v. 675, no. 3-4, p. 344-350.

Kamatani, N., W. A. Nelson-Rees, and D. A. Carson, 1981, Selective killing of human malignant cell lines deficient in methylthioadenosine phosphorylase, a purine metabolic enzyme: Proc.Natl.Acad.Sci.U.S.A, v. 78, no. 2, p. 1219-1223.

Kido, J., Y. Ashida, K. Shinkai, H. Akedo, A. Isoai, H. Kumagai, and H. Inoue, 1991, Effects of methylthiodeoxyadenosine and its analogs on in vitro invasion of rat ascites hepatoma cells and methylation of their phospholipids: Jpn.J.Cancer Res., v. 82, no. 10, p. 1104-1111.

Kirovski, G. et al., 2011, Down-regulation of methylthioadenosine phosphorylase (MTAP) induces progression of hepatocellular carcinoma via accumulation of 5'-deoxy-5'-methylthioadenosine (MTA): Am.J.Pathol., v. 178, no. 3, p. 1145-1152.

Ko, K., H. Yang, M. Noureddin, A. Iglesia-Ara, M. Xia, C. Wagner, Z. Luka, J. M. Mato, and S. C. Lu, 2008, Changes in S-adenosylmethionine and GSH homeostasis during endotoxemia in mice: Lab Invest, v. 88, no. 10, p. 1121-1129.

Kotb, M., and N. M. Kredich, 1985, S-Adenosylmethionine synthetase from human lymphocytes. Purification and characterization: J.Biol.Chem., v. 260, no. 7, p. 3923-3930.

Kotb, M., S. H. Mudd, J. M. Mato, A. M. Geller, N. M. Kredich, J. Y. Chou, and G. L. Cantoni, 1997, Consensus nomenclature for the mammalian methionine adenosyltransferase genes and gene products: Trends Genet., v. 13, no. 2, p. 51-52.

Krawitt, E. L., 2006, Autoimmune hepatitis: N.Engl.J.Med., v. 354, no. 1, p. 54-66.

Latasa, M. U. et al., 2010, Oral methylthioadenosine administration attenuates fibrosis and chronic liver disease progression in Mdr2-/- mice: PLoS.One., v. 5, no. 12, p. e15690.

Law, R. E., J. B. Stimmel, M. A. Damore, C. Carter, S. Clarke, and R. Wall, 1992, Lipopolysaccharide-induced NF-kappa B activation in mouse 70Z/3 pre-B lymphocytes is inhibited by mevinolin and 5'-methylthioadenosine: roles of protein

isoprenylation and carboxyl methylation reactions: Mol.Cell Biol., v. 12, no. 1, p. 103-111.

Lee, S. H., and Y. D. Cho, 1998, Induction of apoptosis in leukemia U937 cells by 5'-deoxy-5'-methylthioadenosine, a potent inhibitor of protein carboxylmethyltransferase: Exp.Cell Res., v. 240, no. 2, p. 282-292.

Lee, T. D., M. R. Sadda, M. H. Mendler, T. Bottiglieri, G. Kanel, J. M. Mato, and S. C. Lu, 2004, Abnormal hepatic methionine and glutathione metabolism in patients with alcoholic hepatitis: Alcohol Clin.Exp.Res., v. 28, no. 1, p. 173-181.

Li, T. W., H. Yang, H. Peng, M. Xia, J. M. Mato, and S. C. Lu, 2012, Effects of S-adenosylmethionine and methylthioadenosine on inflammation-induced colon cancer in mice: Carcinogenesis, v. 33, no. 2, p. 427-435.

Liao, Y. J. et al., 2009, Characterization of a glycine N-methyltransferase gene knockout mouse model for hepatocellular carcinoma: Implications of the gender disparity in liver cancer susceptibility: Int.J.Cancer, v. 124, no. 4, p. 816-826.

Liew, C. T. et al., 1999, High frequency of p16INK4A gene alterations in hepatocellular carcinoma: Oncogene, v. 18, no. 3, p. 789-795.

Lim, S. O., J. M. Gu, M. S. Kim, H. S. Kim, Y. N. Park, C. K. Park, J. W. Cho, Y. M. Park, and G. Jung, 2008, Epigenetic changes induced by reactive oxygen species in hepatocellular carcinoma: methylation of the E-cadherin promoter: Gastroenterology, v. 135, no. 6, p. 2128-40, 2140.

Lu, S. C., L. Alvarez, Z. Z. Huang, L. Chen, W. An, F. J. Corrales, M. A. Avila, G. Kanel, and J. M. Mato, 2001, Methionine adenosyltransferase 1A knockout mice are predisposed to liver injury and exhibit increased expression of genes involved in proliferation: Proc.Natl.Acad.Sci.U.S.A, v. 98, no. 10, p. 5560-5565.

Lu, S. C., and J. M. Mato, 2008, S-Adenosylmethionine in cell growth, apoptosis and liver cancer: J.Gastroenterol.Hepatol., v. 23 Suppl 1, p. S73-S77.

Lu, S. C., and J. M. Mato, 2012, S-adenosylmethionine in liver health, injury, and cancer: Physiol Rev., v. 92, no. 4, p. 1515-1542.

Ludwig, J., T. R. Viggiano, D. B. McGill, and B. J. Oh, 1980, Nonalcoholic steatohepatitis: Mayo Clinic experiences with a hitherto unnamed disease: Mayo Clin.Proc., v. 55, no. 7, p. 434-438.

Maher, P. A., 1993, Inhibition of the tyrosine kinase activity of the fibroblast growth factor receptor by the methyltransferase inhibitor 5'-methylthioadenosine: J.Biol.Chem., v. 268, no. 6, p. 4244-4249.

Mann, J., and D. A. Mann, 2009, Transcriptional regulation of hepatic stellate cells: Adv.Drug Deliv.Rev., v. 61, no. 7-8, p. 497-512.

Mann, J., F. Oakley, F. Akiboye, A. Elsharkawy, A. W. Thorne, and D. A. Mann, 2007, Regulation of myofibroblast transdifferentiation by DNA methylation and MeCP2: implications for wound healing and fibrogenesis: Cell Death.Differ., v. 14, no. 2, p. 275-285.

Martinez-Chantar, M. L. et al., 2002, Spontaneous oxidative stress and liver tumors in mice lacking methionine adenosyltransferase 1A: FASEB J., v. 16, no. 10, p. 1292-1294.

Martinez-Chantar, M. L., M. U. Latasa, M. Varela-Rey, S. C. Lu, E. R. Garcia-Trevijano, J. M. Mato, and M. A. Avila, 2003, L-methionine availability regulates expression of the methionine adenosyltransferase 2A gene in human hepatocarcinoma cells: role of S-adenosylmethionine: J.Biol.Chem., v. 278, no. 22, p. 19885-19890.

Martinez-Chantar, M. L. et al., 2008, Loss of the glycine N-methyltransferase gene leads to steatosis and hepatocellular carcinoma in mice: Hepatology, v. 47, no. 4, p. 1191-1199.

Mato, J. M., L. Alvarez, P. Ortiz, and M. A. Pajares, 1997, S-adenosylmethionine synthesis: molecular mechanisms and clinical implications: Pharmacol.Ther., v. 73, no. 3, p. 265-280.

Matsuzawa, N. et al., 2007, Lipid-induced oxidative stress causes steatohepatitis in mice fed an atherogenic diet: Hepatology, v. 46, no. 5, p. 1392-1403.

Mezzano, S., C. Aros, A. Droguett, M. E. Burgos, L. Ardiles, C. Flores, H. Schneider, M. Ruiz-Ortega, and J. Egido, 2004, NF-kappaB activation and overexpression of regulated genes in human diabetic nephropathy: Nephrol.Dial.Transplant., v. 19, no. 10, p. 2505-2512.

Min, J. Y., S. O. Lim, and G. Jung, 2010, Downregulation of catalase by reactive oxygen species via hypermethylation of CpG island II on the catalase promoter: FEBS Lett., v. 584, no. 11, p. 2427-2432.

Moreno, B., B. Fernandez-Diez, P. A. di, and P. Villoslada, 2010, Preclinical studies of methylthioadenosine for the treatment of multiple sclerosis: Mult.Scler., v. 16, no. 9, p. 1102-1108.

Mowen, K. A., J. Tang, W. Zhu, B. T. Schurter, K. Shuai, H. R. Herschman, and M. David, 2001, Arginine methylation of STAT1 modulates IFNalpha/beta-induced transcription: Cell, v. 104, no. 5, p. 731-741.

Navarro, V. J., and J. R. Senior, 2006, Drug-related hepatotoxicity: N.Engl.J.Med., v. 354, no. 7, p. 731-739.

Nobori, T., J. G. Karras, R. F. Della, T. A. Waltz, P. P. Chen, and D. A. Carson, 1991, Absence of methylthioadenosine phosphorylase in human gliomas: Cancer Res., v. 51, no. 12, p. 3193-3197.

Nobori, T., I. Szinai, D. Amox, B. Parker, O. I. Olopade, D. L. Buchhagen, and D. A. Carson, 1993, Methylthioadenosine phosphorylase deficiency in human non-small cell lung cancers: Cancer Res., v. 53, no. 5, p. 1098-1101.

Nobori, T., K. Takabayashi, P. Tran, L. Orvis, A. Batova, A. L. Yu, and D. A. Carson, 1996, Genomic cloning of methylthioadenosine phosphorylase: a purine metabolic enzyme deficient in multiple different cancers: Proc.Natl.Acad.Sci.U.S.A, v. 93, no. 12, p. 6203-6208.

Novo, E. et al., 2006, Overexpression of Bcl-2 by activated human hepatic stellate cells: resistance to apoptosis as a mechanism of progressive hepatic fibrogenesis in humans: Gut, v. 55, no. 8, p. 1174-1182.

Oakley, F. et al., 2005, Inhibition of inhibitor of kappaB kinases stimulates hepatic stellate cell apoptosis and accelerated recovery from rat liver fibrosis: Gastroenterology, v. 128, no. 1, p. 108-120.

Olopade, O. I. et al., 1995, Construction of a 2.8-megabase yeast artificial chromosome contig and cloning of the human methylthioadenosine phosphorylase gene from the tumor suppressor region on 9p21: Proc.Natl.Acad.Sci.U.S.A, v. 92, no. 14, p. 6489-6493.

Parola, M., and G. Robino, 2001, Oxidative stress-related molecules and liver fibrosis: J.Hepatol., v. 35, no. 2, p. 297-306.

Parry, D., S. Bates, D. J. Mann, and G. Peters, 1995, Lack of cyclin D-Cdk complexes in Rb-negative cells correlates with high levels of p16INK4/MTS1 tumour suppressor gene product: EMBO J., v. 14, no. 3, p. 503-511.

Pascale, R. M., M. M. Simile, M. R. De Miglio, and F. Feo, 2002, Chemoprevention of hepatocarcinogenesis: S-adenosyl-L-methionine: Alcohol, v. 27, no. 3, p. 193-198.

Pegg, A. E., 1988, Polyamine metabolism and its importance in neoplastic growth and a target for chemotherapy: Cancer Res., v. 48, no. 4, p. 759-774.

Pegg, A. E., and H. G. Williams-Ashman, 1969, Phosphate-stimulated breakdown of 5'-methylthioadenosine by rat ventral prostate: Biochem.J., v. 115, no. 2, p. 241-247.

Pinzani, M., and K. Rombouts, 2004, Liver fibrosis: from the bench to clinical targets: Dig.Liver Dis., v. 36, no. 4, p. 231-242.

Pinzani, M., M. Rosselli, and M. Zuckermann, 2011, Liver cirrhosis: Best.Pract.Res.Clin.Gastroenterol., v. 25, no. 2, p. 281-290.

Qu, L., and S. M. Lemon, 2010, Hepatitis A and hepatitis C viruses: divergent infection outcomes marked by similarities in induction and evasion of interferon responses: Semin.Liver Dis., v. 30, no. 4, p. 319-332.

Ragione, F. D., and A. Iolascon, 1997, Inactivation of cyclin-dependent kinase inhibitor genes and development of human acute leukemias: Leuk.Lymphoma, v. 25, no. 1-2, p. 23-35.

Ramani, K., H. Yang, J. Kuhlenkamp, L. Tomasi, H. Tsukamoto, J. M. Mato, and S. C. Lu, 2010, Changes in the expression of methionine adenosyltransferase genes and S-adenosylmethionine homeostasis during hepatic stellate cell activation: Hepatology, v. 51, no. 3, p. 986-995.

Riscoe, M. K., P. A. Tower, and A. J. Ferro, 1984, Mechanism of action of 5'-methylthioadenosine in S49 cells: Biochem.Pharmacol., v. 33, no. 22, p. 3639-3643.

Roberts, R., and A. F. Stewart, 2012, The genetics of coronary artery disease: Curr.Opin.Cardiol., v. 27, no. 3, p. 221-227.

Rosencrantz, R., and M. Schilsky, 2011, Wilson disease: pathogenesis and clinical considerations in diagnosis and treatment: Semin.Liver Dis., v. 31, no. 3, p. 245-259.

Rountree, C. B., S. Senadheera, J. M. Mato, G. M. Crooks, and S. C. Lu, 2008, Expansion of liver cancer stem cells during aging in methionine adenosyltransferase 1A-deficient mice: Hepatology, v. 47, no. 4, p. 1288-1297.

Sanchez-Valle, V., N. C. Chavez-Tapia, M. Uribe, and N. Mendez-Sanchez, 2012, Role of oxidative stress and molecular changes in liver fibrosis: a review: Curr.Med.Chem., v. 19, no. 28, p. 4850-4860.

Sandhu, C., J. Garbe, N. Bhattacharya, J. Daksis, C. H. Pan, P. Yaswen, J. Koh, J. M. Slingerland, and M. R. Stampfer, 1997, Transforming growth factor beta stabilizes p15INK4B protein, increases p15INK4B-cdk4 complexes, and inhibits cyclin D1-cdk4 association in human mammary epithelial cells: Mol.Cell Biol., v. 17, no. 5, p. 2458-2467.

Savarese, T. M., G. W. Crabtree, and R. E. Parks, Jr., 1981, 5'-Methylthioadenosine phosphorylase-L. Substrate activity of 5'-deoxyadenosine with the enzyme from Sarcoma 180 cells: Biochem.Pharmacol., v. 30, no. 3, p. 189-199.

Sceusi, E. L., D. S. Loose, and C. J. Wray, 2011, Clinical implications of DNA methylation in hepatocellular carcinoma: HPB (Oxford), v. 13, no. 6, p. 369-376.

Schuppan, D., and N. H. Afdhal, 2008, Liver cirrhosis: Lancet, v. 371, no. 9615, p. 838-851.

Schwabe, R. F., R. Bataller, and D. A. Brenner, 2003, Human hepatic stellate cells express CCR5 and RANTES to induce proliferation and migration: Am.J.Physiol Gastrointest.Liver Physiol, v. 285, no. 5, p. G949-G958.

Simile, M. M. et al., 2001, 5'-Methylthioadenosine administration prevents lipid peroxidation and fibrogenesis induced in rat liver by carbon-tetrachloride intoxication: J.Hepatol., v. 34, no. 3, p. 386-394.

Stevens, A. P., K. Dettmer, G. Kirovski, K. Samejima, C. Hellerbrand, A. K. Bosserhoff, and P. J. Oefner, 2010, Quantification of intermediates of the methionine and polyamine metabolism by liquid chromatography-tandem mass spectrometry in cultured tumor cells and liver biopsies: J.Chromatogr.A, v. 1217, no. 19, p. 3282-3288.

Stevens, A. P., K. Dettmer, S. Wallner, A. K. Bosserhoff, and P. J. Oefner, 2008, Quantitative analysis of 5'-deoxy-5'-methylthioadenosine in melanoma cells by liquid chromatography-stable isotope ratio tandem mass spectrometry: J.Chromatogr.B Analyt.Technol.Biomed.Life Sci., v. 876, no. 1, p. 123-128.

Stevens, A. P., B. Spangler, S. Wallner, M. Kreutz, K. Dettmer, P. J. Oefner, and A. K. Bosserhoff, 2009, Direct and tumor microenvironment mediated influences of

5'-deoxy-5'-(methylthio)adenosine on tumor progression of malignant melanoma: J.Cell Biochem., v. 106, no. 2, p. 210-219.

Strassburg, C. P., 2008, Pharmacogenetics of Gilbert's syndrome: Pharmacogenomics., v. 9, no. 6, p. 703-715.

Straub, B. K., and P. Schirmacher, 2010, Pathology and biopsy assessment of non-alcoholic fatty liver disease: Dig.Dis., v. 28, no. 1, p. 197-202.

Subhi, A. L., P. Diegelman, C. W. Porter, B. Tang, Z. J. Lu, G. D. Markham, and W. D. Kruger, 2003, Methylthioadenosine phosphorylase regulates ornithine decarboxylase by production of downstream metabolites: J.Biol.Chem., v. 278, no. 50, p. 49868-49873.

Subhi, A. L., B. Tang, B. R. Balsara, D. A. Altomare, J. R. Testa, H. S. Cooper, J. P. Hoffman, N. J. Meropol, and W. D. Kruger, 2004, Loss of methylthioadenosine phosphorylase and elevated ornithine decarboxylase is common in pancreatic cancer: Clin.Cancer Res., v. 10, no. 21, p. 7290-7296.

Tamm, I., Y. Wang, E. Sausville, D. A. Scudiero, N. Vigna, T. Oltersdorf, and J. C. Reed, 1998, IAP-family protein survivin inhibits caspase activity and apoptosis induced by Fas (CD95), Bax, caspases, and anticancer drugs: Cancer Res., v. 58, no. 23, p. 5315-5320.

Tanaka, Y., J. M. Maher, C. Chen, and C. D. Klaassen, 2007, Hepatic ischemia-reperfusion induces renal heme oxygenase-1 via NF-E2-related factor 2 in rats and mice: Mol.Pharmacol., v. 71, no. 3, p. 817-825.

Tomasi, M. L., A. Iglesias-Ara, H. Yang, K. Ramani, F. Feo, M. R. Pascale, M. L. Martinez-Chantar, J. M. Mato, and S. C. Lu, 2009, S-adenosylmethionine regulates apurinic/apyrimidinic endonuclease 1 stability: implication in hepatocarcinogenesis: Gastroenterology, v. 136, no. 3, p. 1025-1036.

Tomasi, M. L. et al., 2010, S-adenosylmethionine regulates dual-specificity mitogen-activated protein kinase phosphatase expression in mouse and human hepatocytes: Hepatology, v. 51, no. 6, p. 2152-2161.

Toohey, J. I., 1977, Methylthio group cleavage from methylthioadenosine. Description of an enzyme and its relationship to the methylthio requirement of certain cells in culture: Biochem.Biophys.Res.Commun., v. 78, no. 4, p. 1273-1280.

Tsihlias, J., L. Kapusta, and J. Slingerland, 1999, The prognostic significance of altered cyclin-dependent kinase inhibitors in human cancer: Annu.Rev.Med., v. 50, p. 401-423.

Ubagai, T., K. J. Lei, S. Huang, S. H. Mudd, H. L. Levy, and J. Y. Chou, 1995, Molecular mechanisms of an inborn error of methionine pathway. Methionine adenosyltransferase deficiency: J.Clin.Invest, v. 96, no. 4, p. 1943-1947.

van Bokhoven, M. A., C. T. van Deursen, and D. W. Swinkels, 2011, Diagnosis and management of hereditary haemochromatosis: BMJ, v. 342, p. c7251.

Varela-Rey, M., N. Beraza, S. C. Lu, J. M. Mato, and M. L. Martinez-Chantar, 2011, Role of AMP-activated protein kinase in the control of hepatocyte priming and proliferation during liver regeneration: Exp.Biol.Med.(Maywood.), v. 236, no. 4, p. 402-408.

Vazquez-Chantada, M. et al., 2009, Evidence for LKB1/AMP-activated protein kinase/ endothelial nitric oxide synthase cascade regulated by hepatocyte growth factor, S-adenosylmethionine, and nitric oxide in hepatocyte proliferation: Hepatology, v. 49, no. 2, p. 608-617.

Vazquez-Chantada, M. et al., 2010, HuR/methyl-HuR and AUF1 regulate the MAT expressed during liver proliferation, differentiation, and carcinogenesis: Gastroenterology, v. 138, no. 5, p. 1943-1953.

Veal, N., C. L. Hsieh, S. Xiong, J. M. Mato, S. Lu, and H. Tsukamoto, 2004, Inhibition of lipopolysaccharide-stimulated TNF-alpha promoter activity by S-adenosylmethionine and 5'-methylthioadenosine: Am.J.Physiol Gastrointest.Liver Physiol, v. 287, no. 2, p. G352-G362.

Watanabe, F. et al., 2009, Immunohistochemical diagnosis of methylthioadenosine phosphorylase (MTAP) deficiency in non-small cell lung carcinoma: Lung Cancer, v. 63, no. 1, p. 39-44.

Watson, M. R., K. Wallace, R. G. Gieling, D. M. Manas, E. Jaffray, R. T. Hay, D. A. Mann, and F. Oakley, 2008, NF-kappaB is a critical regulator of the survival of rodent and human hepatic myofibroblasts: J.Hepatol., v. 48, no. 4, p. 589-597.

White, D. L., F. Kanwal, and H. B. El-Serag, 2012, Association between nonalcoholic fatty liver disease and risk for hepatocellular cancer, based on systematic review: Clin.Gastroenterol.Hepatol., v. 10, no. 12, p. 1342-1359.

Williams-Ashman, H. G., J. Seidenfeld, and P. Galletti, 1982, Trends in the biochemical pharmacology of 5'-deoxy-5'-methylthioadenosine: Biochem.Pharmacol., v. 31, no. 3, p. 277-288.

Wong, Y. F., T. K. Chung, T. H. Cheung, T. Nobori, and A. M. Chang, 1998, MTAP gene deletion in endometrial cancer: Gynecol.Obstet.Invest, v. 45, no. 4, p. 272-276.

Wright, M. C., R. Issa, D. E. Smart, N. Trim, G. I. Murray, J. N. Primrose, M. J. Arthur, J. P. Iredale, and D. A. Mann, 2001, Gliotoxin stimulates the apoptosis of human and rat hepatic stellate cells and enhances the resolution of liver fibrosis in rats: Gastroenterology, v. 121, no. 3, p. 685-698.

Yang, H., A. I. Ara, N. Magilnick, M. Xia, K. Ramani, H. Chen, T. D. Lee, J. M. Mato, and S. C. Lu, 2008, Expression pattern, regulation, and functions of methionine adenosyltransferase 2beta splicing variants in hepatoma cells: Gastroenterology, v. 134, no. 1, p. 281-291.

Yang, H., K. Ko, M. Xia, T. W. Li, P. Oh, J. Li, and S. C. Lu, 2010, Induction of avian musculoaponeurotic fibrosarcoma proteins by toxic bile acid inhibits expression of glutathione synthetic enzymes and contributes to cholestatic liver injury in mice: Hepatology, v. 51, no. 4, p. 1291-1301.

Yang, H., K. Ramani, M. Xia, K. S. Ko, T. W. Li, P. Oh, J. Li, and S. C. Lu, 2009, Dysregulation of glutathione synthesis during cholestasis in mice: molecular mechanisms and therapeutic implications: Hepatology, v. 49, no. 6, p. 1982-1991.

Zhang, D. Y., and S. L. Friedman, 2012, Fibrosis-dependent mechanisms of hepatocarcinogenesis: Hepatology, v. 56, no. 2, p. 769-775.

Zhang, H., Z. H. Chen, and T. M. Savarese, 1996, Codeletion of the genes for p16INK4, methylthioadenosine phosphorylase, interferon-alpha1, interferon-beta1, and other 9p21 markers in human malignant cell lines: Cancer Genet.Cytogenet., v. 86, no. 1, p. 22-28.

Ziech, D., R. Franco, A. G. Georgakilas, S. Georgakila, V. Malamou-Mitsi, O. Schoneveld, A. Pappa, and M. I. Panayiotidis, 2010, The role of reactive oxygen species and oxidative stress in environmental carcinogenesis and biomarker development: Chem.Biol.Interact., v. 188, no. 2, p. 334-339.

Ziech, D., R. Franco, A. Pappa, and M. I. Panayiotidis, 2011, Reactive oxygen species (ROS)--induced genetic and epigenetic alterations in human carcinogenesis: Mutat.Res., v. 711, no. 1-2, p. 167-173.

8 Abbreviations

AEC	3-amino-9-ethylcarbazole
AMP	adenosine monophosphate
AdoMet	S-adenosyl- L -methionine
AdOx	adenosine-2′,3′-dialdehyde, adenosine periodate oxidized
ALF	acute liver failure
AMV-RT	avian myeloblastosis virus reverse transcriptase
AOM/DSS	azoxymethane/ dextran sodium sulphate
APS	ammonium persulfate
As_2O_3	arsenic trioxide
AT	arsenic trioxide
ATP	adenosine triphosphate
Aza	5-Azacytidine
BCA	bicinchoninic acid
BDL	bile duct ligation
Bp	base pairs
BSA	bovine serum albumin
ca.	circa
cAMP	cyclic adenosine monophosphate
CCl_4	carbon tetrachloride
CCL5	chemokine Ligand 5 = RANTES (Regulated on Activation, Normal T cell Expressed and Secreted)
CCL2	chemokine ligand 2 = MCP-1 (monocyte chemotactic protein-1)
cDNA	complementary DNA
Coll I	Collagen I
Ctrl.	control
Cy2	Cyanine dye 2

Da	dalton (=1.66018 x 10-24 g)
DAPI	4’, 6-diamino-2-phenylindole
DMEM	Dulbecco’s modified eagle medium
DNA	deoxyribonucleic acid
e.g.	*exempli gratia*
ECM	extracellular matrix
EDTA	ethylene diamine tetraacetic acid
et al.	*et alii*
FCS	fetal calf serum
FITC	fluorescein isothiocyanate
g	gram
h	hour
H2DCFDA	2',7'-dichlorodihydrofluorescein diacetate
H_2Odest.	destilled water
HCC	hepatocellular carcinoma
HMOX	heme oxygenase (decycling) 1
HRP	horse radish peroxidase
HSC(s)	hepatic stellate cell(s)
IAP	Inhibitor of Apoptosis
Ig	immunoglobulin
IκBα	inhibitory kappa B alpha
kDa	kilodalton
l	liter
LC-ESI- MS/MS	liquid chromatography-electrospray ionization-tandem mass spectrometry
LPS	Lipopolysaccharides
M	molar, mol/l
mA	milliampere
MCP-1	monocyte chemoattractant protein-1 = CCl2
mg	milligram
min	minute

ml	milliliter
mM	millimolar
mm	millimeter
mmol	millimol
MMPs	matrix metalloproteinase
mRNA	messenger RNA
MTA	5'-deoxy-5'-(methylthio)adenosine
MTAP	methylthioadenosine phosphorylase
MTOB	4-methylthio-2-oxobutanoic acid
MTR-1P	methylthioribose 1-phosphate
NAC	N-Acetyl- L-Cysteine
NAFLD	Non-alcoholic fatty liver disease
NASH	Non-alcoholic steatohepatitis
NFκB	nuclear factor kappa B
ng	nanogram
ODC	ornithine decarboxylase
PBS	phosphate buffered saline
PCR	polymerase chain reaction
pH	*pondus hydrogenii*
PHHs	primary human hepatocytes
PI	propidium iodide
qRT-PCR	quantitative realtime-PCR
RANTES	Regulated on Activation, Normal T cell Expressed and Secreted = CCl5
ROS	reactive oxygen species
rpm	rounds per minute
RT	room temperature
s	second
SAM	S-adenosyl- L -methionine
SDS	sodium dodecyl sulfate
STS	staurosporine
TBS	tris-buffered saline
TE	tris EDTA

TEMED	N, N, N', N'-tetramethylethylenediamine
TIMP	tissue inhibitors of matrix metalloproteinases
Tris	tris(hydroxymethyl)aminomethane
TRITC	isothiocyanate derivative
Tween	Polyoxyethylene sorbitan monolaurate
UK	United Kingdom
USA	United States of America
µg	microgram
µl	microliter
µm	microgram
µM	micromolar
°C	degree Celsius

9 Appendix

9.1 Curriculum vitae

Diplom Biologin Barbara Czech

Adresse	Straubinger Straße 19 93055 Regensburg
geboren	am 15.10.1983 in Simbach am Inn
Familienstand	ledig
Konfession	römisch-katholisch
Staatsangehörigkeit	deutsch
seit 09/2009	Promotion als wissenschaftlicher Mitarbeiter am Universitätsklinikum Regensburg in der Abteilung Innere Medizin I in der Arbeitsgruppe von Prof. Dr. Claus Hellerbrand.
07/2009	Diplom im Fach Biologie: Hauptfächer: Zellbiologie, Biochemie, Tierphysiologie Bewertung: sehr gut
10/2008-07/2009	Diplomarbeit am Lehrstuhl für zelluläre und molekulare Neurobiologie von Prof. Dr. Inga Neumann: „Auswirkungen von Oxytocin auf die Emotionalität bei Ratten.“
10/2003-07/2009	Studium der Biologie an der Universität Regensburg
07/2003	Abitur am Gymnasium in Pfarrkirchen

9.2 Advanced training and courses

2010	Teilnahme an der Weiterbildungsveranstaltung „Versuchstierkunde und Tierschutz (nach den FELASA-B – Richtlinien)“ am Universitätsklinikum Regensburg
03/2010	Teilnahme an der „Fortbildungsveranstaltung für Projektleiter und Beauftragte für Biologische Sicherheit (BBS)“ am Universitätsklinikum Regensburg
27.-28.01.2011	Falk Workshop Liver and Immunology
26.-27.01.2012	Falk Work Inflammation and Cancer
24.-25.02.2013	Falk Work Targeted Therapies in Hepatology

9.3 Publications

2013

1. Czech B, Neumann ID, Müller M, Reber SO, Hellerbrand C
   Combination of chronic psychosocial stress and a NASH inducing diet in mice
   International Journal of Clinical and Experimental Pathology 2013

2012

2. Valletta D, Czech B, Thasler WE, Müller M, Bosserhoff AK, Hellerbrand C
   Expression and function of the atypical cadherin FAT1 in chronic liver disease
   Biochemical and Biophysical Research Communications 2012

3. Saugspier M, Dorn C, Czech B, Gehrig M, Heilmann J, Hellerbrand C.
   Hop bitter acids inhibit tumorigenicity of hepatocellular carcinoma cells *in vitro*
   Oncology Reports 2012

2011

4. Schnabl B, Czech B, Valletta D, Weiss TS, Kirovski G, Hellerbrand C
   Increased expression of zinc finger protein 267 in non-alcoholic fatty liver disease
   International Journal of Clinical and Experimental Pathology 2011

5. Kirovski G, Stevens AP, Czech B, Dettmer K, Weiss TS, Wild P, Hartmann A, Bosserhoff AK, Oefner PJ, Hellerbrand C.
   Down-regulation of methylthioadenosine phosphorylase (MTAP) induces progression of hepatocellular carcinoma via accumulation of 5'-deoxy-5'-methylthioadenosine (MTA)
   American Journal of Pathology 2011

9.4 Presentations

Symposium: Tumor Metabolism meets Immunology (2013, Regensburg)

Czech B, Valletta D, Saugspier M, Müller M, Bosserhoff AK, Hellerbrand C

Effect of increased glucose transporter 1 (GLUT1) expression in activated hepatic stellate cells

29. Jahrestagung der Deutschen Arbeitsgemeinschaft zum Studium der Leber (2013, Hannover)

Czech B, Valletta D, Dettmer K, Müller M, Bosserhoff AK, Oefner PJ, Hellerbrand C

Downregulation of methylthioadenosine phosphorylase (MTAP) expression in chronic liver disease promotes hepatic inflammation and fibrosis

Czech B, Valletta D, Saugspier M, Müller M, Bosserhoff AK, Hellerbrand C

Effect of increased glucose transporter 1 (GLUT1) expression in activated hepatic stellate cells

Czech B, Weigand K, Neumann ID, Müller M Reber SO, Hellerbrand C

Combination of psychosocial stress and a NASH-inducing diet in mice

Falk Workshop Targeted Therapies in Hepatology (2013, Hannover)

Czech B, Hellerbrand C

Upregulation of Myc-associated zinc finger protein (MAZ) in the pathogenesis of chronic liver disease

47th Annual Meeting of the European Association for the Study of the Liver (2012, Barcelona)

Czech B, Valletta D, Saugspier M, Dettmer K, Weiss TS, Bosserhoff AK, Oefner PJ, Hellerbrand C

Downregulation of methylthioadenosine phosphorylase (MTAP) expression in chronic liver disease promotes hepatic inflammation and fibrosis

28. Jahrestagung der Deutschen Arbeitsgemeinschaft zum Studium der Leber (2012, Hamburg)

Czech B, Valletta D, Hellerbrand C

Increased expression of the glucose transporter GLUT1 in liver fibrosis

Czech B, Valletta D, Saugspier M, Dettmer K, Weiss TS, Bosserhoff AK, Oefner PJ, Hellerbrand C

Downregulation of methylthioadenosine phosphorylase (MTAP) expression in chronic liver disease promotes hepatic inflammation and fibrosis

Falk Workshop Inflammation and Cancer (2012, Hamburg)

Czech B, Valletta D, Hellerbrand C

Monoacylglycerol lipase (MAGL) is downregulated in hepatocellular carcinoma

27. Jahrestagung der Deutschen Arbeitsgemeinschaft zum Studium der Leber (2011, Regensburg)

Czech B, Kirovski G, Stevens AP, Saugspier M, Dorn C, Bosserhoff AK, Oefner PJ, Hellerbrand C

Expression and function of methylthioadenosine phosphorylase (MTAP) in chronic liver disease

9.5 Awards/ Grants

Falk Foundation Travel Award 2013, Hannover, Germany

EASL (European Association for the Study of the Liver) Travel Award 2012, Barcelona, Spain

Falk Foundation Travel Award 2012, Hamburg, Germany

9.6 Danksagung

Last but not least ist es mir ein großes Anliegen, Danke zu sagen, zu all den Menschen, ohne die ich dieses Ziel niemals hätte erreichen können.

Ganz besonderer Dank gilt meinem Doktorvater **Prof. Dr. Claus Hellerbrand**. Lieber Claus, vielen Dank, für die Zeit, die du meiner Arbeit geschenkt hast, für Dein Wissen, das du mit mir geteilt hast, für Deinen Glauben, den du an das Projekt hattest und vor allem für Deine immerwährende positive Art. Darüber hinaus, vielen Dank für Deine Fähigkeit, Kritik so anzubringen, dass ich besser geworden bin und Deine nicht endende innere Motivation ☺.

Vielen Dank an Frau **Prof. Dr. Müller- Schilling** für die Möglichkeit, diese Arbeit an ihrem Lehrstuhl durchgeführt haben zu dürfen.

Vielen Dank auch an meine Mentorin **Prof. Dr. Marina Kreutz**, die mich außerordentlich unterstützt hat- sowohl emotional als auch mental ☺. Sei es durch Ihr Charisma oder durch Ihr Gespür für ihre Mitmenschen und Ihre Kompetenz. Durch Ihre Art, Ihre Erfahrung und Ihr Wissen und den daraus folgenden Ideen wurde diese Arbeit sehr bereichert.

Größter Dank auch an meinen Mentor **Prof. Dr. Peter Oefner**, der sehr viel Zeit und Energie in dieses Projekt gesteckt hat und ohne dessen Unterstützung diese Arbeit in vielerlei Hinsicht nicht möglich gewesen wäre. Vielen Dank für Ihre konstruktive Kritik und Ihr Interesse, dass Sie mir und meiner Arbeit geschenkt haben.

Vielen Dank auch an **Dr. Katja Dettmer**, **Dr. Axel Stevens** und **Nadine Nürnberger** für die MTA Messungen. Danke für eure stets positive, lockere und kompetente Art, eure schnelle Arbeit und eure konstruktiven Beiträge. Ohne euch wäre die Arbeit nicht so schlüssig geworden.

Ich bedanke mich bei **Prof. Dr. Frank Schweda** für die Übernahme der Rolle als Prüfungsvorsitzender.

Ich danke auch Herrn **Rudi Jung** für die Unterstützung bei den immunohistochemischen Färbungen.

Größten Dank an **Peter Karl** und **Herbert Gabler** für die stets lockere und humorvolle Stimmung im Tierstall. Und vor allem für eure ständige Unterstützung.

Vielen Dank an meine liebsten Kollegen, der Lebergruppe: **Abdo, Andi, Birgitta, Conny, Christoph, Daniela, Heidi, Karin, Leandra, Margit, Marina, Michael, Monika, Ruth, Sebastian.** Vielen Dank für das außerordentliche Arbeitsklima, die immerwährende gegenseitige Hilfe und den Zusammenhalt als TEAM- es hätte nicht besser sein können.

Vielen Dank an meinen langjährigen Labornachbarn **Michael**, der durch seine Art jeden Tag mit ihm zu etwas Besonderem gemacht hat. Er hat mich so herzlich ins Team integriert und mich an seinem Wissen teilhaben lassen, deswegen ist es nicht mehr dasselbe, seit DU nicht mehr da bist, liebster **Michi**…

Größter Dank gebührt auch dem hochgeschätzten Kollegen **Dr. Dorn**. Der, zum einen, durch seinen außergewöhnlichen Humor und zum anderen durch seine herausragende Kompetenz das Fortschreiten dieser Arbeit sehr bereichert hat.

Ganz riesengroßer Dank gebührt auch meiner ALLERLIEBSTEN, BESTEN, SCHLAUSTEN Kollegin, **Daniela**. Du hast die größten Krisen mit mir durchgestanden, hast mich immer unterstützt und warst jederzeit bereit mir zu helfen, egal ob beruflich oder privat. Ich vermisse dich sehr und ich hoffe, dass du so tolle neue Kollegen hast, wie du eine bist.

Vielen Dank an **Maria** für ihre freundschaftliche Art und ihre Kompetenz in der Arbeit mit Primärzellen und vor allem für die zur Verfügung Stellung humaner Zellen. Durch dich ist es uns eine Freude geworden, den Zellanruf zu bekommen ☺.

Größter Dank auch an **Claudia**, die versucht hat, mir Methoden beizubringen, von denen ich vorher noch nie was gehört hatte. Aber vor allem Danke für dich, für

deine positive, fröhliche Art, durchs Leben zu gehen, du hast mir so manchen Tag im H1 durch Deine bloße Anwesenheit gerettet ☺.

Frau **Martina Meisinger** danke ich für die vielen stillen Arbeiten im Hintergrund, die einem das Leben im Labor sehr erleichtern.

Besonders bedanken möchte ich mich auch bei **Dr. Kathrin Renner-Sattler**. Vielen Dank für Deine schlauen Ratschläge, Dein Interesse an dem Fortschritt meiner Arbeit, Deine offene Art und Deine soziale Kompetenz, ich habe viel von Dir gelernt ☺.

Vielen Dank an das **komplette Umfeld im H1**, an all die netten Menschen, die ich durch meine Arbeit hier kennengelernt habe, für die lustigen Plaudereien am Gang und in der Küche ☼☺.

Ein riesengroßer Dank auch an meine **Isi**. Die mich glücklicherweise schon sehr lange begleitet. Über das Sudium, bis hin zum Doktor bist du mir die beste Freundin geworden, die ich mir vorstellen kann und ich danke Dir für all Deine klugen Ratschläge um meine Arbeit aber vor allem dafür, dass DU da bist.

Liebsten Dank an **Gerrit**, der mich sehr dabei unterstützt hat, diese Arbeit zum Abschluss zu bringen. Ich weiss durch dich was es heisst:
“You'll never walk alone “. Vielen Dank, dass du IMMER für mich da bist!

Ich danke der **Familie Bambauer** für die Unterstützung und Fürsorge seit ich ein kleines Kind war. Ihr habt immer an mich geglaubt, das hat mir sehr geholfen.

Der größte Dank geht an **meine Eltern** und meine Schwester **Veronika**. Danke für eure immerwährende Unterstützung jeglicher Art, für die klugen Ratschläge und die Art mit mir in Krisen klarzukommen. Ohne euch, wäre ich niemals dahin gekommen, wo ich bin. **Veronika** hat stets meine Launen ertragen und mich immer wieder motiviert, wenns mal gar nicht mehr ging und neben dem Dank bin ich auch unglaublich stolz darauf, dass sie meine Schwester ist!

Selbstständigkeitserklärung

Ich, Barbara Czech geboren am 15.10.1983 in Simbach am Inn erkläre hiermit, dass ich die vorliegende Arbeit ohne unzulässige Hilfe Dritter und ohne Benutzung anderer als der angegebenen Hilfsmittel angefertigt habe. Die aus anderen Quellen direkt oder indirekt übernommenen Daten und Konzepte sind unter Angabe der Quelle gekennzeichnet. Insbesondere habe ich nicht die entgeltliche Hilfe von Vermittlungs- bzw. Beratungsdiensten (Promotionsberater oder andere Personen) in Anspruch genommen.

Die Arbeit wurde bisher weder im In- noch im Ausland in gleicher oder ähnlicher Form einer anderen Prüfungsbehörde vorgelegt.

…… ……..

(Ort, Datum) (Unterschrift)